

UC Berkeley

UC Berkeley Previously Published Works

Title

Search for top squarks in events with a Higgs or Z boson using 139 fb⁻¹ of pp collision data at s=13 TeV with the ATLAS detector

Permalink

<https://escholarship.org/uc/item/01r5j2k5>

Journal

European Physical Journal C, 80(11)

ISSN

1434-6044

Authors

Aad, G
Abbott, B
Abbott, DC
et al.

Publication Date

2020-11-01

DOI

10.1140/epjc/s10052-020-08469-8

Peer reviewed



Search for top squarks in events with a Higgs or Z boson using 139 fb^{-1} of pp collision data at $\sqrt{s} = 13 \text{ TeV}$ with the ATLAS detector

The ATLAS Collaboration

This paper presents a search for direct top squark pair production in events with missing transverse momentum plus either a pair of jets consistent with Standard Model Higgs boson decay into b -quarks or a same-flavour opposite-sign dilepton pair with an invariant mass consistent with a Z boson. The analysis is performed using the proton–proton collision data at $\sqrt{s} = 13 \text{ TeV}$ collected with the ATLAS detector during the LHC Run-2, corresponding to an integrated luminosity of 139 fb^{-1} . No excess is observed in the data above the Standard Model predictions. The results are interpreted in simplified models featuring direct production of pairs of either the lighter top squark (\tilde{t}_1) or the heavier top squark (\tilde{t}_2), excluding at 95% confidence level \tilde{t}_1 and \tilde{t}_2 masses up to about 1220 and 875 GeV, respectively.

arXiv:2006.05880v2 [hep-ex] 17 Dec 2020

1 Introduction

Supersymmetry (SUSY) [1–6] is one of the most studied frameworks to extend the Standard Model (SM) beyond the electroweak scale. It predicts new bosonic (fermionic) partners for the known fermions (bosons). Assuming R -parity conservation [7], SUSY particles are produced in pairs and the lightest supersymmetric particle (LSP) is stable, providing a possible dark-matter candidate. The SUSY partners of the Higgs bosons and electroweak gauge bosons mix to form the mass eigenstates known as charginos ($\tilde{\chi}_k^\pm$, $k = 1, 2$) and neutralinos ($\tilde{\chi}_m^0$, $m = 1, 2, 3, 4$), where the increasing index denotes increasing mass. The scalar partners of right-handed and left-handed quarks, \tilde{q}_R and \tilde{q}_L squarks, mix to form two mass eigenstates, \tilde{q}_1 and \tilde{q}_2 , with \tilde{q}_1 defined to be the lighter of the two. To address the SM hierarchy problem [8–11], TeV-scale masses are favoured [12, 13] for the supersymmetric partners of the gluons, and the top squarks [14, 15].

Top squark production with SM Higgs (h) or Z bosons in the decay chain can appear either in production of the lighter top squark mass eigenstate (\tilde{t}_1) decaying via $\tilde{t}_1 \rightarrow t\tilde{\chi}_2^0$ with $\tilde{\chi}_2^0 \rightarrow h/Z\tilde{\chi}_1^0$, or in production of the heavier top squark mass eigenstate (\tilde{t}_2) decaying via $\tilde{t}_2 \rightarrow Z\tilde{t}_1$ with $\tilde{t}_1 \rightarrow t^{(*)}\tilde{\chi}_1^0$, as illustrated in Figure 1. Unlike other top squark models, these signals can be efficiently distinguished from the SM top quark pair production ($t\bar{t}$) background by requiring either a same-flavour opposite-sign (SF-OS) lepton pair originating from the $Z \rightarrow \ell^+\ell^-$ ($\ell \equiv e, \mu$) decay or a pair of b -tagged jets originating from the $h \rightarrow b\bar{b}$ decay, plus the presence of an additional lepton produced in the decay of the top squarks in the event.

Simplified models [16–18] are used for the analysis optimisation and interpretation of the results. In these models, direct top squark pair production is considered and all SUSY particles are decoupled except for the top squarks and the neutralinos involved in their decay. In all cases the $\tilde{\chi}_1^0$ is assumed to be the LSP. Simplified models featuring direct \tilde{t}_1 production with $\tilde{t}_1 \rightarrow t\tilde{\chi}_2^0$ and decays via either Higgs ($\tilde{\chi}_2^0 \rightarrow h\tilde{\chi}_1^0$) or Z ($\tilde{\chi}_2^0 \rightarrow Z\tilde{\chi}_1^0$) bosons with different branching ratio values are considered. In these models, the $\tilde{\chi}_1^0$ is assumed to be very light and the $\tilde{\chi}_2^0 - \tilde{\chi}_1^0$ mass difference to be large enough to allow on-shell Higgs or Z boson decays.

Additional simplified models featuring direct \tilde{t}_2 production with $\tilde{t}_2 \rightarrow Z\tilde{t}_1$ decays and $\tilde{t}_1 \rightarrow t^{(*)}\tilde{\chi}_1^0$ are also considered. The mass difference between the \tilde{t}_1 and $\tilde{\chi}_1^0$ is set to be smaller than the W boson mass, and the four-body decay $\tilde{t}_1 \rightarrow bff'\tilde{\chi}_1^0$ is assumed to occur, where f and f' are two fermions from the W^* decay, such as $\tilde{t}_1 \rightarrow b\ell\nu\tilde{\chi}_1^0$. Direct production of \tilde{t}_1 pairs is not considered in the \tilde{t}_2 production simplified models. The \tilde{t}_1 pair production contribution to the selections presented in this paper has been found to be negligible.

This paper presents the results of a search for top squarks in final states with Higgs or Z bosons at $\sqrt{s} = 13$ TeV using the complete data sample collected with the ATLAS detector [19] in proton–proton (pp) collisions during Run-2 of the LHC (2015–2018), corresponding to 139 fb^{-1} . Searches for top squark production in events involving Higgs or Z bosons have been performed previously by both ATLAS [20, 21] and CMS [22, 23].

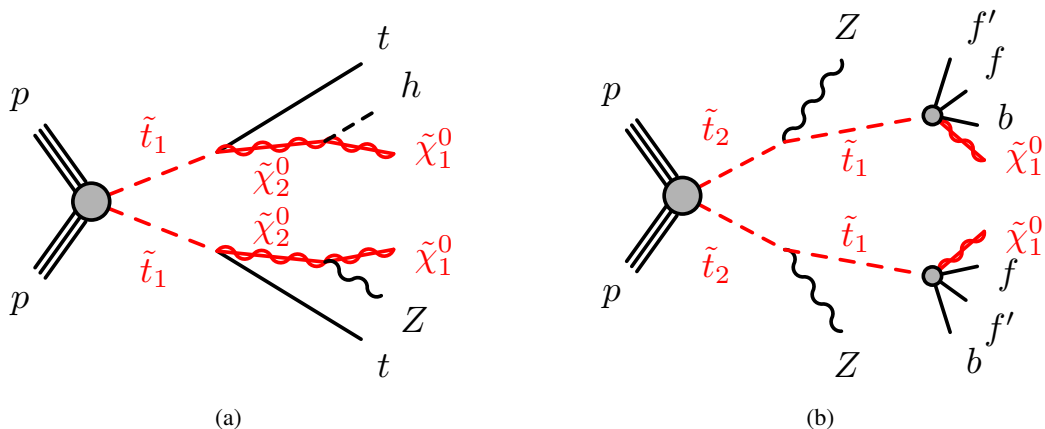


Figure 1: Diagrams for the top squark pair production processes considered in this analysis: (a) $\tilde{t}_1 \rightarrow t\tilde{\chi}_2^0$ with $\tilde{\chi}_2^0 \rightarrow h/Z\tilde{\chi}_1^0$ decays (showing for illustration the case where the two $\tilde{\chi}_2^0$ decay differently, although events with the same $\tilde{\chi}_2^0$ decays are also considered in the analysis), and (b) $\tilde{t}_2 \rightarrow Z\tilde{t}_1$ with $\tilde{t}_1 \rightarrow bff'\tilde{\chi}_1^0$ decays.

2 ATLAS detector

The ATLAS detector [19, 24] at the LHC is a multipurpose particle detector with a forward–backward symmetric cylindrical geometry and a near 4π coverage in solid angle.¹ It consists of an inner tracking detector (ID) surrounded by a thin superconducting solenoid providing a 2 T axial magnetic field, electromagnetic (EM) and hadron calorimeters, and a muon spectrometer (MS). The inner tracking detector covers the pseudorapidity range $|\eta| < 2.5$. It consists of silicon pixel, silicon microstrip, and transition radiation tracking detectors. Lead/liquid-argon (LAr) sampling calorimeters provide EM energy measurements with high granularity. A steel/scintillator-tile hadron calorimeter covers the central pseudorapidity range $|\eta| < 1.7$. The endcap and forward regions are instrumented with LAr calorimeters for both the EM and hadronic energy measurements up to $|\eta| = 4.9$. The muon spectrometer surrounds the calorimeters and is based on three large air-core toroidal superconducting magnets with eight coils each. The field integral of the toroids ranges between 2 and 6 T m across most of the detector. The muon spectrometer includes a system of precision tracking chambers and fast detectors for triggering. A two-level trigger system is used to select events [25]. The first-level trigger is implemented in hardware and uses a subset of the detector information to reduce the accepted rate to at most 100 kHz. This is followed by a software-based trigger that reduces the accepted event rate to 1 kHz on average depending on the data-taking conditions.

3 Data set and simulated event samples

The data were collected by the ATLAS detector during the LHC Run-2 (2015–2018) with a peak instantaneous luminosity of $\mathcal{L} = 2.1 \times 10^{34} \text{ cm}^{-2}\text{s}^{-1}$, resulting in a mean number of pp interactions per

¹ ATLAS uses a right-handed coordinate system with its origin at the nominal interaction point (IP) in the centre of the detector and the z -axis along the beam pipe. The x -axis points from the IP to the centre of the LHC ring, and the y -axis points upwards. Cylindrical coordinates (r, ϕ) are used in the transverse plane, ϕ being the azimuthal angle around the z -axis. The pseudorapidity is defined in terms of the polar angle θ as $\eta = -\ln \tan(\theta/2)$, and the rapidity is defined as $y = (1/2)[(E + p_z)/(E - p_z)]$.

Table 1: Simulated signal and background event samples: the corresponding event generator used for the hard-scatter process, the generator used to model the parton showering, the source of the cross-section used for normalisation, the PDF set and the underlying-event tune are shown.

Physics process	Generator	Parton shower	Cross-section normalisation	PDF set	Tune
SUSY Signals	MG5_AMC@NLO 2.6.2 [34]	PYTHIA 8.212 [35]	NNLO+NNLL [36–39]	NNPDF2.3LO [40]	A14 [41]
$t\bar{t}Z/\gamma^*, t\bar{t}W$	MG5_AMC@NLO 2.3.3	PYTHIA 8.210	NLO [34]	NNPDF2.3LO	A14
Diboson	SHERPA 2.2.2 [32]	SHERPA 2.2.2	Generator NLO	NNPDF3.0NNLO [42]	SHERPA default
$t\bar{t}$	POWHEG-BOX v2 [43]	PYTHIA 8.230	NNLO+NNLL [44–49]	NNPDF3.0NLO	A14
$t\bar{t}h$	POWHEG-BOX v2	PYTHIA 8.230	NLO [50]	NNPDF2.3LO	A14
Single-top, Wt	POWHEG-BOX v2	PYTHIA 8.230	NNLO+NNLL [51–53]	NNPDF3.0NLO	A14
Wh, Zh	PYTHIA 8.186 [54]	PYTHIA 8.186	NLO [50]	NNPDF2.3LO	A14
$t\bar{t}WW, t\bar{t}t\bar{t}$	MG5_AMC@NLO 2.2.2	PYTHIA 8.186	NLO [34]	NNPDF2.3LO	A14
$t\bar{t}t$	MG5_AMC@NLO 2.2.2	PYTHIA 8.186	Generator LO	NNPDF2.3LO	A14
tZ	MG5_AMC@NLO 2.3.3	PYTHIA 8.186	Generator LO	NNPDF2.3LO	A14
tWZ	MG5_AMC@NLO 2.3.3	PYTHIA 8.212	Generator NLO	NNPDF2.3LO	A14
Triboson	SHERPA 2.2.2	SHERPA 2.2.2	Generator NLO	NNPDF3.0NNLO	SHERPA default

bunch crossing of $\langle\mu\rangle = 34$. Data quality requirements are applied to ensure that all subdetectors were operating normally, and that the LHC beams were in stable-collision mode. The integrated luminosity of the resulting data sample is 139 fb^{-1} . The uncertainty in the combined 2015–2018 integrated luminosity is 1.7%. It is derived from the calibration of the luminosity scale using x – y beam-separation scans, following a methodology similar to that detailed in Ref. [26], and using the LUCID-2 detector for the baseline luminosity measurements [27].

Monte Carlo (MC) simulated event samples are used to aid the estimation of the background from SM processes and to model the SUSY signal. The choices of MC event generator, parton shower and hadronisation, the cross-section normalisation, the parton distribution function (PDF) set and the set of tuned parameters (tune) for the underlying event of these samples are summarised in Table 1. More details of the event generator configurations can be found in Refs. [28–31]. Cross-sections calculated at next-to-next-to-leading order (NNLO) in quantum chromodynamics (QCD) including resummation of next-to-next-to-leading logarithmic (NNLL) soft-gluon terms were used for top quark production processes. For production of top quark pairs in association with vector or Higgs bosons, cross-sections calculated at next-to-leading order (NLO) were used, and the event generator NLO cross-sections from SHERPA [32] were used when normalising the multi-boson backgrounds. In all MC samples, except those produced by SHERPA, the EvtGen v1.2.0 program [33] was used to model the properties of the bottom and charm hadron decays.

SUSY signal samples were generated with MG5_AMC@NLO 2.6.2 [34] interfaced to PYTHIA 8.212 [35] for the parton showering (PS) and hadronisation. The matrix element (ME) calculation was performed at tree level and includes the emission of up to two additional partons for all signal samples. MADSPIN [55] was used to model the $\tilde{t}_1 \rightarrow b f f' \tilde{\chi}_1^0$ decays. MADSPIN emulates kinematic distributions to a good approximation without calculating the full ME. The PDF set used for the generation of the signal samples was NNPDF2.3LO [40] with the A14 [41] set of tuned underlying-event and shower parameters (UE tune). The ME–PS matching was performed with the CKKW-L prescription [56], with a matching scale set to one quarter of the top squark mass. All signal cross-sections were calculated to approximate NNLO in the strong coupling constant, adding the resummation of soft gluon emission at NNLL accuracy (approximate NNLO+NNLL) [36–39]. The nominal cross-section and its uncertainty were derived using the PDF4LHC15_mc PDF set, following the recommendations of Ref. [57].

To simulate the effects of additional pp collisions in the same and nearby bunch crossings (pile-up), additional interactions were generated using the soft QCD processes provided by PYTHIA 8.186 with the A3 tune [58] and the MSTW2008LO PDF set [59], and overlaid onto each simulated hard-scatter event. The MC samples were reweighted so that the pile-up distribution matches the one observed in the data. The MC samples were processed through an ATLAS detector simulation [60] based on GEANT 4 [61] or, in the case of $t\bar{t}$ and the SUSY signal samples, a fast simulation using a parameterisation of the calorimeter response and GEANT 4 for the other parts of the detector. All MC samples were reconstructed in the same manner as the data.

4 Event selection

Candidate events are required to have a reconstructed vertex [62] with at least two associated tracks with transverse momentum (p_T) larger than 500 MeV that are consistent with originating from the beam collision region in the x - y plane. The primary vertex in the event is the vertex with the highest sum of squared transverse momenta of associated tracks.

Two categories of leptons (electrons and muons) are defined: ‘candidate’ and ‘signal’ (the latter being a subset of the ‘candidate’ leptons satisfying tighter selection criteria). Electron candidates are reconstructed from isolated electromagnetic calorimeter energy deposits matched to ID tracks and are required to have $|\eta| < 2.47$, a transverse momentum $p_T > 4.5$ GeV, and to satisfy the ‘LooseAndBLayer’ requirement defined in Ref. [63], which is based on a likelihood using measurements of shower shapes in the calorimeter and track properties in the ID as input variables.

Muon candidates are reconstructed in the region $|\eta| < 2.4$ from MS tracks matching ID tracks. Candidate muons are required to have $p_T > 4$ GeV and satisfy the ‘medium’ identification requirements defined in Ref. [64], based on the number of hits in the different ID and MS subsystems, and on the ratio of the charge and momentum (q/p) measured in the ID and MS divided by the sum in quadrature of their corresponding uncertainties.

The tracks associated with the lepton candidates are required to have a significance of the transverse impact parameter relative to the reconstructed primary vertex, d_0 , of $|d_0|/\sigma(d_0) < 5$ for electrons and $|d_0|/\sigma(d_0) < 3$ for muons, and a longitudinal impact parameter relative to the reconstructed primary vertex, z_0 , satisfying $|z_0 \sin \theta| < 0.5$ mm.

Jets are reconstructed from three-dimensional energy clusters in the calorimeter [65] using the anti- k_t jet clustering algorithm [66] with a radius parameter $R = 0.4$. Only jet candidates with $p_T > 20$ GeV and $|\eta| < 2.8$ are considered. Jets are calibrated using MC simulation with corrections obtained from in situ techniques [67]. To reduce the effects of pile-up, jets with $p_T < 120$ GeV and $|\eta| < 2.5$ are required to have a significant fraction of their associated tracks compatible with originating from the primary vertex, as defined by the jet vertex tagger [68]. This requirement reduces the fraction of jets from pile-up to 1%, with an efficiency for hard-scatter jets of about 90%. Events are discarded if they contain any jet with $p_T > 20$ GeV not satisfying basic quality selection criteria designed to reject detector noise and non-collision backgrounds [69].

Identification of jets containing b -hadrons (b -tagging) is performed with a multivariate discriminant that makes use of track impact parameters and reconstructed secondary vertices [70, 71]. Jets are considered as b -tagged if they fulfil a requirement corresponding to a 77% average efficiency obtained for jets containing b -hadrons in simulated $t\bar{t}$ events. The rejection factors for light-quark and gluon jets, jets containing

c -hadrons and jets containing hadronically decaying τ -leptons in simulated $t\bar{t}$ events are approximately 113, 16 and 4, respectively.

Jet candidates with $p_T < 200$ GeV within an angular distance $\Delta R = \sqrt{(\Delta y)^2 + (\Delta\phi)^2} = 0.2$ of an electron candidate are discarded, unless the jet has a value of the b -tagging discriminant larger than the value corresponding to approximately 85% b -tagging efficiency, in which case the lepton is discarded since it is likely to have originated from a semileptonic b -hadron decay. The same procedure is applied to jets within $\Delta R = 0.2$ of a muon candidate irrespective of the jet p_T . Any remaining electron candidate within $\Delta R = 0.4$ of a non-pile-up jet, and any muon candidate within $\Delta R = \min\{0.4, 0.04 + p_T(\mu)/10 \text{ GeV}\}$ of a non-pile-up jet is discarded. In the latter case, if the jet has fewer than three associated tracks, the muon is retained and the jet is discarded instead to avoid inefficiencies for high-energy muons undergoing significant energy loss in the calorimeter. Finally, any electron candidate sharing an ID track with a remaining muon candidate is also removed.

Tighter requirements on the lepton candidates are imposed, which are then referred to as ‘signal’ electrons or muons. Signal electrons must satisfy the ‘Medium’ identification requirement as defined in Ref. [63] and signal muons must have $p_T > 5$ GeV. Isolation requirements are applied to both the signal electrons and muons. The scalar sum of the p_T of tracks within a variable-size cone around the lepton, excluding its own track, must be less than 6% of the lepton p_T ; these tracks are required to be associated with the primary vertex to limit sensitivity to pile-up. The size of the track isolation cone for electrons (muons) is given by the smaller of $\Delta R = 10 \text{ GeV}/p_T$ and $\Delta R = 0.2$ (0.3). In addition, in the case of electrons the energy of calorimeter energy clusters in a cone of $\Delta R_\eta = \sqrt{(\Delta\eta)^2 + (\Delta\phi)^2} = 0.2$ around the electron (excluding the deposition from the electron itself) must be less than 6% of the electron p_T .

Simulated events are corrected for differences between data and MC simulation in jet vertex tagger and b -tagging efficiencies as well as b -tagging mis-tag rates [68, 71–73]. Corrections are also applied to account for minor differences between data and MC simulation in the signal-lepton trigger, reconstruction, identification and isolation efficiencies.

The missing transverse momentum vector, whose magnitude is denoted by E_T^{miss} , is defined as the negative vector sum of the transverse momenta of all identified electrons, muons and jets, plus an additional soft term. The soft term is constructed from all tracks that originate from the primary vertex but are not associated with any identified lepton or jet. In this way, the E_T^{miss} is adjusted for the best calibration of leptons and jets, while contributions from pile-up interactions are suppressed through the soft term [74, 75].

The events are classified into two exclusive categories: at least three leptons (referred to as 3ℓ selection, aimed at top squark decays involving Z bosons), or exactly one lepton (referred to as 1ℓ selection, aimed at top squark decays involving Higgs bosons). The selection requirements for each of these categories are described below.

4.1 3ℓ selection

In this selection, events are accepted if they satisfy a trigger requiring either two electrons, two muons or an electron and a muon. The requirements imposed offline on the p_T , identification and isolation of the leptons involved in the trigger decision are tighter than those applied online, so as to be on the trigger efficiency plateau [25]. The presence of at least three signal leptons (electrons or muons, referred to collectively with the symbol ℓ), with at least one SF-OS lepton pair whose invariant mass is compatible

with the Z boson mass ($|m_{\ell\ell} - m_Z| < 15$ GeV, with $m_Z = 91.2$ GeV) is required. In addition, the leading (highest p_T) lepton is required to have $p_T > 40$ GeV and the subleading to have $p_T > 20$ GeV. The SF-OS requirements are not applied for the validation of the background induced by fake and non-prompt leptons in Section 5.1.

Four overlapping signal regions (SRs) are optimised for the best discovery sensitivity, two for each of the simplified models described in Section 1. The requirements in each SR are summarised in Table 2.

Signal region SR_{1A}^Z is optimised for large $\tilde{\chi}_2^0 - \tilde{\chi}_1^0$ mass splittings in the $\tilde{t}_1 \rightarrow t\tilde{\chi}_2^0$ with $\tilde{\chi}_2^0 \rightarrow h/Z\tilde{\chi}_1^0$ model. It includes requirements on $m_{T2}^{3\ell}$, a variation of the transverse mass m_{T2} which is used to bind the masses of a pair of particles that are presumed to have each decayed semi-invisibly into one visible and one invisible particle [76, 77]. In the case of $m_{T2}^{3\ell}$, the two visible legs of the two semi-invisible decays are set to be the third leading lepton and the system of the SF-OS lepton pair with an invariant mass closest to m_Z . Models with small mass differences between the $\tilde{\chi}_2^0$ and the $\tilde{\chi}_1^0$ are targeted with SR_{1B}^Z , which instead imposes requirements on the transverse momentum of the SF-OS lepton pair ($p_T^{\ell\ell}$).

Two SRs are optimised for the $\tilde{t}_2 \rightarrow Z\tilde{t}_1$ with $\tilde{t}_1 \rightarrow bff'\tilde{\chi}_1^0$ model, SR_{2A}^Z and SR_{2B}^Z , targeting small and large mass splittings between the \tilde{t}_2 and the $\tilde{\chi}_1^0$, respectively. Due to the overall soft kinematics of the particles in compressed \tilde{t}_2 signals, SR_{2A}^Z features upper bounds on the p_T of the third leading lepton and on $p_T^{\ell\ell}$, as well as no requirement on the number of b -tagged jets since they are likely to be soft in this scenario. SR_{2B}^Z also includes an upper bound on the third leading lepton p_T but requires the presence of b -tagged jets and large E_T^{miss} and $p_T^{\ell\ell}$.

The requirement on the number of signal leptons makes the SR_{1A}^Z and SR_{1B}^Z selections insensitive to potential contributions from alternative \tilde{t}_1 decays with each $\tilde{t}_1 \rightarrow t\tilde{\chi}_1^0$. The acceptance for mixed decay scenarios, with $\tilde{t}_1\tilde{t}_1 \rightarrow t\tilde{\chi}_1^0 t\tilde{\chi}_2^0$ was found to depend linearly on the branching fraction of \tilde{t}_1 to $t\tilde{\chi}_2^0$. The signal lepton multiplicity requirement depletes the contribution from the direct production of \tilde{t}_1 pairs to SR_{2A}^Z and SR_{2B}^Z .

4.2 1ℓ selection

Events in this selection are accepted if they satisfy a combination of single-lepton and E_T^{miss} trigger requirements, the latter being used only for events with $E_T^{\text{miss}} > 230$ GeV and lepton $p_T < 30$ GeV. The offline requirements on the E_T^{miss} , p_T , identification and isolation of the lepton are tighter than those applied online, so as to be on the trigger efficiency plateau [25]. The presence of exactly one signal lepton (electron or muon) is required.

The identification of Higgs boson candidates decaying into b -quarks is performed using a neural network that uses as input the four-momentum and b -tagging information of pairs of jets. The scaled jet p_T/m_{jj} observable is used to prevent the dijet invariant mass being used as the primary discriminating variable. The network is trained with the PyTorch package [78] using as signal dijet pairs originating from Higgs boson decays in the simulated $t\bar{t}H$ process, and as background dijet pairs in $t\bar{t}$ and $t\bar{t}H$ not originating from Higgs boson decays. A jet pair is tagged as a Higgs boson candidate if the corresponding neural network score is above a threshold optimised to target models predicting sizeable branching fractions of $\tilde{\chi}_2^0$ into Higgs bosons. The efficiency to correctly identify jet pairs originating from Higgs boson decays in signal events is 50%–54% depending on the \tilde{t}_1 mass, as evaluated on a simulated event sample selected by

Table 2: Definition of the signal regions used in the 3ℓ selection (see text for further description).

Requirement / Region	SR _{1A} ^Z	SR _{1B} ^Z	SR _{2A} ^Z	SR _{2B} ^Z
Number of signal leptons		≥ 3		
Number of SF-OS pairs		≥ 1		
Leading lepton p_T [GeV]		> 40		
Subleading lepton p_T [GeV]		> 20		
$ m_{\ell\ell}^{\text{SF-OS}} - m_Z $ [GeV]		< 15		
Third leading lepton p_T [GeV]	> 20	> 20	< 20	< 60
$n_{\text{jets}} (p_T > 30 \text{ GeV})$	≥ 4	≥ 5	≥ 3	≥ 3
$n_{b\text{-tagged jets}} (p_T > 30 \text{ GeV})$	≥ 1	≥ 1	–	≥ 1
Leading jet p_T [GeV]	–	–	> 150	–
Leading b -tagged jet p_T [GeV]	–	> 100	–	–
E_T^{miss} [GeV]	> 250	> 150	> 200	> 350
$p_T^{\ell\ell}$ [GeV]	–	> 150	< 50	> 150
$m_{T2}^{3\ell}$ [GeV]	> 100	–	–	–

requiring one signal lepton and at least two b -tagged jets. Using the same selection, the probability of tagging a jet pair in $t\bar{t}$ events is approximately 0.05%.

Two overlapping SRs are optimised for the best discovery sensitivity in the $\tilde{t}_1 \rightarrow t\tilde{\chi}_2^0$ simplified model discussed in Section 1, and their requirements are summarised in Table 3. Both require the presence of at least four b -tagged jets and at least one Higgs boson candidate ($n_{h\text{-cand}}$). The SRs include requirements on the transverse mass m_T (computed as $m_T = \sqrt{2p_T^\ell E_T^{\text{miss}}(1 - \cos \Delta\phi)}$ where $\Delta\phi$ is the azimuthal angle between the missing transverse momentum vector and the lepton), and on the object-based E_T^{miss} -significance [79] (\mathcal{S}), which is used to discriminate events where the E_T^{miss} is due to invisible particles in the final state from events where the E_T^{miss} is due to poorly measured particles and jets. The requirements on $n_{b\text{-tagged jets}}$ and $n_{h\text{-cand}}$ reduce the potential contributions from alternative \tilde{t}_1 decays with each $\tilde{t}_1 \rightarrow t\tilde{\chi}_1^0$ to a negligible level. Analogously to the 3ℓ selection, the acceptance for mixed decay scenarios with $\tilde{t}_1\tilde{t}_1 \rightarrow t\tilde{\chi}_1^0 t\tilde{\chi}_2^0$ has been found to depend linearly on the branching fraction of \tilde{t}_1 to $t\tilde{\chi}_2^0$.

Signal region SR_{1A}^h is optimised for small $\tilde{\chi}_2^0 - \tilde{\chi}_1^0$ mass splittings, while large $\tilde{\chi}_2^0 - \tilde{\chi}_1^0$ mass splittings are targeted by SR_{1B}^h.

Table 3: Definition of the signal regions used in the 1ℓ selection (see text for further description).

Requirement / Region	SR_{1A}^h	SR_{1B}^h
Number of signal leptons	1	
$n_{h\text{-cand}}$	≥ 1	
$n_{b\text{-tagged jets}} (p_T > 30 \text{ GeV})$	≥ 4	
$n_{\text{jets}} (p_T > 60 \text{ GeV})$	≥ 4	≥ 6
$m_T [\text{GeV}]$	> 150	> 150
\mathcal{S}	> 12	> 7

5 Background estimation

The dominant SM background contribution to the 3ℓ SRs is expected to originate from $t\bar{t}Z$ production, with minor contributions from multi-boson production (mainly WZ) and backgrounds containing hadrons misidentified as leptons (hereafter referred to as ‘fake’ leptons) or non-prompt leptons from decays of hadrons (mainly in $t\bar{t}$ events). The main background affecting the 1ℓ SRs is expected to originate from $t\bar{t}$ production in association with heavy-flavour quarks.

The background from fake/non-prompt (FNP) leptons is estimated in a data-driven way, while the normalisation of the main backgrounds ($t\bar{t}Z$ and multi-boson in the 3ℓ selection; $t\bar{t}$ in the 1ℓ selection) is obtained by fitting the yield from MC simulation to the observed data in dedicated control regions (CRs) enhanced in a particular background component, and then extrapolating this yield to the SRs. Backgrounds from other sources, which provide a subdominant contribution to the SRs, are determined from MC simulation only.

The expected SM background is determined separately in each SR from a profile likelihood fit [80] implemented in the HistFitter framework [81]. The fit uses as a constraint the observed event yield in the fitted regions to adjust the normalisation of the main backgrounds. The quality of the resulting background model is judged by performing a ‘background-only’ fit to data using exclusively the event yield in the CRs to adjust the normalisation of the backgrounds. The agreement of the resulting background model is compared with the data yields in dedicated validation regions (VRs). Systematic uncertainties related to the MC modelling affect the expected yields in the SRs and CRs, and are taken into account to determine the uncertainty in the background prediction. Each source of uncertainty is described by a single nuisance parameter, and correlations between background processes and selections are taken into account. The VRs, used to assess the quality of the background model, are not used to constrain the nuisance parameters in the fit. The fit does not significantly affect either the uncertainty or the central value of these nuisance parameters. The systematic uncertainties considered in the fit are described in Section 6.

5.1 Fake/non-prompt lepton background

A method similar to that described in Refs. [82, 83] is used for the estimation of the FNP lepton background. Two types of lepton identification criteria are defined for this evaluation: ‘tight’ and ‘loose’, corresponding

to the signal and candidate electrons and muons described in Section 4. With the number of observed events with tight or loose leptons, the method estimates the number of events containing prompt or FNP leptons using as input the probability for loose prompt or FNP leptons to satisfy the tight criteria. The probability for prompt loose leptons to satisfy the tight selection is determined from $t\bar{t}Z$ MC simulation, applying correction factors obtained by comparing $Z \rightarrow \ell^+\ell^-$ ($\ell = e, \mu$) events in data and MC simulation. The equivalent probability for loose FNP leptons to satisfy the tight selection is measured in a data sample enhanced in $t\bar{t}$ using events with one electron and one muon with the same charge plus at least one b -tagged jet.

The estimates for the FNP background are validated in dedicated regions with selection criteria similar to those defining the 3ℓ SRs but with reduced contributions from processes with three prompt leptons. Two VRs are defined as detailed in Table 4, with $\text{VR}_{1\text{F}}^Z$ probing the lepton p_{T} regime in $\text{SR}_{1\text{A}}^Z$ and $\text{SR}_{1\text{B}}^Z$, while $\text{VR}_{2\text{F}}^Z$ includes soft lepton requirements as in $\text{SR}_{2\text{A}}^Z$ and $\text{SR}_{2\text{B}}^Z$. To enhance fakes and be mutually exclusive with the SR, events in these VRs are required to have no SF-OS dilepton pairs and to have at least one different-flavour opposite-sign (DF-OS) dilepton pair. The observed and expected yields in these VRs are shown in Table 5, with a purity of FNP leptons above 55% and with good agreement between data and the background estimates.

The contribution of the FNP background in the 1ℓ selection is negligible.

Table 4: Definition of the validation regions used for the FNP lepton estimation (see text for further description).

Requirement / Region	$\text{VR}_{1\text{F}}^Z$	$\text{VR}_{2\text{F}}^Z$
Number of signal leptons	≥ 3	
Number of SF-OS pairs	0	
Number of DF-OS pairs	≥ 1	
Leading lepton p_{T} [GeV]	> 40	
Subleading lepton p_{T} [GeV]	> 20	
Third leading lepton p_{T} [GeV]	> 20	< 60
$n_{\text{jets}} (p_{\text{T}} > 30 \text{ GeV})$	≥ 3	≥ 3
$n_{b\text{-tagged jets}} (p_{\text{T}} > 30 \text{ GeV})$	≥ 1	–
$E_{\text{T}}^{\text{miss}}$ [GeV]	> 50	> 150

5.2 Estimation of the $t\bar{t}Z$ and multi-boson background in the 3ℓ selection

The two dedicated control regions used for the $t\bar{t}Z$ ($\text{CR}_{t\bar{t}Z}^Z$) and multi-boson (CR_{VV}^Z) background estimation in the 3ℓ selection are defined in Table 6. To ensure mutual exclusion with the SRs, only events with $50 \text{ GeV} < E_{\text{T}}^{\text{miss}} < 100 \text{ GeV}$ are included in $\text{CR}_{t\bar{t}Z}^Z$, while a b -tagged jet veto and a $50 \text{ GeV} < E_{\text{T}}^{\text{miss}} < 200 \text{ GeV}$ requirement are applied in CR_{VV}^Z .

To validate the background estimates and provide a statistically independent cross-check of the extrapolation to the SRs, three validation regions are defined, as shown in Table 6. The $\text{VR}_{t\bar{t}Z}^Z$ region primarily validates

Table 5: Background fit results for the FNP validation regions. The ‘Others’ category is dominated by $t\bar{t}W$ production and also contains the contributions from $t\bar{t}h$, $t\bar{t}WW$, $t\bar{t}t$, $t\bar{t}\bar{t}$, Wh , and Zh production. Combined statistical and systematic uncertainties are given. Some of the uncertainties are correlated and therefore the overall sum in quadrature does not necessarily add to the total systematic uncertainty. The number of $t\bar{t}Z$ and multi-boson background events is estimated as described in Section 5.2.

	VR_{1F}^Z	VR_{2F}^Z
Observed events	84	98
Total (post-fit) SM events	104 ± 28	98 ± 33
Post-fit, multi-boson	0.7 ± 0.2	2.7 ± 0.7
Post-fit, $t\bar{t}Z$	9.1 ± 1.7	2.6 ± 0.6
Fake/non-prompt leptons	54 ± 27	76 ± 33
tZ , tWZ	0.9 ± 0.5	0.40 ± 0.21
Others	39 ± 6	16.2 ± 3.1

the $t\bar{t}Z$ background estimate. The $\text{VR}_{VV}^{Z,\text{n-jet}}$ and $\text{VR}_{VV}^{Z,b\text{-tag}}$ regions validate the multi-boson background estimate, the former focusing on the extrapolation in jet multiplicity and the latter releasing the b -tagged jet veto. The overlap between these multi-boson VRs is around 50%.

Table 7 shows the observed and expected yields in the CRs and VRs for each background source, and Figure 2 shows the jet multiplicity distribution after the background fit for these CRs and VRs. The normalisation factors for the $t\bar{t}Z$ and multi-boson backgrounds do not differ from unity by more than 20% and the post-fit MC-simulated jet multiplicity distributions agree well with the data.

Table 6: Definition of the control and validation regions used for the $t\bar{t}Z$ and multi-boson background estimation.

Requirement / Region	$\text{CR}_{t\bar{t}Z}^Z$	$\text{VR}_{t\bar{t}Z}^Z$	CR_{VV}^Z	$\text{VR}_{VV}^{Z,\text{n-jet}}$	$\text{VR}_{VV}^{Z,b\text{-tag}}$
Number of signal leptons		≥ 3			
Number of SF-OS pairs		≥ 1			
Leading lepton p_T [GeV]		> 40			
$ m_{\ell\ell}^{\text{SF-OS}} - m_Z $ [GeV]		< 15			
Second leading lepton p_T [GeV]	> 20	> 20	> 20	> 40	> 40
Third leading lepton p_T [GeV]	> 20	> 20	> 20	> 40	> 40
$n_{\text{jets}}(p_T > 30 \text{ GeV})$	≥ 4	≥ 3	≥ 3	≥ 3	3
$n_{b\text{-tagged jets}}(p_T > 30 \text{ GeV})$	≥ 1	≥ 1	0	0	≥ 0
E_T^{miss} [GeV]	50–100	100–150	50–200	200–300	200–300

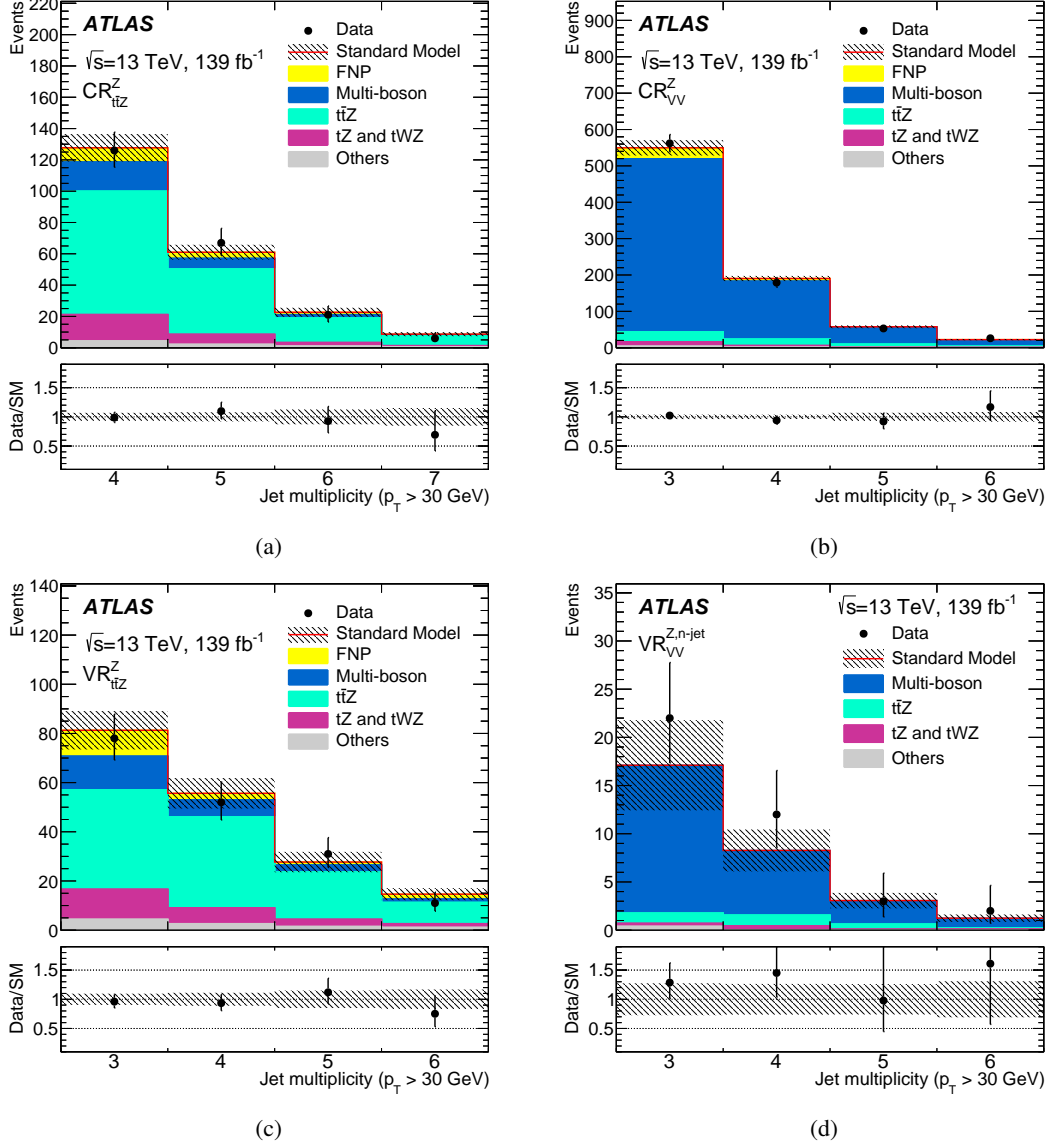


Figure 2: Jet multiplicity distributions in control and validation regions (a) $CR_{t\bar{t}Z}^Z$, (b) CR_{VV}^Z , (c) $VR_{t\bar{t}Z}^Z$ and (d) $VR_{VV}^{Z,n-jet}$ after normalising the $t\bar{t}Z$ and multi-boson background processes via the simultaneous fit described in Section 5. The contributions from all SM backgrounds are shown as a histogram stack; the bands represent the total uncertainty in the background prediction. The ‘Others’ category contains the contributions from $t\bar{t}h$, $t\bar{t}W$, $t\bar{t}WW$, $t\bar{t}t$, $t\bar{t}t\bar{t}$, Wh , and Zh production. The ‘FNP’ category represents the background from fake or non-prompt leptons. The last bin in each figure contains the overflow. The lower panels show the ratio of the observed data to the total SM background prediction, with bands representing the total uncertainty in the background prediction.

Table 7: Background fit results for the control and validation regions for the $t\bar{t}Z$ and multi-boson backgrounds. The pre-fit predictions from MC simulation are given for comparison for those backgrounds ($t\bar{t}Z$, multi-boson) that are normalised to data. The ‘Others’ category contains the contributions from $t\bar{t}h$, $t\bar{t}W$, $t\bar{t}WW$, $t\bar{t}t$, $t\bar{t}t\bar{t}$, Wh , and Zh production. Combined statistical and systematic uncertainties are given. Some of the uncertainties are correlated and therefore the overall sum in quadrature does not necessarily add to the total systematic uncertainty. The number of events with fake/non-prompt leptons is estimated with the data-driven technique described in Section 5.1.

	$CR_{t\bar{t}Z}^Z$	$VR_{t\bar{t}Z}^Z$	CR_{VV}^Z	$VR_{VV}^{Z,n\text{-jet}}$	$VR_{VV}^{Z,b\text{-tag}}$
Observed events	220	172	820	39	34
Total (post-fit) SM events	220 \pm 15	179 \pm 16	820 \pm 29	30 \pm 8	26 \pm 6
Post-fit, multi-boson	28 \pm 7	25 \pm 8	698 \pm 34	26 \pm 8	17 \pm 6
Post-fit, $t\bar{t}Z$	142 \pm 22	105 \pm 20	57 \pm 11	2.8 \pm 0.6	5.4 \pm 1.2
Fake/non-prompt leptons	15.1 \pm 1.7	16.7 \pm 1.9	41 \pm 15	<1.5	0.9 ^{+1.1} _{-0.9}
tZ , tWZ	27 \pm 14	23 \pm 12	19 \pm 10	0.9 \pm 0.5	1.7 \pm 0.9
Others	8.0 \pm 1.4	9.7 \pm 2.1	5.8 \pm 1.3	0.46 \pm 0.09	0.62 \pm 0.12
Pre-fit, multi-boson	35.4 \pm 3.5	31 \pm 7	870 \pm 200	32 \pm 7	22 \pm 5
Pre-fit, $t\bar{t}Z$	154 \pm 14	114 \pm 5	61.7 \pm 3.4	3.1 \pm 0.4	5.8 \pm 0.6

5.3 Estimation of the $t\bar{t}$ background in the 1ℓ selection

The $t\bar{t}$ background represents more than 70% of the total background in the 1ℓ SRs and it is estimated with the aid of a dedicated control region ($\text{CR}_{t\bar{t}}^h$), defined in Table 8. Compared to the SRs in Table 3, this region does not apply any selection on the number of Higgs boson candidates and features relaxed requirements on m_T , while only events with exactly four jets and $7 < \mathcal{S} < 10$ are included in this CR to ensure orthogonality with the SRs. Table 9 shows the observed and expected yields in the CR for each background source, and Figure 3 shows the distribution of the transverse mass and number of Higgs boson candidates after the background fit. The normalisation factor for the $t\bar{t}$ background was found to be 1.09 ± 0.13 .

The extrapolation across \mathcal{S} and m_T between $\text{CR}_{t\bar{t}}^h$ and the SRs is tested in several validation regions. Figure 4 shows the definition, the observed number of events and expected yields in these regions, which feature either the same b -tagged jets multiplicity as the SRs with relaxed m_T requirements, or the same m_T selections as the SRs requiring exactly three b -tagged jets. Good agreement between the background estimation and the data is observed in all these validation regions.

Table 8: Definition of the control region used for the $t\bar{t}$ background estimation.

Requirement / Region	$\text{CR}_{t\bar{t}}^h$
Number of signal leptons	1
$n_{h\text{-cand}}$	-
$n_{b\text{-tagged jets}} (p_T > 30 \text{ GeV})$	≥ 4
$n_{\text{jets}} (p_T > 60 \text{ GeV})$	4
$m_T [\text{GeV}]$	> 100
\mathcal{S}	7–10

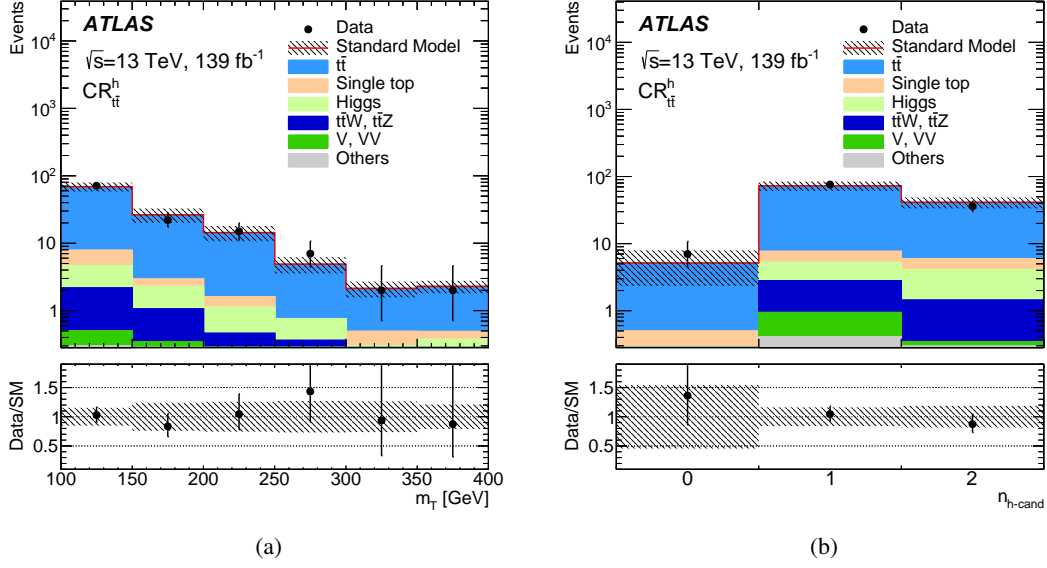


Figure 3: (a) Transverse mass and (b) number of Higgs boson candidates distributions in $CR_{t\bar{t}}^h$ after normalising the $t\bar{t}$ background process via the simultaneous fit described in Section 5. The contributions from all SM backgrounds are shown as a histogram stack; the bands represent the total uncertainty in the background prediction. The ‘Higgs’ category contains the contributions from gluon–gluon fusion, vector-boson fusion, Wh , Zh and $t\bar{t}h$ production. The ‘Others’ category contains the contributions from $t\bar{t}WW$, $t\bar{t}WZ$, $t\bar{t}t$ and $t\bar{t}t\bar{t}$ production. The last bin in each figure contains the overflow. The lower panels show the ratio of the observed data to the total SM background prediction, with bands representing the total uncertainty in the background prediction.

Table 9: Background fit results for the $t\bar{t}$ background control region in the 1ℓ selection. The pre-fit predictions from MC simulation are given for comparison for those backgrounds ($t\bar{t}$) that are normalised to data. The ‘Higgs’ category contains the contributions from gluon–gluon fusion, vector-boson fusion, Wh , Zh and $t\bar{t}h$ production. The ‘Others’ category contains the contributions from $t\bar{t}WW$, $t\bar{t}WZ$, $t\bar{t}t$ and $t\bar{t}t\bar{t}$ production. Combined statistical and systematic uncertainties are given. Some of the uncertainties are correlated and therefore the overall sum in quadrature does not necessarily add to the total systematic uncertainty.

	$CR_{t\bar{t}}^h$
Observed events	119
Total (post-fit) SM events	119 ± 11
Post-fit, $t\bar{t}$	105 ± 11
V, VV	0.6 ± 0.5
$t\bar{t}W, t\bar{t}Z$	3.0 ± 0.7
Higgs	5.1 ± 1.8
Single top	4.6 ± 1.5
Others	0.73 ± 0.16
Pre-fit, $t\bar{t}$	96 ± 6

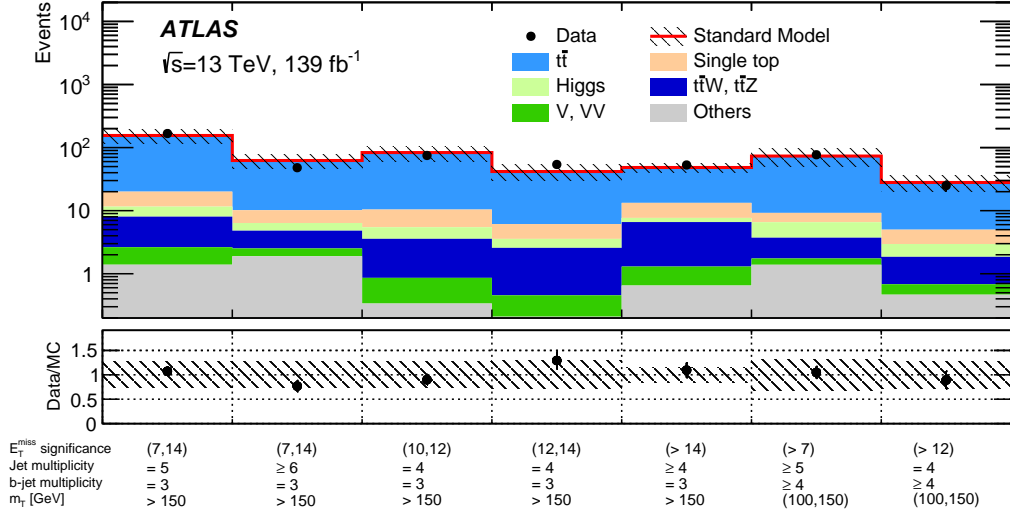


Figure 4: Comparison of the observed and expected event yields in the different kinematic regions used to validate the $t\bar{t}$ background estimation in the 1ℓ selection. The ‘Higgs’ category contains the contributions from gluon–gluon fusion, vector-boson fusion, Wh , Zh and $t\bar{t}h$ production. The ‘Others’ category contains the contributions from $t\bar{t}WW$, $t\bar{t}WZ$, $t\bar{t}t$ and $t\bar{t}t\bar{t}$ production. The lower panel shows the ratio of the observed data to the total SM background prediction, with bands representing the total uncertainty in the background prediction.

6 Systematic uncertainties

The main sources of systematic uncertainty affecting the analysis SRs are related to the theoretical and modelling uncertainties in the background, the limited number of events in the CRs and MC simulated samples, the uncertainties in the FNP probabilities, as well as the jet energy scale and resolution. The effects of the systematic uncertainties are evaluated for all signal samples and background processes. Since the normalisation of the dominant background processes is extracted in dedicated CRs, the systematic uncertainties only affect the extrapolation to the SRs in these cases. Figure 5 summarises the contributions from the different sources of systematic uncertainty to the total SM background predictions in the signal regions.

The jet energy scale and resolution uncertainties are derived as a function of the p_T and η of the jet, as well as of the pile-up conditions and the jet flavour composition (more like a quark or a gluon) of the selected jet sample. They are determined using a combination of data and simulated event samples, through measurements of the jet response asymmetry in dijet, Z +jet and γ +jet events [67, 84].

Systematic uncertainties in the b -tagging efficiency are estimated by varying the η -, p_T - and flavour-dependent scale factors applied to each jet in the simulation within a range that reflects the systematic uncertainty in the measured tagging efficiency and mis-tag rates in data [71–73].

Other detector-related systematic uncertainties, such as those related to the E_T^{miss} modelling, as well as lepton reconstruction efficiency, energy scale and energy resolution are found to have a small impact on the results.

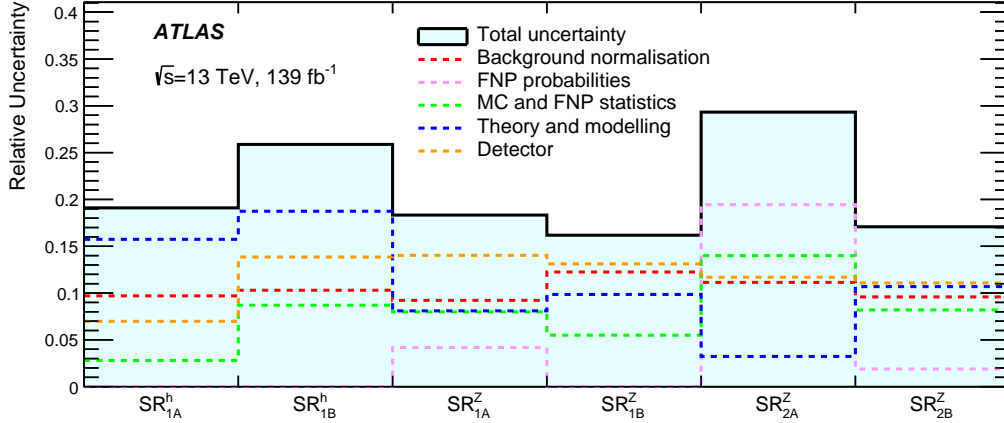


Figure 5: Comparison of the relative uncertainty for the total background yield in each SR, including the contribution from the different sources of uncertainty. The ‘Detector’ category contains all detector-related systematic uncertainties and is dominated by jet energy scale and resolution, and b -tagging uncertainties.

Systematic uncertainties are assigned to the FNP background estimation to account for different compositions (heavy flavour, light flavour or conversions) between the signal and control regions, as well as the contamination from prompt leptons in the regions used to measure the FNP probabilities.

The diboson background MC modelling uncertainties are estimated by varying the renormalisation, factorisation and resummation scales used to generate the samples [30]. For the $t\bar{t}Z$ background, uncertainties due to parton shower and hadronisation modelling are evaluated by comparing the predictions from MG5_AMC@NLO interfaced to PYTHIA and HERWIG 7.0.4 [85], while the uncertainties related to the choice of renormalisation and factorisation scales are assessed by varying the corresponding event generator parameters up and down by a factor of two around their nominal values [31]. For the $t\bar{t}$ background, uncertainties due to parton shower and hadronisation modelling are evaluated by comparing the predictions from POWHEG-BOX interfaced to PYTHIA and HERWIG 7.0.4 [85], while the uncertainties due the choice of generator are evaluated by comparing the predictions from POWHEG-BOX and MG5_AMC@NLO both interfaced to PYTHIA. Variations of the $t\bar{t}$ initial- and final-state radiation, renormalisation and factorisation scales are also considered [86].

The cross-sections used to normalise the MC samples are varied according to the uncertainty in the cross-section calculation, i.e. 6% for diboson, 12% for $t\bar{t}Z$, 13% for $t\bar{t}W$ [34] and 5% for single top production. For $t\bar{t}WW$, tZ , tWZ , $t\bar{t}h$, Wh , Zh , $t\bar{t}t$, $t\bar{t}t\bar{t}$, and triboson production processes, which constitute a small background, a 50% uncertainty in the event yields is assumed.

7 Results

The observed number of events and expected yields are shown in Tables 10 and 11 for each of the inclusive 3ℓ and 1ℓ SRs, respectively. Figures 6 and 7 show kinematic distributions after applying all the SR selection requirements except those on E_T^{miss} , $p_T^{\ell\ell}$ or \mathcal{S} and jet multiplicity. The data agree with the SM background predictions and these results are interpreted as exclusion limits for several beyond-the-SM (BSM) scenarios.

The HistFitter framework, which utilises a profile-likelihood-ratio test statistic [80], is used to estimate 95% confidence intervals using the CL_s prescription [87]. The likelihood is built from the product of probability density functions describing the observed numbers of events in the SR and the associated CRs. The statistical uncertainties in the CRs and SRs are modelled using Poisson distributions. Systematic uncertainties enter the likelihood as nuisance parameters that are constrained by Gaussian distributions whose widths correspond to the sizes of these uncertainties. Table 10 also shows upper limits (at the 95% CL) on the number of BSM events S^{95} , and on the visible BSM cross-section $\sigma_{\text{vis}} = S_{\text{obs}}^{95} / \int \mathcal{L} dt$, defined as the product of the production cross-section, acceptance and efficiency.

Model-dependent limits are also set in specific classes of SUSY models. For each signal hypothesis, the background fit is repeated taking into account the signal contamination in the CRs, which is found to be below 12% for signal models close to the existing exclusion limits [20]. Correlations of the uncertainties between the SM backgrounds and the signals are taken into account.

To enhance the exclusion power in the SUSY models considered, a ‘shape-fit’ approach is used where several mutually exclusive bins in different kinematic variables are defined in order to take advantage of the different signal-to-background ratios in the different bins. Table 12 shows the definition of these bins, which loosen a few of the requirements of the discovery SRs to increase the acceptance for different classes of models across the phase space (Tables 2 and 3). SR_{2A}^Z is used in the exclusion fits with no changes. The observed number of events and expected yields in all these bins are shown in Figures 8 and 9.

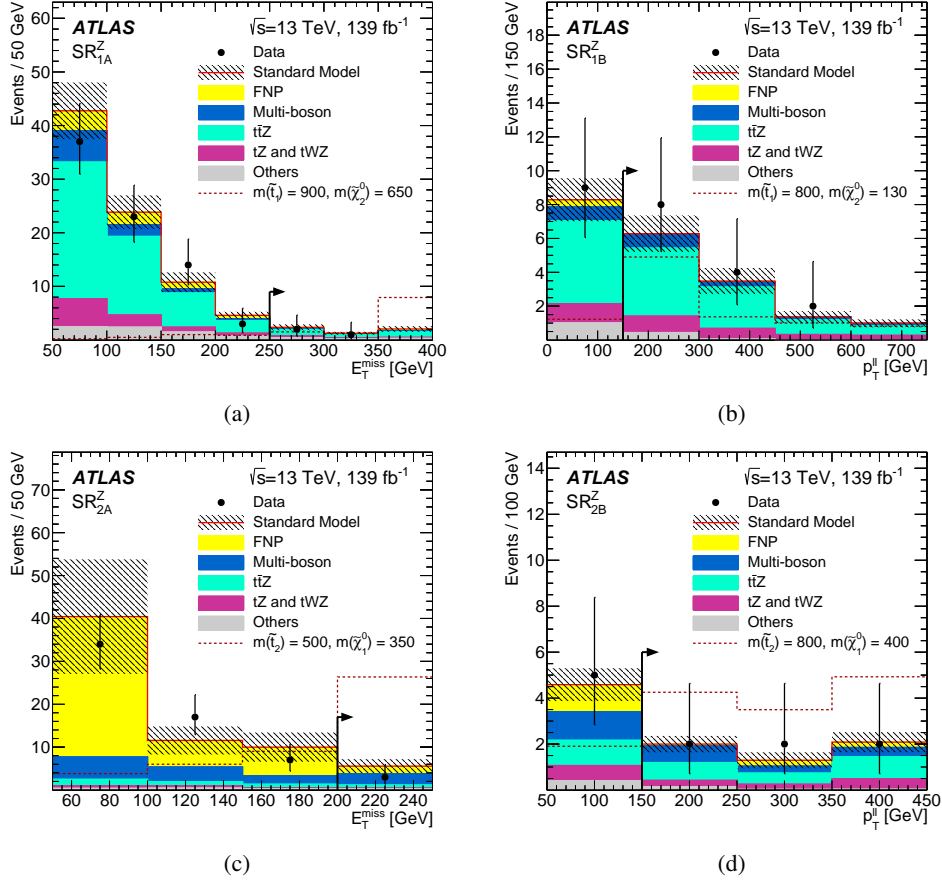


Figure 6: Distributions of (a) E_T^{miss} in SR_{1A}^Z , (b) $p_T^{\ell\ell}$ in SR_{1B}^Z , (c) E_T^{miss} in SR_{2A}^Z , and (d) $p_T^{\ell\ell}$ in SR_{2B}^Z for events passing all the SR requirements except those on the variable being plotted (the requirements are indicated by the arrows). The contributions from all SM backgrounds are shown after the background fit described in Section 5; the hashed bands represent the total uncertainty. The ‘Others’ category contains the contributions from $t\bar{t}h$, $t\bar{t}W$, $t\bar{t}WW$, $t\bar{t}t$, $t\bar{t}t\bar{t}$, Wh , and Zh production. The ‘FNP’ category represents the background from fake or non-prompt leptons. The expected distributions for selected signal models are also shown as dashed lines. The last bin in each figure contains the overflow.

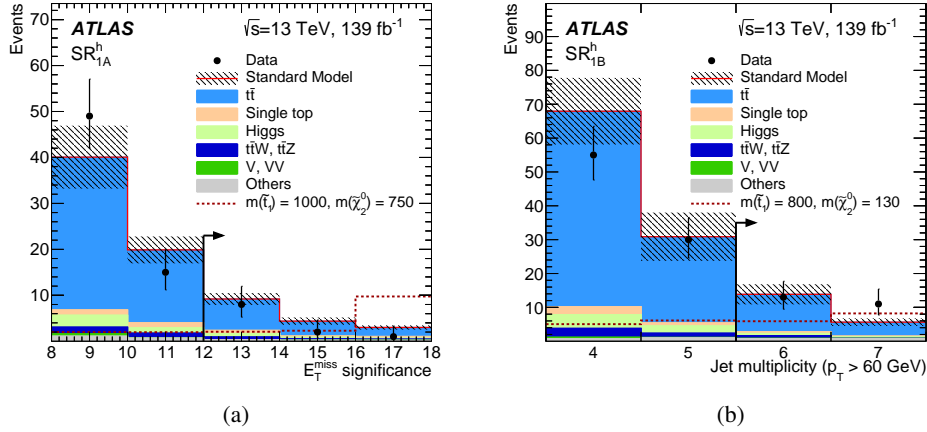


Figure 7: Distributions of (a) E_T^{miss} significance in SR_{1A}^h and (b) jet multiplicity in SR_{1B}^h , for events passing all the SR requirements except those on the variable being plotted (the requirements are indicated by the arrows). The contributions from all SM backgrounds are shown after the background fit described in Section 5; the hashed bands represent the total uncertainty. The ‘Higgs’ category contains the contributions from gluon–gluon fusion, vector-boson fusion, Wh , Zh and $t\bar{t}h$ production. The ‘Others’ category contains the contributions from $t\bar{t}WW$, $t\bar{t}WZ$, $t\bar{t}t$ and $t\bar{t}t\bar{t}$ production. The expected distributions for selected signal models are also shown as dashed lines. The last bin in each figure contains the overflow.

Table 10: Observed and expected numbers of events in the 3ℓ signal regions. The pre-fit predictions from MC simulation are given for comparison for those backgrounds ($t\bar{t}Z$, multi-boson) that are normalised to data in dedicated control regions. The ‘Others’ category is dominated by $t\bar{t}W$ production and also contains the contributions from $t\bar{t}h$, $t\bar{t}WW$, $t\bar{t}t$, $t\bar{t}t\bar{t}$, Wh , and Zh production. Combined statistical and systematic uncertainties are given. The table also includes model-independent 95% CL upper limits on the visible number of BSM events (S_{obs}^{95}), the number of BSM events given the expected number of background events (S_{exp}^{95}) and the visible BSM cross-section (σ_{vis}), as well as the discovery p -value (p_0) for the background-only hypothesis, all calculated from pseudo-experiments. The value of p_0 is capped at 0.5 if the observed number of events is below the expected number of events.

	SR_{1A}^Z	SR_{1B}^Z	SR_{2A}^Z	SR_{2B}^Z
Observed events	3	14	3	6
Total (post-fit) SM events	5.7 ± 1.0	12.1 ± 2.0	5.6 ± 1.6	5.5 ± 0.9
Post-fit, multi-boson	0.49 ± 0.22	1.5 ± 0.5	2.6 ± 1.0	1.4 ± 0.6
Post-fit, $t\bar{t}Z$	2.8 ± 0.9	7.9 ± 1.9	0.70 ± 0.23	2.2 ± 0.7
Fake or non-prompt leptons	0.74 ± 0.24	0.04 ± 0.02	1.8 ± 1.1	0.65 ± 0.12
tZ , tWZ	0.8 ± 0.4	2.2 ± 1.2	0.19 ± 0.10	1.0 ± 0.5
Others	0.84 ± 0.18	0.51 ± 0.11	0.25 ± 0.07	0.19 ± 0.04
Pre-fit, multi-boson	0.61 ± 0.23	1.9 ± 0.5	3.3 ± 0.9	1.8 ± 0.7
Pre-fit, $t\bar{t}Z$	3.0 ± 0.7	8.5 ± 1.6	0.76 ± 0.21	2.4 ± 0.5
S_{obs}^{95}	4.5	11.7	4.9	7.0
S_{exp}^{95}	$6.2^{+2.6}_{-1.6}$	$9.2^{+4.1}_{-1.3}$	$6.1^{+2.6}_{-1.7}$	$6.6^{+2.5}_{-1.8}$
σ_{vis} [fb]	0.03	0.08	0.03	0.05
p_0	0.50	0.31	0.50	0.4

Table 11: Observed and expected numbers of events in the 1ℓ signal regions. The pre-fit predictions from MC simulation are given for comparison for the $t\bar{t}$ background that is normalised to data in a dedicated control region. The ‘Higgs’ category contains the contributions from gluon–gluon fusion, vector-boson fusion, Wh , Zh and $t\bar{t}h$ production. The ‘Others’ category contains the contributions from $t\bar{t}WW$, $t\bar{t}WZ$, $t\bar{t}t$ and $t\bar{t}t\bar{t}$ production. Combined statistical and systematic uncertainties are given. The table also includes model-independent 95% CL upper limits on the visible number of BSM events (S_{obs}^{95}), the number of BSM events given the expected number of background events (S_{exp}^{95}) and the visible BSM cross-section (σ_{vis}), as well as the discovery p -value (p_0) for the background-only hypothesis, all calculated from pseudo-experiments. The value of p_0 is capped at 0.5 if the observed number of events is below the expected number of events.

	SR_{1A}^h	SR_{1B}^h
Observed events	11	24
Total (post-fit) SM events	17 ± 3	19 ± 5
Post-fit, $t\bar{t}$	12 ± 3	15 ± 5
V, VV	0.05 ± 0.05	0.13 ± 0.08
$t\bar{t}W, t\bar{t}Z$	1.16 ± 0.26	0.95 ± 0.25
Higgs	1.19 ± 0.21	0.9 ± 0.4
Single top	1.38 ± 0.23	0.74 ± 0.22
Others	0.68 ± 0.13	1.53 ± 0.32
Pre-fit, $t\bar{t}$	11.0 ± 2.4	14 ± 4
S_{obs}^{95}	7.0	18.1
S_{exp}^{95}	$10.3^{+4.4}_{-3.2}$	$14.2^{+6.0}_{-3.8}$
σ_{vis} [fb]	0.05	0.13
p_0	0.50	0.25

Table 12: Selection criteria used in the shape-fit to derive the model-dependent exclusion limits. The additional SR labelled as SR_{1AB}^h overlaps with both SR_{1A}^h and SR_{1B}^h defined in Table 3.

SR_{1A}^Z	E_T^{miss} [GeV]	200–250, 250–300, 300–350, >350
SR_{1B}^Z	$p_T^{\ell\ell}$ [GeV]	150–300, 300–450, 450–600, >600
SR_{2B}^Z	E_T^{miss} [GeV]	300–350, >350
	$p_T^{\ell\ell}$ [GeV]	50–150, >150
SR_{1A}^h	$n_{h\text{-cand}}$	1, ≥ 2
	$n_{\text{jets}} (p_T > 60 \text{ GeV})$	4
	S	10–12, 12–14
SR_{1B}^h	$n_{h\text{-cand}}$	1, ≥ 2
	$n_{\text{jets}} (p_T > 60 \text{ GeV})$	5, ≥ 6
	S	7–14
SR_{1AB}^h	$n_{h\text{-cand}}$	≥ 1
	$n_{\text{jets}} (p_T > 60 \text{ GeV})$	≥ 4
	S	≥ 14

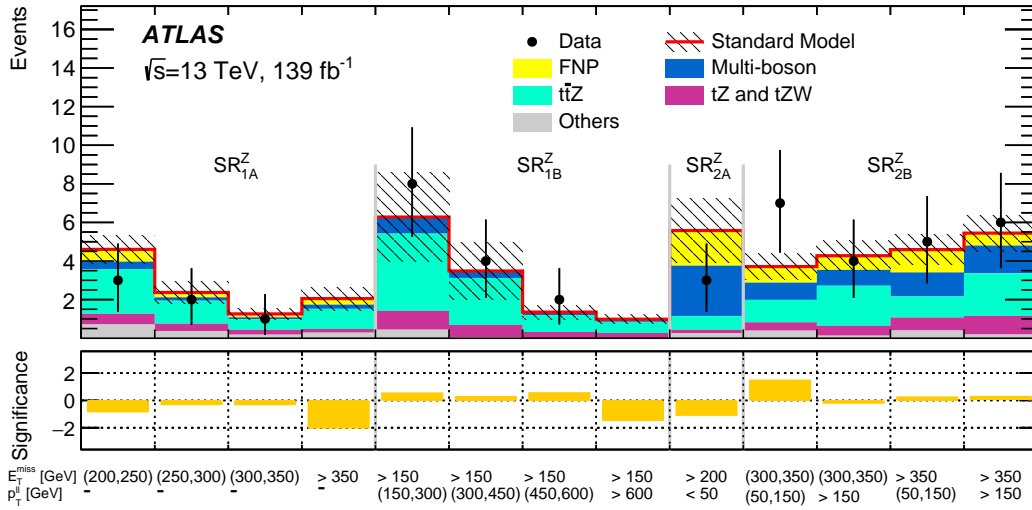


Figure 8: Comparison of the observed and expected event yields in all the 3ℓ SRs and bins used for the model-dependent exclusion limits. The ‘Others’ category contains the contributions from $t\bar{t}h$, $t\bar{t}W$, $t\bar{t}WW$, $t\bar{t}t$, $t\bar{t}t\bar{t}$, Wh , and Zh production. The ‘FNP’ category represents the background from fake or non-prompt leptons. The lower panel shows the significance in each SR bin, computed as described in Ref. [88].

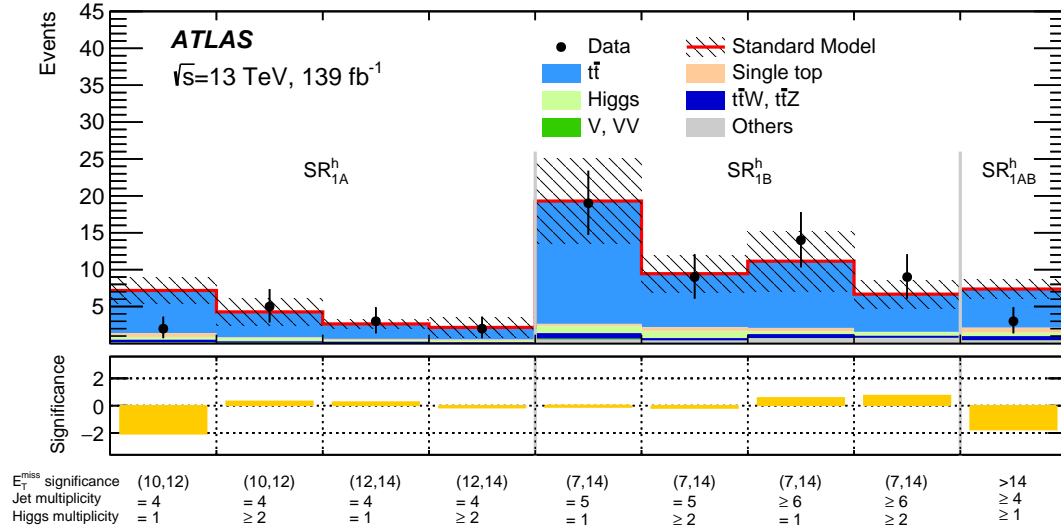


Figure 9: Comparison of the observed and expected event yields in all the 1ℓ SRs and bins used for the model-dependent exclusion limits. The ‘Higgs’ category contains the contributions from gluon–gluon fusion, vector-boson fusion, Wh , Zh and $t\bar{t}h$ production. The ‘Others’ category contains the contributions from $t\bar{t}WW$, $t\bar{t}WZ$, $t\bar{t}t$ and $t\bar{t}t\bar{t}$ production. The lower panel shows the significance in each SR bin, computed as described in Ref. [88].

Figure 10 shows the exclusion limits in the $\tilde{t}_1 \rightarrow t\tilde{\chi}_2^0$ with $\tilde{\chi}_2^0 \rightarrow h/Z\tilde{\chi}_1^0$ simplified model with 50% branching ratios to each $\tilde{\chi}_2^0$ decay mode. These results are obtained from the statistical combination of the shape-fit bins of SR_{1A}^Z , SR_{1B}^Z , SR_{1A}^h , SR_{1B}^h and SR_{1AB}^h shown in Table 12. The bins of SR_{1A}^h , SR_{1B}^h and SR_{1AB}^h are separately combined with the bins of SR_{1A}^Z and SR_{1B}^Z . For each combination of sparticle masses, only the option among those two with best expected sensitivity is considered for the final limit setting. The change in best expected combination is responsible for the kink at \tilde{t}_1 masses of about 900–1000 GeV and $\tilde{\chi}_2^0$ masses below 200 GeV. For $\tilde{\chi}_2^0$ masses above 225 GeV, \tilde{t}_1 masses up to about 1100 GeV are excluded at 95% CL, while \tilde{t}_1 masses below 1220 GeV are excluded for a $\tilde{\chi}_2^0$ mass of 925 GeV. These results improve upon the existing limits on the \tilde{t}_1 mass in this model by approximately 300 GeV [20].

The same statistical combination strategy is also used to obtain exclusion limits in the $\tilde{t}_1 \rightarrow t\tilde{\chi}_2^0$ with $\tilde{\chi}_2^0 \rightarrow h/Z\tilde{\chi}_1^0$ simplified model for different $\tilde{\chi}_2^0 \rightarrow h/Z\tilde{\chi}_1^0$ decay branching ratios, shown in Figure 11. For $\tilde{\chi}_2^0$ masses above 300 GeV, the exclusion limits on \tilde{t}_1 masses vary by at most 40 GeV depending on the $\tilde{\chi}_2^0 \rightarrow h/Z\tilde{\chi}_1^0$ branching ratios. However, for $\tilde{\chi}_2^0$ masses below 200 GeV the exclusion limits on \tilde{t}_1 masses are up to 300 GeV better for models featuring only $\tilde{\chi}_2^0 \rightarrow Z\tilde{\chi}_1^0$ decays compared with models only considering the $\tilde{\chi}_2^0 \rightarrow h\tilde{\chi}_1^0$ decays.

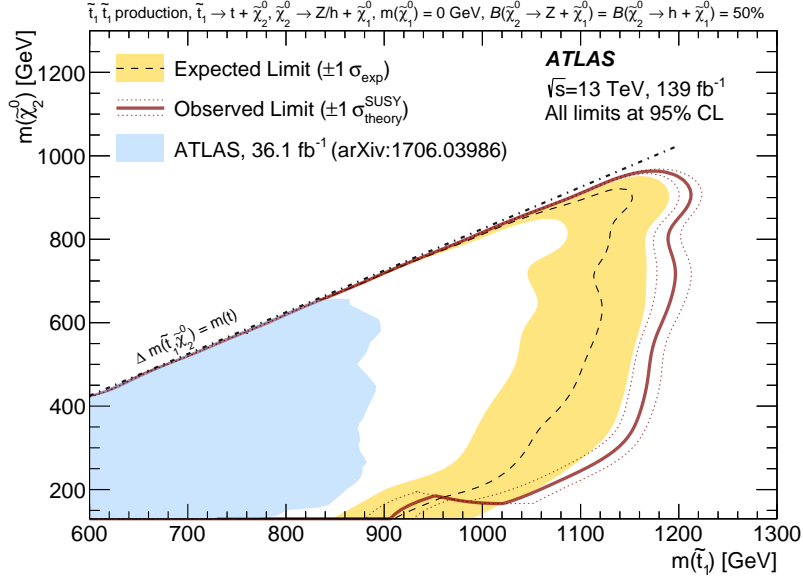


Figure 10: Exclusion limits at 95% CL on the masses of the \tilde{t}_1 and $\tilde{\chi}_2^0$, for a fixed $m(\tilde{\chi}_1^0) = 0$ GeV, assuming $\mathcal{B}(\tilde{\chi}_2^0 \rightarrow Z\tilde{\chi}_1^0) = 0.5$ and $\mathcal{B}(\tilde{\chi}_2^0 \rightarrow h\tilde{\chi}_1^0) = 0.5$. The dashed line and the shaded band are the expected limit and its $\pm 1\sigma$ uncertainty, respectively. The thick solid line is the observed limit for the central value of the signal cross-section. The expected and observed limits do not include the effect of the theoretical uncertainties in the signal cross-section. The dotted lines show the effect on the observed limit of varying the signal cross-section by $\pm 1\sigma$ of the theoretical uncertainty. Results are compared with the observed limits obtained by the previous ATLAS search in Ref. [20].

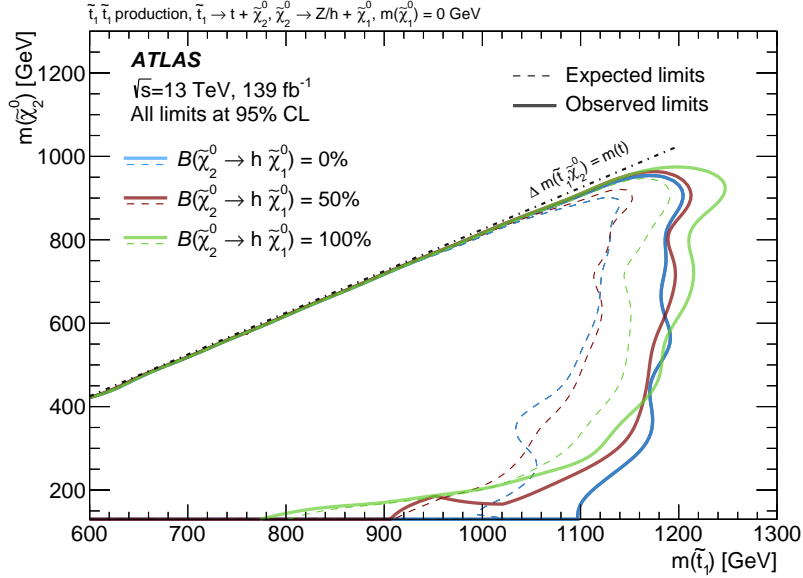


Figure 11: Exclusion limits at 95% CL on the masses of the \tilde{t}_1 and $\tilde{\chi}_2^0$, for a fixed $m(\tilde{\chi}_1^0) = 0$ GeV and different values of $\mathcal{B}(\tilde{\chi}_2^0 \rightarrow h\tilde{\chi}_1^0)$ with $\mathcal{B}(\tilde{\chi}_2^0 \rightarrow Z\tilde{\chi}_1^0) = 1 - \mathcal{B}(\tilde{\chi}_2^0 \rightarrow h\tilde{\chi}_1^0)$. The dashed and solid lines are the expected and observed limits for the central value of the signal cross-section, respectively. The expected and observed limits do not include the effect of the theoretical uncertainties in the signal cross-section.

Figure 12 shows the exclusion limits in the $\tilde{t}_2 \rightarrow Z\tilde{t}_1$ with $\tilde{t}_1 \rightarrow bff'\tilde{\chi}_1^0$ simplified model for a mass difference between the \tilde{t}_1 and $\tilde{\chi}_1^0$ of 40 GeV. Several options for the \tilde{t}_1 and $\tilde{\chi}_1^0$ mass difference are also considered and the sensitivity is found to appreciably decrease only for values below 20 GeV. These results are obtained from the statistical combination of SR_{2A}^Z and the shape-fit bins of SR_{2B}^Z shown in Table 12. The shape of the contour is driven by SR_{2A}^Z and SR_{2B}^Z being most sensitive to small and large mass splittings between the \tilde{t}_2 and the $\tilde{\chi}_1^0$ respectively. Masses of the \tilde{t}_2 up to 875 GeV are excluded at 95% CL for a $\tilde{\chi}_1^0$ mass of about 350 GeV and $\tilde{\chi}_1^0$ masses of approximately 520 (450) GeV are excluded for \tilde{t}_2 masses of 650 (800) GeV, extending beyond the previous limits on the $\tilde{\chi}_1^0$ mass from Ref. [89] by up to 160 GeV.

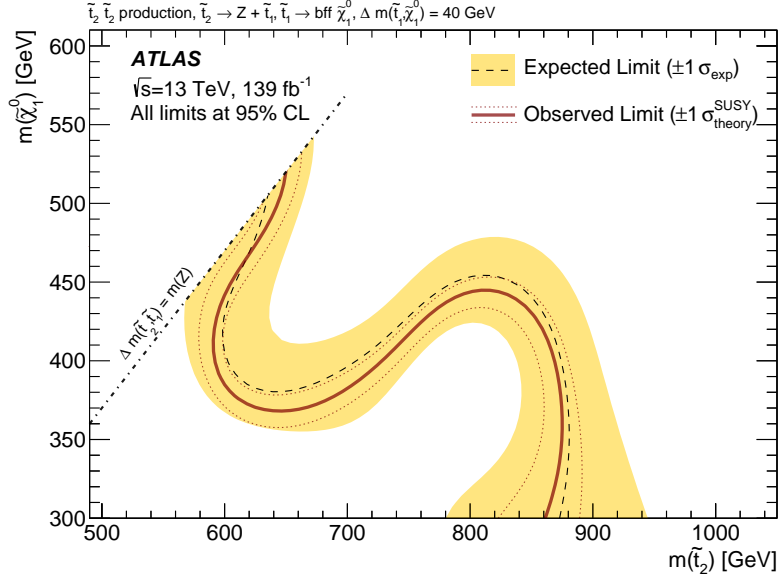


Figure 12: Exclusion limits at 95% CL on the masses of the \tilde{t}_2 and $\tilde{\chi}_1^0$, for a fixed $m(\tilde{t}_1) - m(\tilde{\chi}_1^0) = 40$ GeV and assuming $\mathcal{B}(\tilde{t}_2 \rightarrow Z\tilde{t}_1) = 1$. The dashed line and the shaded band are the expected limit and its $\pm 1\sigma$ uncertainty, respectively. The thick solid line is the observed limit for the central value of the signal cross-section. The expected and observed limits do not include the effect of the theoretical uncertainties in the signal cross-section. The dotted lines show the effect on the observed limit of varying the signal cross-section by $\pm 1\sigma$ of the theoretical uncertainty.

8 Conclusion

A search for direct top squark pair production in events with a leptonically decaying Z boson or a SM Higgs boson decaying into a b -quark pair is presented. The analysis uses 139 fb^{-1} of proton–proton collision data at $\sqrt{s} = 13$ TeV recorded by the ATLAS detector at the LHC. No excess over the SM background predictions is observed, and exclusion limits are presented for a selection of simplified models. The limits exclude, at 95% confidence level, \tilde{t}_1 masses up to 1220 GeV in models featuring \tilde{t}_1 production and $\tilde{t}_1 \rightarrow t\tilde{\chi}_2^0$ with $\tilde{\chi}_2^0 \rightarrow Z/h\tilde{\chi}_1^0$ decays, and \tilde{t}_2 masses up to 875 GeV in models featuring \tilde{t}_2 production and $\tilde{t}_2 \rightarrow Z\tilde{t}_1$ with $\tilde{t}_1 \rightarrow bff'\tilde{\chi}_1^0$ decays. Compared with previous limits, these results extend the mass parameter space exclusion by up to 300 GeV in \tilde{t}_1 mass and by up to 160 GeV in $\tilde{\chi}_1^0$ mass in the considered \tilde{t}_2 model.

Acknowledgements

We thank CERN for the very successful operation of the LHC, as well as the support staff from our institutions without whom ATLAS could not be operated efficiently.

We acknowledge the support of ANPCyT, Argentina; YerPhI, Armenia; ARC, Australia; BMFWF and FWF, Austria; ANAS, Azerbaijan; SSTC, Belarus; CNPq and FAPESP, Brazil; NSERC, NRC and CFI, Canada; CERN; CONICYT, Chile; CAS, MOST and NSFC, China; COLCIENCIAS, Colombia; MSMT CR, MPO CR and VSC CR, Czech Republic; DNRF and DNSRC, Denmark; IN2P3-CNRS and CEA-DRF/IRFU, France; SRNSFG, Georgia; BMBF, HGF and MPG, Germany; GSRT, Greece; RGC and Hong Kong SAR, China; ISF and Benozio Center, Israel; INFN, Italy; MEXT and JSPS, Japan; CNRST, Morocco; NWO, Netherlands; RCN, Norway; MNiSW and NCN, Poland; FCT, Portugal; MNE/IFA, Romania; MES of Russia and NRC KI, Russia Federation; JINR; MESTD, Serbia; MSSR, Slovakia; ARRS and MIZŠ, Slovenia; DST/NRF, South Africa; MINECO, Spain; SRC and Wallenberg Foundation, Sweden; SERI, SNSF and Cantons of Bern and Geneva, Switzerland; MOST, Taiwan; TAEK, Turkey; STFC, United Kingdom; DOE and NSF, United States of America. In addition, individual groups and members have received support from BCKDF, CANARIE, Compute Canada and CRC, Canada; ERC, ERDF, Horizon 2020, Marie Skłodowska-Curie Actions and COST, European Union; Investissements d’Avenir Labex, Investissements d’Avenir Idex and ANR, France; DFG and AvH Foundation, Germany; Herakleitos, Thales and Aristeia programmes co-financed by EU-ESF and the Greek NSRF, Greece; BSF-NSF and GIF, Israel; CERCA Programme Generalitat de Catalunya and PROMETEO Programme Generalitat Valenciana, Spain; Göran Gustafssons Stiftelse, Sweden; The Royal Society and Leverhulme Trust, United Kingdom.

The crucial computing support from all WLCG partners is acknowledged gratefully, in particular from CERN, the ATLAS Tier-1 facilities at TRIUMF (Canada), NDGF (Denmark, Norway, Sweden), CC-IN2P3 (France), KIT/GridKA (Germany), INFN-CNAF (Italy), NL-T1 (Netherlands), PIC (Spain), ASGC (Taiwan), RAL (UK) and BNL (USA), the Tier-2 facilities worldwide and large non-WLCG resource providers. Major contributors of computing resources are listed in Ref. [90].

References

- [1] Y. Golfand and E. Likhtman, *Extension of the Algebra of Poincare Group Generators and Violation of P Invariance*, JETP Lett. **13** (1971) 323, [Pisma Zh. Eksp. Teor. Fiz. **13** (1971) 452].
- [2] D. Volkov and V. Akulov, *Is the neutrino a goldstone particle?*, Phys. Lett. B **46** (1973) 109.
- [3] J. Wess and B. Zumino, *Supergauge transformations in four dimensions*, Nucl. Phys. B **70** (1974) 39.
- [4] J. Wess and B. Zumino, *Supergauge invariant extension of quantum electrodynamics*, Nucl. Phys. B **78** (1974) 1.
- [5] S. Ferrara and B. Zumino, *Supergauge invariant Yang-Mills theories*, Nucl. Phys. B **79** (1974) 413.
- [6] A. Salam and J. Strathdee, *Super-symmetry and non-Abelian gauges*, Phys. Lett. B **51** (1974) 353.
- [7] G. R. Farrar and P. Fayet, *Phenomenology of the production, decay, and detection of new hadronic states associated with supersymmetry*, Phys. Lett. B **76** (1978) 575.
- [8] N. Sakai, *Naturalnes in supersymmetric GUTS*, Z. Phys. C **11** (1981) 153.
- [9] S. Dimopoulos, S. Raby and F. Wilczek, *Supersymmetry and the scale of unification*, Phys. Rev. D **24** (1981) 1681.
- [10] L. E. Ibáñez and G. G. Ross, *Low-energy predictions in supersymmetric grand unified theories*, Phys. Lett. B **105** (1981) 439.
- [11] S. Dimopoulos and H. Georgi, *Softly broken supersymmetry and SU(5)*, Nucl. Phys. B **193** (1981) 150.
- [12] R. Barbieri and G. Giudice, *Upper bounds on supersymmetric particle masses*, Nucl. Phys. B **306** (1988) 63.
- [13] B. de Carlos and J. Casas, *One-loop analysis of the electroweak breaking in supersymmetric models and the fine-tuning problem*, Phys. Lett. B **309** (1993) 320, arXiv: hep-ph/9303291.
- [14] K. Inoue, A. Kakuto, H. Komatsu and S. Takeshita, *Aspects of Grand Unified Models with Softly Broken Supersymmetry*, Prog. Theor. Phys. **68** (1982) 927, Erratum: Prog. Theor. Phys. **70** (1983) 330.
- [15] J. R. Ellis and S. Rudaz, *Search for supersymmetry in toponium decays*, Phys. Lett. B **128** (1983) 248.
- [16] J. Alwall, M.-P. Le, M. Lisanti and J. G. Wacker, *Searching for directly decaying gluinos at the Tevatron*, Phys. Lett. B **666** (2008) 34, arXiv: 0803.0019 [hep-ph].
- [17] J. Alwall, P. Schuster and N. Toro, *Simplified models for a first characterization of new physics at the LHC*, Phys. Rev. D **79** (2009) 075020, arXiv: 0810.3921 [hep-ph].
- [18] D. Alves et al., *Simplified models for LHC new physics searches*, J. Phys. G **39** (2012) 105005, arXiv: 1105.2838 [hep-ph].
- [19] ATLAS Collaboration, *The ATLAS Experiment at the CERN Large Hadron Collider*, JINST **3** (2008) S08003.
- [20] ATLAS Collaboration, *Search for direct top squark pair production in events with a Higgs or Z boson, and missing transverse momentum in $\sqrt{s} = 13$ TeV pp collisions with the ATLAS detector*, JHEP **08** (2017) 006, arXiv: 1706.03986 [hep-ex].
- [21] ATLAS Collaboration, *Search for direct top squark pair production in events with a Z boson, b-jets and missing transverse momentum in $\sqrt{s} = 8$ TeV pp collisions with the ATLAS detector*, Eur. Phys. J. C **74** (2014) 2883, arXiv: 1403.5222 [hep-ex].
- [22] CMS Collaboration, *Search for top-squark pairs decaying into Higgs or Z bosons in pp collisions at $\sqrt{s} = 8$ TeV*, Phys. Lett. B **736** (2014) 371, arXiv: 1405.3886 [hep-ex].

- [23] CMS Collaboration, *Search for top-squark pairs decaying into Higgs or Z bosons in pp collisions at $\sqrt{s}=8$ TeV*, *Phys. Lett. B* **736** (2014) 371, arXiv: [1405.3886 \[hep-ex\]](#).
- [24] B. Abbott et al., *Production and integration of the ATLAS Insertable B-Layer*, *JINST* **13** (2018) T05008, arXiv: [1803.00844 \[physics.ins-det\]](#).
- [25] ATLAS Collaboration, *Performance of the ATLAS trigger system in 2015*, *Eur. Phys. J. C* **77** (2017) 317, arXiv: [1611.09661 \[hep-ex\]](#).
- [26] ATLAS Collaboration, *Luminosity determination in pp collisions at $\sqrt{s} = 8$ TeV using the ATLAS detector at the LHC*, *Eur. Phys. J. C* **76** (2016) 653, arXiv: [1608.03953 \[hep-ex\]](#).
- [27] G. Avoni et al., *The new LUCID-2 detector for luminosity measurement and monitoring in ATLAS*, *JINST* **13** (2018) P07017.
- [28] ATLAS Collaboration, *Simulation of top-quark production for the ATLAS experiment at $\sqrt{s} = 13$ TeV*, ATL-PHYS-PUB-2016-004, 2016, URL: <https://cds.cern.ch/record/2120417>.
- [29] ATLAS Collaboration, *Monte Carlo Generators for the Production of a W or Z/ γ^* Boson in Association with Jets at ATLAS in Run 2*, ATL-PHYS-PUB-2016-003, 2016, URL: <https://cds.cern.ch/record/2120133>.
- [30] ATLAS Collaboration, *Multi-boson simulation for 13 TeV ATLAS analyses*, ATL-PHYS-PUB-2016-002, 2016, URL: <https://cds.cern.ch/record/2119986>.
- [31] ATLAS Collaboration, *Modelling of the $t\bar{t}H$ and $t\bar{t}V$ ($V = W, Z$) processes for $\sqrt{s} = 13$ TeV ATLAS analyses*, ATL-PHYS-PUB-2016-005, 2016, URL: <https://cds.cern.ch/record/2120826>.
- [32] T. Gleisberg et al., *Event generation with SHERPA 1.1*, *JHEP* **02** (2009) 007, arXiv: [0811.4622 \[hep-ph\]](#).
- [33] D. J. Lange, *The EvtGen particle decay simulation package*, *Nucl. Instrum. Meth. A* **462** (2001) 152.
- [34] J. Alwall et al., *The automated computation of tree-level and next-to-leading order differential cross sections, and their matching to parton shower simulations*, *JHEP* **07** (2014) 079, arXiv: [1405.0301 \[hep-ph\]](#).
- [35] T. Sjöstrand et al., *An introduction to PYTHIA 8.2*, *Comput. Phys. Commun.* **191** (2015) 159, arXiv: [1410.3012 \[hep-ph\]](#).
- [36] W. Beenakker, C. Borschensky, M. Krämer, A. Kulesza and E. Laenen, *NNLL-fast: predictions for coloured supersymmetric particle production at the LHC with threshold and Coulomb resummation*, *JHEP* **12** (2016) 133, arXiv: [1607.07741 \[hep-ph\]](#).
- [37] W. Beenakker, M. Kramer, T. Plehn, M. Spira and P. Zerwas, *Stop production at hadron colliders*, *Nucl. Phys. B* **515** (1998) 3, arXiv: [hep-ph/9710451 \[hep-ph\]](#).
- [38] W. Beenakker, S. Brensing, M. Kramer, A. Kulesza, E. Laenen et al., *Supersymmetric top and bottom squark production at hadron colliders*, *JHEP* **08** (2010) 098, arXiv: [1006.4771 \[hep-ph\]](#).
- [39] W. Beenakker et al., *NNLL resummation for stop pair-production at the LHC*, *JHEP* **05** (2016) 153, arXiv: [1601.02954 \[hep-ph\]](#).
- [40] R. D. Ball et al., *Parton distributions with LHC data*, *Nucl. Phys. B* **867** (2013) 244, arXiv: [1207.1303 \[hep-ph\]](#).
- [41] ATLAS Collaboration, *ATLAS Pythia 8 tunes to 7 TeV data*, ATL-PHYS-PUB-2014-021, 2014, URL: <https://cds.cern.ch/record/1966419>.

- [42] R. D. Ball et al., *Parton distributions for the LHC Run II*, *JHEP* **04** (2015) 040, arXiv: [1410.8849 \[hep-ph\]](#).
- [43] S. Frixione, P. Nason and C. Oleari, *Matching NLO QCD computations with Parton Shower simulations: the POWHEG method*, *JHEP* **11** (2007) 070, arXiv: [0709.2092 \[hep-ph\]](#).
- [44] M. Czakon, P. Fiedler and A. Mitov, *Total Top-Quark Pair-Production Cross Section at Hadron Colliders Through $O(\alpha_s^4)$* , *Phys. Rev. Lett.* **110** (2013) 252004, arXiv: [1303.6254 \[hep-ph\]](#).
- [45] M. Czakon and A. Mitov, *NNLO corrections to top pair production at hadron colliders: the quark-gluon reaction*, *JHEP* **01** (2013) 080, arXiv: [1210.6832 \[hep-ph\]](#).
- [46] M. Czakon and A. Mitov, *NNLO corrections to top-pair production at hadron colliders: the all-fermionic scattering channels*, *JHEP* **12** (2012) 054, arXiv: [1207.0236 \[hep-ph\]](#).
- [47] P. Bärnreuther, M. Czakon and A. Mitov, *Percent Level Precision Physics at the Tevatron: First Genuine NNLO QCD Corrections to $q\bar{q} \rightarrow t\bar{t} + X$* , *Phys. Rev. Lett.* **109** (2012) 132001, arXiv: [1204.5201 \[hep-ph\]](#).
- [48] M. Cacciari, M. Czakon, M. Mangano, A. Mitov and P. Nason, *Top-pair production at hadron colliders with next-to-next-to-leading logarithmic soft-gluon resummation*, *Phys. Lett. B* **710** (2012) 612, arXiv: [1111.5869 \[hep-ph\]](#).
- [49] M. Czakon and A. Mitov, *Top++: A program for the calculation of the top-pair cross-section at hadron colliders*, *Comput. Phys. Commun.* **185** (2014) 2930, arXiv: [1112.5675 \[hep-ph\]](#).
- [50] LHC Higgs Cross Section Working Group, *Handbook of LHC Higgs Cross Sections: 2. Differential Distributions*, (2012), arXiv: [1201.3084 \[hep-ph\]](#).
- [51] N. Kidonakis, *Next-to-next-to-leading-order collinear and soft gluon corrections for t-channel single top quark production*, *Phys. Rev. D* **83** (2011) 091503, arXiv: [1103.2792 \[hep-ph\]](#).
- [52] N. Kidonakis, *Two-loop soft anomalous dimensions for single top quark associated production with a W- or H-*, *Phys. Rev. D* **82** (2010) 054018, arXiv: [1005.4451 \[hep-ph\]](#).
- [53] N. Kidonakis, *NNLL resummation for s-channel single top quark production*, *Phys. Rev. D* **81** (2010) 054028, arXiv: [1001.5034 \[hep-ph\]](#).
- [54] T. Sjöstrand, S. Mrenna and P. Z. Skands, *A brief introduction to PYTHIA 8.1*, *Comput. Phys. Commun.* **178** (2008) 852, arXiv: [0710.3820 \[hep-ph\]](#).
- [55] P. Artoisenet, R. Frederix, O. Mattelaer and R. Rietkerk, *Automatic spin-entangled decays of heavy resonances in Monte Carlo simulations*, *JHEP* **03** (2013) 015, arXiv: [1212.3460 \[hep-ph\]](#).
- [56] L. Lönnblad and S. Prestel, *Matching tree-level matrix elements with interleaved showers*, *JHEP* **03** (2012) 019, arXiv: [1109.4829 \[hep-ph\]](#).
- [57] J. Butterworth et al., *PDF4LHC recommendations for LHC Run II*, *J. Phys. G* **43** (2016) 023001, arXiv: [1510.03865 \[hep-ph\]](#).
- [58] ATLAS Collaboration, *The Pythia 8 A3 tune description of ATLAS minimum bias and inelastic measurements incorporating the Donnachie–Landshoff diffractive model*, ATL-PHYS-PUB-2016-017, 2016, URL: <https://cds.cern.ch/record/2206965>.
- [59] A. D. Martin, W. J. Stirling, R. S. Thorne and G. Watt, *Parton distributions for the LHC*, *Eur. Phys. J. C* **63** (2009) 189, arXiv: [0901.0002 \[hep-ph\]](#).
- [60] ATLAS Collaboration, *The ATLAS Simulation Infrastructure*, *Eur. Phys. J. C* **70** (2010) 823, arXiv: [1005.4568 \[physics.ins-det\]](#).

- [61] S. Agostinelli et al., *GEANT4 – a simulation toolkit*, *Nucl. Instrum. Meth. A* **506** (2003) 250.
- [62] ATLAS Collaboration, *Vertex Reconstruction Performance of the ATLAS Detector at $\sqrt{s} = 13$ TeV*, ATL-PHYS-PUB-2015-026, 2015, URL: <https://cds.cern.ch/record/2037717>.
- [63] ATLAS Collaboration, *Electron reconstruction and identification in the ATLAS experiment using the 2015 and 2016 LHC proton–proton collision data at $\sqrt{s} = 13$ TeV*, *Eur. Phys. J. C* **79** (2019) 639, arXiv: [1902.04655](https://arxiv.org/abs/1902.04655) [[hep-ex](#)].
- [64] ATLAS Collaboration, *Muon reconstruction performance of the ATLAS detector in proton–proton collision data at $\sqrt{s} = 13$ TeV*, *Eur. Phys. J. C* **76** (2016) 292, arXiv: [1603.05598](https://arxiv.org/abs/1603.05598) [[hep-ex](#)].
- [65] ATLAS Collaboration, *Properties of jets and inputs to jet reconstruction and calibration with the ATLAS detector using proton–proton collisions at $\sqrt{s} = 13$ TeV*, ATL-PHYS-PUB-2015-036, 2015, URL: <https://cds.cern.ch/record/2044564>.
- [66] M. Cacciari, G. P. Salam and G. Soyez, *The anti- k_r jet clustering algorithm*, *JHEP* **04** (2008) 063, arXiv: [0802.1189](https://arxiv.org/abs/0802.1189) [[hep-ph](#)].
- [67] ATLAS Collaboration, *Jet energy scale measurements and their systematic uncertainties in proton–proton collisions at $\sqrt{s} = 13$ TeV with the ATLAS detector*, *Phys. Rev. D* **96** (2017) 072002, arXiv: [1703.09665](https://arxiv.org/abs/1703.09665) [[hep-ex](#)].
- [68] ATLAS Collaboration, *Performance of pile-up mitigation techniques for jets in pp collisions at $\sqrt{s} = 8$ TeV using the ATLAS detector*, *Eur. Phys. J. C* **76** (2016) 581, arXiv: [1510.03823](https://arxiv.org/abs/1510.03823) [[hep-ex](#)].
- [69] ATLAS Collaboration, *Selection of jets produced in 13 TeV proton–proton collisions with the ATLAS detector*, ATL-CONF-2015-029, 2015, URL: <https://cds.cern.ch/record/2037702>.
- [70] ATLAS Collaboration, *Optimisation and performance studies of the ATLAS b -tagging algorithms for the 2017-18 LHC run*, ATL-PHYS-PUB-2017-013, 2017, URL: <https://cds.cern.ch/record/2273281>.
- [71] ATLAS Collaboration, *ATLAS b -jet identification performance and efficiency measurement with $t\bar{t}$ events in pp collisions at $\sqrt{s} = 13$ TeV*, *Eur. Phys. J. C* **79** (2019) 970, arXiv: [1907.05120](https://arxiv.org/abs/1907.05120) [[hep-ex](#)].
- [72] ATLAS Collaboration, *Measurement of b -tagging efficiency of c -jets in $t\bar{t}$ events using a likelihood approach with the ATLAS detector*, ATL-CONF-2018-001, 2018, URL: <https://cds.cern.ch/record/2306649>.
- [73] ATLAS Collaboration, *Calibration of light-flavour b -jet mistagging rates using ATLAS proton–proton collision data at $\sqrt{s} = 13$ TeV*, ATL-CONF-2018-006, 2018, URL: <https://cds.cern.ch/record/2314418>.
- [74] ATLAS Collaboration, *Performance of missing transverse momentum reconstruction with the ATLAS detector in the first proton–proton collisions at $\sqrt{s} = 13$ TeV*, ATL-PHYS-PUB-2015-027, 2015, URL: <https://cds.cern.ch/record/2037904>.
- [75] ATLAS Collaboration, *E_T^{miss} performance in the ATLAS detector using 2015–2016 LHC pp collisions*, ATL-CONF-2018-023, 2018, URL: <https://cds.cern.ch/record/2625233>.
- [76] C. G. Lester and D. J. Summers, *Measuring masses of semi-invisibly decaying particles pair produced at hadron colliders*, *Phys. Lett. B* **463** (1999) 99, arXiv: [hep-ph/9906349](https://arxiv.org/abs/hep-ph/9906349) [[hep-ph](#)].
- [77] A. Barr, C. G. Lester and P. Stephens, *A variable for measuring masses at hadron colliders when missing energy is expected; m_{T2} : The truth behind the glamour*, *J. Phys. G* **29** (2003) 2343.

- [78] A. Paszke et al., ‘PyTorch: An Imperative Style, High-Performance Deep Learning Library’, *Advances in Neural Information Processing Systems 32*, ed. by H. Wallach et al., Curran Associates, Inc., 2019 8024, URL: <http://papers.neurips.cc/paper/9015-pytorch-an-imperative-style-high-performance-deep-learning-library.pdf>.
- [79] ATLAS Collaboration, *Object-based missing transverse momentum significance in the ATLAS Detector*, ATLAS-CONF-2018-038, 2018, URL: <https://cds.cern.ch/record/2630948>.
- [80] G. Cowan, K. Cranmer, E. Gross and O. Vitells, *Asymptotic formulae for likelihood-based tests of new physics*, *Eur. Phys. J. C* **71** (2011) 1554, arXiv: [1007.1727](https://arxiv.org/abs/1007.1727) [physics.data-an], Erratum: *Eur. Phys. J. C* **73** (2013) 2501.
- [81] M. Baak et al., *HistFitter software framework for statistical data analysis*, *Eur. Phys. J. C* **75** (2015) 153, arXiv: [1410.1280](https://arxiv.org/abs/1410.1280) [hep-ex].
- [82] ATLAS Collaboration, *Measurement of the top quark-pair production cross section with ATLAS in pp collisions at $\sqrt{s} = 7$ TeV*, *Eur. Phys. J. C* **71** (2011) 1577, arXiv: [1012.1792](https://arxiv.org/abs/1012.1792) [hep-ex].
- [83] ATLAS Collaboration, *Measurement of the top quark pair production cross section in pp collisions at $\sqrt{s} = 7$ TeV in dilepton final states with ATLAS*, *Phys. Lett. B* **707** (2012) 459, arXiv: [1108.3699](https://arxiv.org/abs/1108.3699) [hep-ex].
- [84] ATLAS Collaboration, *Jet Calibration and Systematic Uncertainties for Jets Reconstructed in the ATLAS Detector at $\sqrt{s} = 13$ TeV*, ATL-PHYS-PUB-2015-015, 2015, URL: <https://cds.cern.ch/record/2037613>.
- [85] J. Bellm et al., *Herwig 7.0/Herwig++ 3.0 release note*, *Eur. Phys. J. C* **76** (2016) 196, arXiv: [1512.01178](https://arxiv.org/abs/1512.01178) [hep-ph].
- [86] ATLAS Collaboration, *Improvements in $t\bar{t}$ modelling using NLO+PS Monte Carlo generators for Run 2*, ATL-PHYS-PUB-2018-009, 2018, URL: <https://cds.cern.ch/record/2630327>.
- [87] A. L. Read, *Presentation of search results: the CL_s technique*, *J. Phys. G* **28** (2002) 2693.
- [88] R. D. Cousins, J. T. Linnemann, J. Tucker, *Evaluation of three methods for calculating statistical significance when incorporating a systematic uncertainty into a test of the background-only hypothesis for a Poisson process*, *Nucl. Instrum. Meth. A* **595** (2008) 480, arXiv: [physics/0702156](https://arxiv.org/abs/physics/0702156) [physics].
- [89] ATLAS Collaboration, *Search for direct top squark pair production in final states with two leptons in $\sqrt{s} = 13$ TeV pp collisions with the ATLAS detector*, *Eur. Phys. J. C* **77** (2017) 898, arXiv: [1708.03247](https://arxiv.org/abs/1708.03247) [hep-ex].
- [90] ATLAS Collaboration, *ATLAS Computing Acknowledgements*, ATL-SOFT-PUB-2020-001, URL: <https://cds.cern.ch/record/2717821>.

The ATLAS Collaboration

G. Aad¹⁰², B. Abbott¹²⁸, D.C. Abbott¹⁰³, A. Abed Abud³⁶, K. Abeling⁵³, D.K. Abhayasinghe⁹⁴, S.H. Abidi¹⁶⁶, O.S. AbouZeid⁴⁰, N.L. Abraham¹⁵⁵, H. Abramowicz¹⁶⁰, H. Abreu¹⁵⁹, Y. Abulaiti⁶, B.S. Acharya^{67a,67b,n}, B. Achkar⁵³, L. Adam¹⁰⁰, C. Adam Bourdarios⁵, L. Adamczyk^{84a}, L. Adamek¹⁶⁶, J. Adelman¹²¹, M. Adersberger¹¹⁴, A. Adiguzel^{12c}, S. Adorni⁵⁴, T. Adye¹⁴³, A.A. Affolder¹⁴⁵, Y. Afik¹⁵⁹, C. Agapopoulou⁶⁵, M.N. Agaras³⁸, A. Aggarwal¹¹⁹, C. Agheorghiesei^{27c}, J.A. Aguilar-Saavedra^{139f,139a,ad}, A. Ahmad³⁶, F. Ahmadov⁸⁰, W.S. Ahmed¹⁰⁴, X. Ai¹⁸, G. Aielli^{74a,74b}, S. Akatsuka⁸⁶, M. Akbiyik¹⁰⁰, T.P.A. Åkesson⁹⁷, E. Akilli⁵⁴, A.V. Akimov¹¹¹, K. Al Houry⁶⁵, G.L. Alberghi^{23b,23a}, J. Albert¹⁷⁵, M.J. Alconada Verzini¹⁶⁰, S. Alderweireldt³⁶, M. Aleksa³⁶, I.N. Aleksandrov⁸⁰, C. Alexa^{27b}, T. Alexopoulos¹⁰, A. Alfonsi¹²⁰, F. Alfonsi^{23b,23a}, M. Alhroob¹²⁸, B. Ali¹⁴¹, S. Ali¹⁵⁷, M. Aliev¹⁶⁵, G. Alimonti^{69a}, C. Allaire³⁶, B.M.M. Allbrooke¹⁵⁵, B.W. Allen¹³¹, P.P. Allport²¹, A. Aloisio^{70a,70b}, F. Alonso⁸⁹, C. Alpigiani¹⁴⁷, E. Alunno Camelia^{74a,74b}, M. Alvarez Estevez⁹⁹, M.G. Alviggi^{70a,70b}, Y. Amaral Coutinho^{81b}, A. Ambler¹⁰⁴, L. Ambroz¹³⁴, C. Amelung²⁶, D. Amidei¹⁰⁶, S.P. Amor Dos Santos^{139a}, S. Amoroso⁴⁶, C.S. Amrouche⁵⁴, F. An⁷⁹, C. Anastopoulos¹⁴⁸, N. Andari¹⁴⁴, T. Andeen¹¹, J.K. Anders²⁰, S.Y. Andrean^{45a,45b}, A. Andreazza^{69a,69b}, V. Andrei^{61a}, C.R. Anelli¹⁷⁵, S. Angelidakis⁹, A. Angerami³⁹, A.V. Anisenkov^{122b,122a}, A. Annovi^{72a}, C. Antel⁵⁴, M.T. Anthony¹⁴⁸, E. Antipov¹²⁹, M. Antonelli⁵¹, D.J.A. Antrim¹⁷⁰, F. Anulli^{73a}, M. Aoki⁸², J.A. Aparisi Pozo¹⁷³, M.A. Aparo¹⁵⁵, L. Aperio Bella⁴⁶, N. Aranzabal Barrio³⁶, V. Araujo Ferraz^{81a}, R. Araujo Pereira^{81b}, C. Arcangeletti⁵¹, A.T.H. Arce⁴⁹, F.A. Arduh⁸⁹, J-F. Arguin¹¹⁰, S. Argyropoulos⁵², J.-H. Arling⁴⁶, A.J. Armbruster³⁶, A. Armstrong¹⁷⁰, O. Arnaez¹⁶⁶, H. Arnold¹²⁰, Z.P. Arrubarrena Tame¹¹⁴, G. Artoni¹³⁴, K. Asai¹²⁶, S. Asai¹⁶², T. Asawatavonvanich¹⁶⁴, N. Asbah⁵⁹, E.M. Asimakopoulou¹⁷¹, L. Asquith¹⁵⁵, J. Assahsah^{35d}, K. Assamagan²⁹, R. Astalos^{28a}, R.J. Atkin^{33a}, M. Atkinson¹⁷², N.B. Atlay¹⁹, H. Atmani⁶⁵, K. Augsten¹⁴¹, V.A. Austrup¹⁸¹, G. Avolio³⁶, M.K. Ayoub^{15a}, G. Azeulos^{110,al}, H. Bachacou¹⁴⁴, K. Bachas¹⁶¹, M. Backes¹³⁴, F. Backman^{45a,45b}, P. Bagnaia^{73a,73b}, M. Bahmani⁸⁵, H. Bahrasemani¹⁵¹, A.J. Bailey¹⁷³, V.R. Bailey¹⁷², J.T. Baines¹⁴³, C. Bakalis¹⁰, O.K. Baker¹⁸², P.J. Bakker¹²⁰, E. Bakos¹⁶, D. Bakshi Gupta⁸, S. Balaji¹⁵⁶, E.M. Baldin^{122b,122a}, P. Balek¹⁷⁹, F. Balli¹⁴⁴, W.K. Balunas¹³⁴, J. Balz¹⁰⁰, E. Banas⁸⁵, M. Bandieramonte¹³⁸, A. Bandyopadhyay²⁴, Sw. Banerjee^{180,i}, L. Barak¹⁶⁰, W.M. Barbe³⁸, E.L. Barberio¹⁰⁵, D. Barberis^{55b,55a}, M. Barbero¹⁰², G. Barbour⁹⁵, T. Barillari¹¹⁵, M-S. Barisits³⁶, J. Barkeloo¹³¹, T. Barklow¹⁵², R. Barnea¹⁵⁹, B.M. Barnett¹⁴³, R.M. Barnett¹⁸, Z. Barnovska-Blenessy^{60a}, A. Baroncelli^{60a}, G. Barone²⁹, A.J. Barr¹³⁴, L. Barranco Navarro^{45a,45b}, F. Barreiro⁹⁹, J. Barreiro Guimarães da Costa^{15a}, U. Barron¹⁶⁰, S. Barsov¹³⁷, F. Bartels^{61a}, R. Bartoldus¹⁵², G. Bartolini¹⁰², A.E. Barton⁹⁰, P. Bartos^{28a}, A. Basalae⁴⁶, A. Basan¹⁰⁰, A. Bassalat^{65,ai}, M.J. Basso¹⁶⁶, R.L. Bates⁵⁷, S. Batlamous^{35e}, J.R. Batley³², B. Batool¹⁵⁰, M. Battaglia¹⁴⁵, M. Bauce^{73a,73b}, F. Bauer¹⁴⁴, K.T. Bauer¹⁷⁰, P. Bauer²⁴, H.S. Bawa³¹, A. Bayirli^{12c}, J.B. Beacham⁴⁹, T. Beau¹³⁵, P.H. Beauchemin¹⁶⁹, F. Becherer⁵², P. Bechtel²⁴, H.C. Beck⁵³, H.P. Beck^{20,p}, K. Becker¹⁷⁷, C. Becot⁴⁶, A. Beddall^{12d}, A.J. Beddall^{12a}, V.A. Bednyakov⁸⁰, M. Bedognetti¹²⁰, C.P. Bee¹⁵⁴, T.A. Beermann¹⁸¹, M. Begalli^{81b}, M. Begel²⁹, A. Behera¹⁵⁴, J.K. Behr⁴⁶, F. Beisiegel²⁴, M. Belfkir⁵, A.S. Bell⁹⁵, G. Bella¹⁶⁰, L. Bellagamba^{23b}, A. Bellerive³⁴, P. Bellos⁹, K. Beloborodov^{122b,122a}, K. Belotskiy¹¹², N.L. Belyaev¹¹², D. Benchekroun^{35a}, N. Benekos¹⁰, Y. Benhammou¹⁶⁰, D.P. Benjamin⁶, M. Benoit⁵⁴, J.R. Bensinger²⁶, S. Bentvelsen¹²⁰, L. Beresford¹³⁴, M. Beretta⁵¹, D. Berge¹⁹, E. Bergeaas Kuutmann¹⁷¹, N. Berger⁵, B. Bergmann¹⁴¹, L.J. Bergsten²⁶, J. Beringer¹⁸, S. Berlendis⁷, G. Bernardi¹³⁵, C. Bernius¹⁵², F.U. Bernlochner²⁴, T. Berry⁹⁴, P. Berta¹⁰⁰, C. Bertella^{15a}, A. Berthold⁴⁸, I.A. Bertram⁹⁰, O. Bessidskaia Bylund¹⁸¹, N. Besson¹⁴⁴, A. Bethani¹⁰¹, S. Bethke¹¹⁵, A. Betti⁴², A.J. Bevan⁹³, J. Beyer¹¹⁵, D.S. Bhattacharya¹⁷⁶, P. Bhattarai²⁶, V.S. Bhopatkar⁶, R. Bi¹³⁸, R.M. Bianchi¹³⁸, O. Biebel¹¹⁴, D. Biedermann¹⁹, R. Bielski³⁶, K. Bierwagen¹⁰⁰, N.V. Biesuz^{72a,72b}, M. Biglietti^{75a}, T.R.V. Billoud¹⁴¹,

M. Bindi⁵³, A. Bingul^{12d}, C. Bini^{73a,73b}, S. Biondi^{23b,23a}, C.J. Birch-sykes¹⁰¹, M. Birman¹⁷⁹, T. Bisanz⁵³,
J.P. Biswal³, D. Biswas^{180,i}, A. Bitadze¹⁰¹, C. Bittrich⁴⁸, K. Bjørke¹³³, T. Blazek^{28a}, I. Bloch⁴⁶,
C. Blocker²⁶, A. Blue⁵⁷, U. Blumenschein⁹³, G.J. Bobbink¹²⁰, V.S. Bobrovnikov^{122b,122a}, S.S. Bocchetta⁹⁷,
D. Boerner⁴⁶, D. Bogavac¹⁴, A.G. Bogdanchikov^{122b,122a}, C. Bohm^{45a}, V. Boisvert⁹⁴, P. Bokan^{53,171,53},
T. Bold^{84a}, A.E. Bolz^{61b}, M. Bomben¹³⁵, M. Bona⁹³, J.S. Bonilla¹³¹, M. Boonekamp¹⁴⁴, C.D. Booth⁹⁴,
A.G. Borbély⁵⁷, H.M. Borecka-Bielska⁹¹, L.S. Borgna⁹⁵, A. Borisov¹²³, G. Borissov⁹⁰, D. Bortoletto¹³⁴,
D. Boscherini^{23b}, M. Bosman¹⁴, J.D. Bossio Sola¹⁰⁴, K. Bouaouda^{35a}, J. Boudreau¹³⁸,
E.V. Bouhova-Thacker⁹⁰, D. Boumediene³⁸, S.K. Boutle⁵⁷, A. Boveia¹²⁷, J. Boyd³⁶, D. Boye^{33c},
I.R. Boyko⁸⁰, A.J. Bozson⁹⁴, J. Bracinik²¹, N. Brahimi^{60d}, G. Brandt¹⁸¹, O. Brandt³², F. Braren⁴⁶,
B. Brau¹⁰³, J.E. Brau¹³¹, W.D. Breaden Madden⁵⁷, K. Brendlinger⁴⁶, R. Brenner¹⁵⁹, L. Brenner³⁶,
R. Brenner¹⁷¹, S. Bressler¹⁷⁹, B. Brickwedde¹⁰⁰, D.L. Briglin²¹, D. Britton⁵⁷, D. Britzger¹¹⁵, I. Brock²⁴,
R. Brock¹⁰⁷, G. Brooijmans³⁹, W.K. Brooks^{146d}, E. Brost²⁹, P.A. Bruckman de Renstrom⁸⁵, B. Brüers⁴⁶,
D. Bruncko^{28b}, A. Bruni^{23b}, G. Bruni^{23b}, L.S. Bruni¹²⁰, S. Bruno^{74a,74b}, M. Bruschi^{23b}, N. Brusino^{73a,73b},
L. Bryngemark¹⁵², T. Buanes¹⁷, Q. Buat¹⁵⁴, P. Buchholz¹⁵⁰, A.G. Buckley⁵⁷, I.A. Budagov⁸⁰,
M.K. Bugge¹³³, F. Bühner⁵², O. Bulekov¹¹², B.A. Bullard⁵⁹, T.J. Burch¹²¹, S. Burdin⁹¹, C.D. Burgard¹²⁰,
A.M. Burger¹²⁹, B. Burghgrave⁸, J.T.P. Burr⁴⁶, C.D. Burton¹¹, J.C. Burzynski¹⁰³, V. Büscher¹⁰⁰,
E. Buschmann⁵³, P.J. Bussey⁵⁷, J.M. Butler²⁵, C.M. Buttar⁵⁷, J.M. Butterworth⁹⁵, P. Butti³⁶,
W. Buttinger³⁶, C.J. Buxo Vazquez¹⁰⁷, A. Buzatu¹⁵⁷, A.R. Buzykaev^{122b,122a}, G. Cabras^{23b,23a},
S. Cabrera Urbán¹⁷³, D. Caforio⁵⁶, H. Cai¹³⁸, V.M.M. Cairo¹⁵², O. Cakir^{4a}, N. Calace³⁶, P. Calafiura¹⁸,
G. Calderini¹³⁵, P. Calfayan⁶⁶, G. Callea⁵⁷, L.P. Caloba^{81b}, A. Caltabiano^{74a,74b}, S. Calvente Lopez⁹⁹,
D. Calvet³⁸, S. Calvet³⁸, T.P. Calvet¹⁰², M. Calvetti^{72a,72b}, R. Camacho Toro¹³⁵, S. Camarda³⁶,
D. Camarero Munoz⁹⁹, P. Camarri^{74a,74b}, M.T. Camerlingo^{75a,75b}, D. Cameron¹³³, C. Camincher³⁶,
S. Campana³⁶, M. Campanelli⁹⁵, A. Camplani⁴⁰, V. Canale^{70a,70b}, A. Canesse¹⁰⁴, M. Cano Bret⁷⁸,
J. Cantero¹²⁹, T. Cao¹⁶⁰, Y. Cao¹⁷², M.D.M. Capeans Garrido³⁶, M. Capua^{41b,41a}, R. Cardarelli^{74a},
F. Cardillo¹⁴⁸, G. Carducci^{41b,41a}, I. Carli¹⁴², T. Carli³⁶, G. Carlino^{70a}, B.T. Carlson¹³⁸,
E.M. Carlson^{175,167a}, L. Carminati^{69a,69b}, R.M.D. Carney¹⁵², S. Caron¹¹⁹, E. Carquin^{146d}, S. Carrá⁴⁶,
G. Carratta^{23b,23a}, J.W.S. Carter¹⁶⁶, T.M. Carter⁵⁰, M.P. Casado^{14,f}, A.F. Casha¹⁶⁶, F.L. Castillo¹⁷³,
L. Castillo Garcia¹⁴, V. Castillo Gimenez¹⁷³, N.F. Castro^{139a,139e}, A. Catinaccio³⁶, J.R. Catmore¹³³,
A. Cattai³⁶, V. Cavaliere²⁹, V. Cavasinni^{72a,72b}, E. Celebi^{12b}, F. Celli¹³⁴, K. Cerny¹³⁰, A.S. Cerqueira^{81a},
A. Cerri¹⁵⁵, L. Cerrito^{74a,74b}, F. Cerutti¹⁸, A. Cervelli^{23b,23a}, S.A. Cetin^{12b}, Z. Chadi^{35a}, D. Chakraborty¹²¹,
J. Chan¹⁸⁰, W.S. Chan¹²⁰, W.Y. Chan⁹¹, J.D. Chapman³², B. Chargeishvili^{158b}, D.G. Charlton²¹,
T.P. Charman⁹³, C.C. Chau³⁴, S. Che¹²⁷, S. Chekanov⁶, S.V. Chekulaev^{167a}, G.A. Chelkov^{80,ag}, B. Chen⁷⁹,
C. Chen^{60a}, C.H. Chen⁷⁹, H. Chen²⁹, J. Chen^{60a}, J. Chen³⁹, J. Chen²⁶, S. Chen¹³⁶, S.J. Chen^{15c},
X. Chen^{15b}, Y. Chen^{60a}, Y-H. Chen⁴⁶, H.C. Cheng^{63a}, H.J. Cheng^{15a}, A. Cheplakov⁸⁰,
E. Cheremushkina¹²³, R. Cherkaoui El Moursli^{35e}, E. Cheu⁷, K. Cheung⁶⁴, T.J.A. Chevalérias¹⁴⁴,
L. Chevalier¹⁴⁴, V. Chiarella⁵¹, G. Chiarelli^{72a}, G. Chiodini^{68a}, A.S. Chisholm²¹, A. Chitan^{27b}, I. Chiu¹⁶²,
Y.H. Chiu¹⁷⁵, M.V. Chizhov⁸⁰, K. Choi¹¹, A.R. Chomont^{73a,73b}, Y.S. Chow¹²⁰, L.D. Christopher^{33e},
M.C. Chu^{63a}, X. Chu^{15a,15d}, J. Chudoba¹⁴⁰, J.J. Chwastowski⁸⁵, L. Chytka¹³⁰, D. Cieri¹¹⁵, K.M. Ciesla⁸⁵,
D. Cinca⁴⁷, V. Cindro⁹², I.A. Cioară^{27b}, A. Ciocio¹⁸, F. Ciroto^{70a,70b}, Z.H. Citron^{179,j}, M. Citterio^{69a},
D.A. Ciubotaru^{27b}, B.M. Ciungu¹⁶⁶, A. Clark⁵⁴, M.R. Clark³⁹, P.J. Clark⁵⁰, S.E. Clawson¹⁰¹,
C. Clement^{45a,45b}, Y. Coadou¹⁰², M. Cobal^{167a,67c}, A. Coccaro^{55b}, J. Cochran⁷⁹, R. Coelho Lopes De Sa¹⁰³,
H. Cohen¹⁶⁰, A.E.C. Coimbra³⁶, B. Cole³⁹, A.P. Colijn¹²⁰, J. Collot⁵⁸, P. Conde Muiño^{139a,139h},
S.H. Connell^{33c}, I.A. Connelly⁵⁷, S. Constantinescu^{27b}, F. Conventi^{70a,am}, A.M. Cooper-Sarkar¹³⁴,
F. Cormier¹⁷⁴, K.J.R. Cormier¹⁶⁶, L.D. Corpe⁹⁵, M. Corradi^{73a,73b}, E.E. Corrigan⁹⁷, F. Corriveau^{104,ab},
M.J. Costa¹⁷³, F. Costanza⁵, D. Costanzo¹⁴⁸, G. Cowan⁹⁴, J.W. Cowley³², J. Crane¹⁰¹, K. Cranmer¹²⁵,
R.A. Creager¹³⁶, S. Crépe-Renaudin⁵⁸, F. Crescioli¹³⁵, M. Cristinziani²⁴, V. Croft¹⁶⁹, G. Crosetti^{41b,41a},
A. Cueto⁵, T. Cuhadar Donszelmann¹⁷⁰, H. Cui^{15a,15d}, A.R. Cukierman¹⁵², W.R. Cunningham⁵⁷,

S. Czekerda⁸⁵, P. Czodrowski³⁶, M.M. Czurylo^{61b}, M.J. Da Cunha Sargedas De Sousa^{60b},
 J.V. Da Fonseca Pinto^{81b}, C. Da Via¹⁰¹, W. Dabrowski^{84a}, F. Dachs³⁶, T. Dado⁴⁷, S. Dahbi^{33e}, T. Dai¹⁰⁶,
 C. Dallapiccola¹⁰³, M. Dam⁴⁰, G. D'amen²⁹, V. D'Amico^{75a,75b}, J. Damp¹⁰⁰, J.R. Dandoy¹³⁶,
 M.F. Daneri³⁰, M. Danninger¹⁵¹, V. Dao³⁶, G. Darbo^{55b}, O. Dartsis⁵, A. Dattagupta¹³¹, T. Daubney⁴⁶,
 S. D'Auria^{69a,69b}, C. David^{167b}, T. Davidek¹⁴², D.R. Davis⁴⁹, I. Dawson¹⁴⁸, K. De⁸, R. De Asmundis^{70a},
 M. De Beurs¹²⁰, S. De Castro^{23b,23a}, N. De Groot¹¹⁹, P. de Jong¹²⁰, H. De la Torre¹⁰⁷, A. De Maria^{15c},
 D. De Pedis^{73a}, A. De Salvo^{73a}, U. De Sanctis^{74a,74b}, M. De Santis^{74a,74b}, A. De Santo¹⁵⁵,
 J.B. De Vivie De Regie⁶⁵, C. Debenedetti¹⁴⁵, D.V. Dedovich⁸⁰, A.M. Deiana⁴², J. Del Peso⁹⁹,
 Y. Delabat Diaz⁴⁶, D. Delgove⁶⁵, F. Deliot¹⁴⁴, C.M. Delitzsch⁷, M. Della Pietra^{70a,70b}, D. Della Volpe⁵⁴,
 A. Dell'Acqua³⁶, L. Dell'Asta^{74a,74b}, M. Delmastro⁵, C. Delporte⁶⁵, P.A. Delsart⁵⁸, D.A. DeMarco¹⁶⁶,
 S. Demers¹⁸², M. Demichev⁸⁰, G. Demontigny¹¹⁰, S.P. Denisov¹²³, L. D'Eramo¹²¹, D. Derendarz⁸⁵,
 J.E. Derkaoui^{35d}, F. Derue¹³⁵, P. Dervan⁹¹, K. Desch²⁴, K. Dette¹⁶⁶, C. Deutsch²⁴, M.R. Devesa³⁰,
 P.O. Deviveiros³⁶, F.A. Di Bello^{73a,73b}, A. Di Ciaccio^{74a,74b}, L. Di Ciaccio⁵, W.K. Di Clemente¹³⁶,
 C. Di Donato^{70a,70b}, A. Di Girolamo³⁶, G. Di Gregorio^{72a,72b}, B. Di Micco^{75a,75b}, R. Di Nardo^{75a,75b},
 K.F. Di Petrillo⁵⁹, R. Di Sipio¹⁶⁶, C. Diaconu¹⁰², F.A. Dias¹²⁰, T. Dias Do Vale^{139a}, M.A. Diaz^{146a},
 F.G. Diaz Capriles²⁴, J. Dickinson¹⁸, M. Didenko¹⁶⁵, E.B. Diehl¹⁰⁶, J. Dietrich¹⁹, S. Díez Cornell⁴⁶,
 C. Diez Pardos¹⁵⁰, A. Dimitrievska¹⁸, W. Ding^{15b}, J. Dingfelder²⁴, S.J. Dittmeier^{61b}, F. Dittus³⁶,
 F. Djama¹⁰², T. Djobava^{158b}, J.I. Djuvsland¹⁷, M.A.B. Do Vale^{81c}, M. Dobre^{27b}, D. Dodsworth²⁶,
 C. Doglioni⁹⁷, J. Dolejsi¹⁴², Z. Dolezal¹⁴², M. Donadelli^{81d}, B. Dong^{60c}, J. Donini³⁸, A. D'onofrio^{15c},
 M. D'Onofrio⁹¹, J. Dopke¹⁴³, A. Doria^{70a}, M.T. Dova⁸⁹, A.T. Doyle⁵⁷, E. Drechsler¹⁵¹, E. Dreyer¹⁵¹,
 T. Dreyer⁵³, A.S. Drobac¹⁶⁹, D. Du^{60b}, T.A. du Pree¹²⁰, Y. Duan^{60d}, F. Dubinin¹¹¹, M. Dubovsky^{28a},
 A. Dubreuil⁵⁴, E. Duchovni¹⁷⁹, G. Duckeck¹¹⁴, O.A. Ducu³⁶, D. Duda¹¹⁵, A. Dudarev³⁶, A.C. Dudder¹⁰⁰,
 E.M. Duffield¹⁸, M. D'uffizi¹⁰¹, L. Duflot⁶⁵, M. Dührssen³⁶, C. Dülsen¹⁸¹, M. Dumancic¹⁷⁹,
 A.E. Dumitriu^{27b}, M. Dunford^{161a}, A. Duperrin¹⁰², H. Duran Yildiz^{4a}, M. Düren⁵⁶, A. Durglishvili^{158b},
 D. Duschinger⁴⁸, B. Dutta⁴⁶, D. Duvnjak¹, G.I. Dyckes¹³⁶, M. Dyndal³⁶, S. Dysch¹⁰¹, B.S. Dziedzic⁸⁵,
 M.G. Eggleston⁴⁹, T. Eifert⁸, G. Eigen¹⁷, K. Einsweiler¹⁸, T. Ekelof¹⁷¹, H. El Jarrari^{35e}, V. Ellajosyula¹⁷¹,
 M. Ellert¹⁷¹, F. Ellinghaus¹⁸¹, A.A. Elliot⁹³, N. Ellis³⁶, J. Elmsheuser²⁹, M. Elsing³⁶, D. Emeliyanov¹⁴³,
 A. Emerman³⁹, Y. Enari¹⁶², M.B. Epland⁴⁹, J. Erdmann⁴⁷, A. Ereditato²⁰, P.A. Erland⁸⁵, M. Errenst¹⁸¹,
 M. Escalier⁶⁵, C. Escobar¹⁷³, O. Estrada Pastor¹⁷³, E. Etzion¹⁶⁰, H. Evans⁶⁶, M.O. Evans¹⁵⁵, A. Ezhilov¹³⁷,
 F. Fabbri⁵⁷, L. Fabbri^{23b,23a}, V. Fabiani¹¹⁹, G. Facini¹⁷⁷, R.M. Fakhruddinov¹²³, S. Falciano^{73a}, P.J. Falke²⁴,
 S. Falke³⁶, J. Faltova¹⁴², Y. Fang^{15a}, Y. Fang^{15a}, G. Fanourakis⁴⁴, M. Fanti^{69a,69b}, M. Faraj^{67a,67c,q},
 A. Farbin⁸, A. Farilla^{75a}, E.M. Farina^{71a,71b}, T. Farooque¹⁰⁷, S.M. Farrington⁵⁰, P. Farthouat³⁶, F. Fassi^{35e},
 P. Fassnacht³⁶, D. Fassouliotis⁹, M. Fauci Giannelli⁵⁰, W.J. Fawcett³², L. Fayard⁶⁵, O.L. Fedin^{137,o},
 W. Fedorko¹⁷⁴, A. Fehr²⁰, M. Feickert¹⁷², L. Feligioni¹⁰², A. Fell¹⁴⁸, C. Feng^{60b}, M. Feng⁴⁹,
 M.J. Fenton¹⁷⁰, A.B. Fenyuk¹²³, S.W. Ferguson⁴³, J. Ferrando⁴⁶, A. Ferrante¹⁷², A. Ferrari¹⁷¹, P. Ferrari¹²⁰,
 R. Ferrari^{71a}, D.E. Ferreira de Lima^{61b}, A. Ferrer¹⁷³, D. Ferrere⁵⁴, C. Ferretti¹⁰⁶, F. Fiedler¹⁰⁰,
 A. Filipčič⁹², F. Filthaut¹¹⁹, K.D. Finelli²⁵, M.C.N. Fiolhais^{139a,139c,a}, L. Fiorini¹⁷³, F. Fischer¹¹⁴,
 J. Fischer¹⁰⁰, W.C. Fisher¹⁰⁷, T. Fitschen²¹, I. Fleck¹⁵⁰, P. Fleischmann¹⁰⁶, T. Flick¹⁸¹, B.M. Flierl¹¹⁴,
 L. Flores¹³⁶, L.R. Flores Castillo^{63a}, F.M. Follega^{76a,76b}, N. Fomin¹⁷, J.H. Foo¹⁶⁶, G.T. Forcolin^{76a,76b},
 B.C. Forland⁶⁶, A. Formica¹⁴⁴, F.A. Förster¹⁴, A.C. Forti¹⁰¹, E. Fortin¹⁰², M.G. Foti¹³⁴, D. Fournier⁶⁵,
 H. Fox⁹⁰, P. Francavilla^{72a,72b}, S. Francescato^{73a,73b}, M. Franchini^{23b,23a}, S. Franchino^{61a}, D. Francis³⁶,
 L. Franco⁵, L. Franconi²⁰, M. Franklin⁵⁹, G. Frattari^{73a,73b}, A.N. Fray⁹³, P.M. Freeman²¹, B. Freund¹¹⁰,
 W.S. Freund^{81b}, E.M. Freundlich⁴⁷, D.C. Frizzell¹²⁸, D. Froidevaux³⁶, J.A. Frost¹³⁴, M. Fujimoto¹²⁶,
 C. Fukunaga¹⁶³, E. Fullana Torregrosa¹⁷³, T. Fusayasu¹¹⁶, J. Fuster¹⁷³, A. Gabrielli^{23b,23a}, A. Gabrielli³⁶,
 S. Gadatsch⁵⁴, P. Gadow¹¹⁵, G. Gagliardi^{55b,55a}, L.G. Gagnon¹¹⁰, G.E. Gallardo¹³⁴, E.J. Gallas¹³⁴,
 B.J. Gallop¹⁴³, R. Gamboa Goni⁹³, K.K. Gan¹²⁷, S. Ganguly¹⁷⁹, J. Gao^{60a}, Y. Gao⁵⁰, Y.S. Gao^{31,l},
 F.M. Garay Walls^{146a}, C. García¹⁷³, J.E. García Navarro¹⁷³, J.A. García Pascual^{15a}, C. Garcia-Argos⁵²,

M. Garcia-Sciveres¹⁸, R.W. Gardner³⁷, N. Garelli¹⁵², S. Gargiulo⁵², C.A. Garner¹⁶⁶, V. Garonne¹³³,
S.J. Gasiorowski¹⁴⁷, P. Gaspar^{81b}, A. Gaudiello^{55b,55a}, G. Gaudio^{71a}, I.L. Gavrilenko¹¹¹, A. Gavriluk¹²⁴,
C. Gay¹⁷⁴, G. Gaycken⁴⁶, E.N. Gazis¹⁰, A.A. Geanta^{27b}, C.M. Gee¹⁴⁵, C.N.P. Gee¹⁴³, J. Geisen⁹⁷,
M. Geisen¹⁰⁰, C. Gemme^{55b}, M.H. Genest⁵⁸, C. Geng¹⁰⁶, S. Gentile^{73a,73b}, S. George⁹⁴, T. Geralis⁴⁴,
L.O. Gerlach⁵³, P. Gessinger-Befurt¹⁰⁰, G. Gessner⁴⁷, S. Ghasemi¹⁵⁰, M. Ghasemi Bostanabad¹⁷⁵,
M. Ghneimat¹⁵⁰, A. Ghosh⁶⁵, A. Ghosh⁷⁸, B. Giacobbe^{23b}, S. Giagu^{73a,73b}, N. Giangiacomi^{23b,23a},
P. Giannetti^{72a}, A. Giannini^{70a,70b}, G. Giannini¹⁴, S.M. Gibson⁹⁴, M. Gignac¹⁴⁵, D.T. Gil^{84b}, B.J. Gilbert³⁹,
D. Gillberg³⁴, G. Gilles¹⁸¹, D.M. Gingrich^{3,al}, M.P. Giordani^{67a,67c}, P.F. Giraud¹⁴⁴, G. Giugliarelli^{67a,67c},
D. Giugni^{69a}, F. Giuli^{74a,74b}, S. Gkaitatzis¹⁶¹, I. Gkialas^{9,g}, E.L. Gkoukousis¹⁴, P. Gkoutoumis¹⁰,
L.K. Gladilin¹¹³, C. Glasman⁹⁹, J. Glatzer¹⁴, P.C.F. Glaysher⁴⁶, A. Glazov⁴⁶, G.R. Gledhill¹³¹,
I. Gnesi^{41b,b}, M. Goblirsch-Kolb²⁶, D. Godin¹¹⁰, S. Goldfarb¹⁰⁵, T. Golling⁵⁴, D. Golubkov¹²³,
A. Gomes^{139a,139b}, R. Goncalves Gama⁵³, R. Gonçalo^{139a,139c}, G. Gonella¹³¹, L. Gonella²¹,
A. Gongadze⁸⁰, F. Gonnella²¹, J.L. Gonski³⁹, S. González de la Hoz¹⁷³, S. Gonzalez Fernandez¹⁴,
R. Gonzalez Lopez⁹¹, C. Gonzalez Renteria¹⁸, R. Gonzalez Suarez¹⁷¹, S. Gonzalez-Sevilla⁵⁴,
G.R. Gonzalvo Rodriguez¹⁷³, L. Goossens³⁶, N.A. Gorasia²¹, P.A. Gorbounov¹²⁴, H.A. Gordon²⁹,
B. Gorini³⁶, E. Gorini^{68a,68b}, A. Gorišek⁹², A.T. Goshaw⁴⁹, M.I. Gostkin⁸⁰, C.A. Gottardo¹¹⁹,
M. Gouighri^{35b}, A.G. Goussiou¹⁴⁷, N. Govender^{33c}, C. Goy⁵, I. Grabowska-Bold^{84a}, E.C. Graham⁹¹,
J. Gramling¹⁷⁰, E. Gramstad¹³³, S. Grancagnolo¹⁹, M. Grandi¹⁵⁵, V. Gratchev¹³⁷, P.M. Gravila^{27f},
F.G. Gravili^{68a,68b}, C. Gray⁵⁷, H.M. Gray¹⁸, C. Grefe²⁴, K. Gregersen⁹⁷, I.M. Gregor⁴⁶, P. Grenier¹⁵²,
K. Grevtsov⁴⁶, C. Grieco¹⁴, N.A. Grieser¹²⁸, A.A. Grillo¹⁴⁵, K. Grimm^{31,k}, S. Grinstein^{14,w}, J.-F. Grivaz⁶⁵,
S. Groh¹⁰⁰, E. Gross¹⁷⁹, J. Grosse-Knetter⁵³, Z.J. Grout⁹⁵, C. Grud¹⁰⁶, A. Grummer¹¹⁸, J.C. Grundy¹³⁴,
L. Guan¹⁰⁶, W. Guan¹⁸⁰, C. Gubbels¹⁷⁴, J. Guenther³⁶, A. Guerguichon⁶⁵, J.G.R. Guerrero Rojas¹⁷³,
F. Guescini¹¹⁵, D. Guest¹⁷⁰, R. Gugel¹⁰⁰, A. Guida⁴⁶, T. Guillemin⁵, S. Guindon³⁶, U. Gul⁵⁷, J. Guo^{60c},
W. Guo¹⁰⁶, Y. Guo^{60a}, Z. Guo¹⁰², R. Gupta⁴⁶, S. Gurbuz^{12c}, G. Gustavino¹²⁸, M. Guth⁵², P. Gutierrez¹²⁸,
C. Gutschow⁹⁵, C. Guyot¹⁴⁴, C. Gwenlan¹³⁴, C.B. Gwilliam⁹¹, E.S. Haaland¹³³, A. Haas¹²⁵, C. Haber¹⁸,
H.K. Hadavand⁸, A. Hadeif^{60a}, M. Haleem¹⁷⁶, J. Haley¹²⁹, J.J. Hall¹⁴⁸, G. Halladjian¹⁰⁷, G.D. Hallewell¹⁰²,
K. Hamano¹⁷⁵, H. Hamdaoui^{35e}, M. Hamer²⁴, G.N. Hamity⁵⁰, K. Han^{60a,v}, L. Han^{60a}, S. Han¹⁸,
Y.F. Han¹⁶⁶, K. Hanagaki^{82,t}, M. Hance¹⁴⁵, D.M. Handl¹¹⁴, M.D. Hank³⁷, R. Hankache¹³⁵, E. Hansen⁹⁷,
J.B. Hansen⁴⁰, J.D. Hansen⁴⁰, M.C. Hansen²⁴, P.H. Hansen⁴⁰, E.C. Hanson¹⁰¹, K. Hara¹⁶⁸,
T. Harenberg¹⁸¹, S. Harkusha¹⁰⁸, P.F. Harrison¹⁷⁷, N.M. Hartman¹⁵², N.M. Hartmann¹¹⁴, Y. Hasegawa¹⁴⁹,
A. Hasib⁵⁰, S. Hassani¹⁴⁴, S. Haug²⁰, R. Hauser¹⁰⁷, L.B. Havener³⁹, M. Havranek¹⁴¹, C.M. Hawkes²¹,
R.J. Hawkings³⁶, S. Hayashida¹¹⁷, D. Hayden¹⁰⁷, C. Hayes¹⁰⁶, R.L. Hayes¹⁷⁴, C.P. Hays¹³⁴, J.M. Hays⁹³,
H.S. Hayward⁹¹, S.J. Haywood¹⁴³, F. He^{60a}, Y. He¹⁶⁴, M.P. Heath⁵⁰, V. Hedberg⁹⁷, S. Heer²⁴,
A.L. Heggelund¹³³, C. Heidegger⁵², K.K. Heidegger⁵², W.D. Heidorn⁷⁹, J. Heilman³⁴, S. Heim⁴⁶,
T. Heim¹⁸, B. Heinemann^{46,aj}, J.G. Heinlein¹³⁶, J.J. Heinrich¹³¹, L. Heinrich³⁶, J. Hejbal¹⁴⁰, L. Helary⁴⁶,
A. Held¹²⁵, S. Hellesund¹³³, C.M. Helling¹⁴⁵, S. Hellman^{45a,45b}, C. Helsen³⁶, R.C.W. Henderson⁹⁰,
Y. Heng¹⁸⁰, L. Henkelmann³², A.M. Henriques Correia³⁶, H. Herde²⁶, Y. Hernández Jiménez^{33e},
H. Herr¹⁰⁰, M.G. Herrmann¹¹⁴, T. Herrmann⁴⁸, G. Herten⁵², R. Hertenberger¹¹⁴, L. Hervas³⁶,
T.C. Herwig¹³⁶, G.G. Hesketh⁹⁵, N.P. Hesse^{167a}, H. Hibi⁸³, A. Higashida¹⁶², S. Higashino⁸²,
E. Higón-Rodríguez¹⁷³, K. Hildebrand³⁷, J.C. Hill³², K.K. Hill²⁹, K.H. Hiller⁴⁶, S.J. Hillier²¹, M. Hils⁴⁸,
I. Hinchliffe¹⁸, F. Hinterkeuser²⁴, M. Hirose¹³², S. Hirose⁵², D. Hirschbuehl¹⁸¹, B. Hiti⁹², O. Hladik¹⁴⁰,
D.R. Hlaluku^{33e}, J. Hobbs¹⁵⁴, N. Hod¹⁷⁹, M.C. Hodgkinson¹⁴⁸, A. Hoecker³⁶, D. Hohn⁵², D. Hohov⁶⁵,
T. Holm²⁴, T.R. Holmes³⁷, M. Holzbock¹¹⁴, L.B.A.H. Hommels³², T.M. Hong¹³⁸, J.C. Honig⁵²,
A. Hönle¹¹⁵, B.H. Hooberman¹⁷², W.H. Hopkins⁶, Y. Horii¹¹⁷, P. Horn⁴⁸, L.A. Horyn³⁷, S. Hou¹⁵⁷,
A. Houmada^{35a}, J. Howarth⁵⁷, J. Hoya⁸⁹, M. Hrabovsky¹³⁰, J. Hrdinka⁷⁷, J. Hrivnac⁶⁵, A. Hrynevich¹⁰⁹,
T. Hryn'ova⁵, P.J. Hsu⁶⁴, S.-C. Hsu¹⁴⁷, Q. Hu²⁹, S. Hu^{60c}, Y.F. Hu^{15a,15d,an}, D.P. Huang⁹⁵, Y. Huang^{60a},
Y. Huang^{15a}, Z. Hubacek¹⁴¹, F. Hubaut¹⁰², M. Huebner²⁴, F. Huegging²⁴, T.B. Huffman¹³⁴, M. Huhtinen³⁶,

R. Hulsken⁵⁸, R.F.H. Hunter³⁴, P. Huo¹⁵⁴, N. Huseynov^{80,ac}, J. Huston¹⁰⁷, J. Huth⁵⁹, R. Hyneman¹⁵², S. Hyrych^{28a}, G. Iacobucci⁵⁴, G. Iakovidis²⁹, I. Ibragimov¹⁵⁰, L. Iconomidou-Fayard⁶⁵, P. Iengo³⁶, R. Ignazzi⁴⁰, O. Igonkina^{120,y,*}, R. Iguchi¹⁶², T. Iizawa⁵⁴, Y. Ikegami⁸², M. Ikeno⁸², N. Ilic^{119,166,ab}, F. Iltzsche⁴⁸, H. Imam^{35a}, G. Introzzi^{71a,71b}, M. Iodice^{75a}, K. Iordanidou^{167a}, V. Ippolito^{73a,73b}, M.F. Isacson¹⁷¹, M. Ishino¹⁶², W. Islam¹²⁹, C. Issever^{19,46}, S. Istin¹⁵⁹, F. Ito¹⁶⁸, J.M. Iturbe Ponce^{63a}, R. Iuppa^{76a,76b}, A. Ivina¹⁷⁹, H. Iwasaki⁸², J.M. Izen⁴³, V. Izzo^{70a}, P. Jacka¹⁴⁰, P. Jackson¹, R.M. Jacobs⁴⁶, B.P. Jaeger¹⁵¹, V. Jain², G. Jäkel¹⁸¹, K.B. Jakobi¹⁰⁰, K. Jakobs⁵², T. Jakoubek¹⁷⁹, J. Jamieson⁵⁷, K.W. Janas^{84a}, R. Jansky⁵⁴, M. Janus⁵³, P.A. Janus^{84a}, G. Jarlskog⁹⁷, A.E. Jaspan⁹¹, N. Javadov^{80,ac}, T. Javûrek³⁶, M. Javurkova¹⁰³, F. Jeanneau¹⁴⁴, L. Jeanty¹³¹, J. Jejelava^{158a}, P. Jenni^{52,c}, N. Jeong⁴⁶, S. Jézéquel⁵, H. Ji¹⁸⁰, J. Jia¹⁵⁴, H. Jiang⁷⁹, Y. Jiang^{60a}, Z. Jiang¹⁵², S. Jiggins⁵², F.A. Jimenez Morales³⁸, J. Jimenez Pena¹¹⁵, S. Jin^{15c}, A. Jinaru^{27b}, O. Jinnouchi¹⁶⁴, H. Jivan^{33e}, P. Johansson¹⁴⁸, K.A. Johns⁷, C.A. Johnson⁶⁶, R.W.L. Jones⁹⁰, S.D. Jones¹⁵⁵, T.J. Jones⁹¹, J. Jongmanns^{61a}, J. Jovicevic³⁶, X. Ju¹⁸, J.J. Junggeburth¹¹⁵, A. Juste Rozas^{14,w}, A. Kaczmarzka⁸⁵, M. Kado^{73a,73b}, H. Kagan¹²⁷, M. Kagan¹⁵², A. Kahn³⁹, C. Kahra¹⁰⁰, T. Kaji¹⁷⁸, E. Kajomovitz¹⁵⁹, C.W. Kalderon²⁹, A. Kaluza¹⁰⁰, A. Kamenshchikov¹²³, M. Kaneda¹⁶², N.J. Kang¹⁴⁵, S. Kang⁷⁹, Y. Kano¹¹⁷, J. Kanzaki⁸², L.S. Kaplan¹⁸⁰, D. Kar^{33e}, K. Karava¹³⁴, M.J. Kareem^{167b}, I. Karkanias¹⁶¹, S.N. Karpov⁸⁰, Z.M. Karpova⁸⁰, V. Kartvelishvili⁹⁰, A.N. Karyukhin¹²³, E. Kasimi¹⁶¹, A. Kastanas^{45a,45b}, C. Kato^{60d,60c}, J. Katzy⁴⁶, K. Kawade¹⁴⁹, K. Kawagoe⁸⁸, T. Kawaguchi¹¹⁷, T. Kawamoto¹⁴⁴, G. Kawamura⁵³, E.F. Kay¹⁷⁵, S. Kazakos¹⁴, V.F. Kazanin^{122b,122a}, R. Keeler¹⁷⁵, R. Kehoe⁴², J.S. Keller³⁴, E. Kellermann⁹⁷, D. Kelsey¹⁵⁵, J.J. Kempster²¹, J. Kendrick²¹, K.E. Kennedy³⁹, O. Kepka¹⁴⁰, S. Kersten¹⁸¹, B.P. Kerševan⁹², S. Ketabchi Haghghat¹⁶⁶, M. Khader¹⁷², F. Khalil-Zada¹³, M. Khandoga¹⁴⁴, A. Khanov¹²⁹, A.G. Kharlamov^{122b,122a}, T. Kharlamova^{122b,122a}, E.E. Khoda¹⁷⁴, A. Khodinov¹⁶⁵, T.J. Khoo⁵⁴, G. Khoraiuli¹⁷⁶, E. Khramov⁸⁰, J. Khubua^{158b}, S. Kido⁸³, M. Kiehn³⁶, C.R. Kilby⁹⁴, E. Kim¹⁶⁴, Y.K. Kim³⁷, N. Kimura⁹⁵, A. Kirchhoff⁵³, D. Kirchmeier⁴⁸, J. Kirk¹⁴³, A.E. Kiryunin¹¹⁵, T. Kishimoto¹⁶², D.P. Kisliuk¹⁶⁶, V. Kitali⁴⁶, C. Kitsaki¹⁰, O. Kivernyk²⁴, T. Klapdor-Kleingrothaus⁵², M. Klassen^{61a}, C. Klein³⁴, M.H. Klein¹⁰⁶, M. Klein⁹¹, U. Klein⁹¹, K. Kleinknecht¹⁰⁰, P. Klimek¹²¹, A. Klimentov²⁹, T. Klingl²⁴, T. Klioutchnikova³⁶, F.F. Klitzner¹¹⁴, P. Kluit¹²⁰, S. Kluth¹¹⁵, E. Kneringer⁷⁷, E.B.F.G. Knoop¹⁰², A. Knue⁵², D. Kobayashi⁸⁸, M. Kobel⁴⁸, M. Kocian¹⁵², T. Kodama¹⁶², P. Kodys¹⁴², D.M. Koeck¹⁵⁵, P.T. Koenig²⁴, T. Koffas³⁴, N.M. Köhler³⁶, M. Kolb¹⁴⁴, I. Koletsou⁵, T. Komarek¹³⁰, T. Kondo⁸², K. Köneke⁵², A.X.Y. Kong¹, A.C. König¹¹⁹, T. Kono¹²⁶, V. Konstantinides⁹⁵, N. Konstantinidis⁹⁵, B. Konya⁹⁷, R. Kopeliansky⁶⁶, S. Koperny^{84a}, K. Korcyl⁸⁵, K. Kordas¹⁶¹, G. Koren¹⁶⁰, A. Korn⁹⁵, I. Korolkov¹⁴, E.V. Korolkova¹⁴⁸, N. Korotkova¹¹³, O. Kortner¹¹⁵, S. Kortner¹¹⁵, V.V. Kostyukhin^{148,165}, A. Kotsokchagia⁶⁵, A. Kotwal⁴⁹, A. Koulouris¹⁰, A. Kourkoumeli-Charalampidi^{71a,71b}, C. Kourkoumelis⁹, E. Kourlitis⁶, V. Kouskoura²⁹, R. Kowalewski¹⁷⁵, W. Kozanecki¹⁰¹, A.S. Kozhin¹²³, V.A. Kramarenko¹¹³, G. Kramberger⁹², D. Krasnopevtsev^{60a}, M.W. Krasny¹³⁵, A. Krasznahorkay³⁶, D. Krauss¹¹⁵, J.A. Kremer¹⁰⁰, J. Kretschmar⁹¹, P. Krieger¹⁶⁶, F. Krieter¹¹⁴, A. Krishnan^{61b}, M. Krivos¹⁴², K. Krizka¹⁸, K. Kroeninger⁴⁷, H. Kroha¹¹⁵, J. Kroll¹⁴⁰, J. Kroll¹³⁶, K.S. Krowpman¹⁰⁷, U. Kruchonak⁸⁰, H. Krüger²⁴, N. Krumnack⁷⁹, M.C. Kruse⁴⁹, J.A. Krzysiak⁸⁵, A. Kubota¹⁶⁴, O. Kuchinskaia¹⁶⁵, S. Kудay^{4b}, J.T. Kuechler⁴⁶, S. Kuehn³⁶, T. Kuhl⁴⁶, V. Kukhtin⁸⁰, Y. Kulchitsky^{108,ae}, S. Kuleshov^{146b}, Y.P. Kulinich¹⁷², M. Kuna⁵⁸, T. Kunigo⁸⁶, A. Kupco¹⁴⁰, T. Kupfer⁴⁷, O. Kuprash⁵², H. Kurashige⁸³, L.L. Kurchaninov^{167a}, Y.A. Kurochkin¹⁰⁸, A. Kurova¹¹², M.G. Kurth^{15a,15d}, E.S. Kuwertz³⁶, M. Kuze¹⁶⁴, A.K. Kvam¹⁴⁷, J. Kvita¹³⁰, T. Kwan¹⁰⁴, F. La Ruffa^{41b,41a}, C. Lacasta¹⁷³, F. Lacava^{73a,73b}, D.P.J. Lack¹⁰¹, H. Lacker¹⁹, D. Lacour¹³⁵, E. Ladygin⁸⁰, R. Lafaye⁵, B. Laforge¹³⁵, T. Lagouri^{146c}, S. Lai⁵³, I.K. Lakomic^{84a}, J.E. Lambert¹²⁸, S. Lammers⁶⁶, W. Lampl⁷, C. Lampoudis¹⁶¹, E. Lançon²⁹, U. Landgraf⁵², M.P.J. Landon⁹³, M.C. Lanfermann⁵⁴, V.S. Lang⁵², J.C. Lange⁵³, R.J. Langenberg¹⁰³, A.J. Lankford¹⁷⁰, F. Lanni²⁹, K. Lantzscht²⁴, A. Lanza^{71a}, A. Lapertosa^{55b,55a}, J.F. Laporte¹⁴⁴, T. Lari^{69a}, F. Lasagni Manghi^{23b,23a}, M. Lassnig³⁶, T.S. Lau^{63a},

A. Laudrain⁶⁵, A. Laurier³⁴, M. Lavorgna^{70a,70b}, S.D. Lawlor⁹⁴, M. Lazzaroni^{69a,69b}, B. Le¹⁰¹,
 E. Le Guirriec¹⁰², A. Lebedev⁷⁹, M. LeBlanc⁷, T. LeCompte⁶, F. Ledroit-Guillon⁵⁸, A.C.A. Lee⁹⁵,
 C.A. Lee²⁹, G.R. Lee¹⁷, L. Lee⁵⁹, S.C. Lee¹⁵⁷, S. Lee⁷⁹, B. Lefebvre^{167a}, H.P. Lefebvre⁹⁴, M. Lefebvre¹⁷⁵,
 C. Leggett¹⁸, K. Lehmann¹⁵¹, N. Lehmann²⁰, G. Lehmann Miotto³⁶, W.A. Leight⁴⁶, A. Leisos^{161,u},
 M.A.L. Leite^{81d}, C.E. Leitgeb¹¹⁴, R. Leitner¹⁴², D. Lellouch^{179,*}, K.J.C. Leney⁴², T. Lenz²⁴, S. Leone^{72a},
 C. Leonidopoulos⁵⁰, A. Leopold¹³⁵, C. Leroy¹¹⁰, R. Les¹⁰⁷, C.G. Lester³², M. Levchenko¹³⁷, J. Levêque⁵,
 D. Levin¹⁰⁶, L.J. Levinson¹⁷⁹, D.J. Lewis²¹, B. Li^{15b}, B. Li¹⁰⁶, C-Q. Li^{60a}, F. Li^{60c}, H. Li^{60a}, H. Li^{60b},
 J. Li^{60c}, K. Li¹⁴⁷, L. Li^{60c}, M. Li^{15a,15d}, Q. Li^{15a,15d}, Q.Y. Li^{60a}, S. Li^{60d,60c}, X. Li⁴⁶, Y. Li⁴⁶, Z. Li^{60b},
 Z. Li¹³⁴, Z. Li¹⁰⁴, Z. Liang^{15a}, M. Liberatore⁴⁶, B. Liberti^{74a}, A. Liblong¹⁶⁶, K. Lie^{63c}, S. Lim²⁹,
 C.Y. Lin³², K. Lin¹⁰⁷, R.A. Linck⁶⁶, R.E. Lindley⁷, J.H. Lindon²¹, A. Linss⁴⁶, A.L. Lioni⁵⁴, E. Lipeles¹³⁶,
 A. Lipniacka¹⁷, T.M. Liss^{172,ak}, A. Lister¹⁷⁴, J.D. Little⁸, B. Liu⁷⁹, B.L. Liu⁶, H.B. Liu²⁹, J.B. Liu^{60a},
 J.K.K. Liu³⁷, K. Liu^{60d}, M. Liu^{60a}, P. Liu^{15a}, X. Liu^{60a}, Y. Liu⁴⁶, Y. Liu^{15a,15d}, Y.L. Liu¹⁰⁶, Y.W. Liu^{60a},
 M. Livan^{71a,71b}, A. Lleres⁵⁸, J. Llorente Merino¹⁵¹, S.L. Lloyd⁹³, C.Y. Lo^{63b}, E.M. Lobodzinska⁴⁶,
 P. Loch⁷, S. Loffredo^{74a,74b}, T. Lohse¹⁹, K. Lohwasser¹⁴⁸, M. Lokajicek¹⁴⁰, J.D. Long¹⁷², R.E. Long⁹⁰,
 I. Longarini^{73a,73b}, L. Longo³⁶, K.A. Looper¹²⁷, I. Lopez Paz¹⁰¹, A. Lopez Solis¹⁴⁸, J. Lorenz¹¹⁴,
 N. Lorenzo Martinez⁵, A.M. Lory¹¹⁴, P.J. Lösel¹¹⁴, A. Lösle⁵², X. Lou⁴⁶, X. Lou^{15a}, A. Lounis⁶⁵, J. Love⁶,
 P.A. Love⁹⁰, J.J. Lozano Bahilo¹⁷³, M. Lu^{60a}, Y.J. Lu⁶⁴, H.J. Lubatti¹⁴⁷, C. Luci^{73a,73b}, F.L. Lucio Alves^{15c},
 A. Lucotte⁵⁸, F. Luehring⁶⁶, I. Luise¹³⁵, L. Luminari^{73a}, B. Lund-Jensen¹⁵³, M.S. Lutz¹⁶⁰, D. Lynn²⁹,
 H. Lyons⁹¹, R. Lysak¹⁴⁰, E. Lytken⁹⁷, F. Lyu^{15a}, V. Lyubushkin⁸⁰, T. Lyubushkina⁸⁰, H. Ma²⁹, L.L. Ma^{60b},
 Y. Ma⁹⁵, D.M. Mac Donell¹⁷⁵, G. Maccarrone⁵¹, A. Macchiolo¹¹⁵, C.M. Macdonald¹⁴⁸,
 J.C. MacDonald¹⁴⁸, J. Machado Miguens¹³⁶, D. Madaffari¹⁷³, R. Madar³⁸, W.F. Mader⁴⁸,
 M. Madugoda Ralalage Don¹²⁹, N. Madysa⁴⁸, J. Maeda⁸³, T. Maeno²⁹, M. Maerker⁴⁸, V. Magerl⁵²,
 N. Magini⁷⁹, J. Magro^{67a,67c,q}, D.J. Mahon³⁹, C. Maidantchik^{81b}, T. Maier¹¹⁴, A. Maio^{139a,139b,139d},
 K. Maj^{84a}, O. Majersky^{28a}, S. Majewski¹³¹, Y. Makida⁸², N. Makovec⁶⁵, B. Malaescu¹³⁵, Pa. Malecki⁸⁵,
 V.P. Maleev¹³⁷, F. Malek⁵⁸, D. Malito^{41b,41a}, U. Mallik⁷⁸, D. Malon⁶, C. Malone³², S. Maltezos¹⁰,
 S. Malyukov⁸⁰, J. Mamuzic¹⁷³, G. Mancini^{70a,70b}, I. Mandić⁹², L. Manhaes de Andrade Filho^{81a},
 I.M. Maniatis¹⁶¹, J. Manjarres Ramos⁴⁸, K.H. Mankinen⁹⁷, A. Mann¹¹⁴, A. Manousos⁷⁷, B. Mansoulie¹⁴⁴,
 I. Mantos¹⁶¹, S. Manzoni¹²⁰, A. Marantis¹⁶¹, G. Marceca³⁰, L. Marchese¹³⁴, G. Marchiori¹³⁵,
 M. Marcisovsky¹⁴⁰, L. Marcoccia^{74a,74b}, C. Marcon⁹⁷, C.A. Marin Tobon³⁶, M. Marjanovic¹²⁸,
 Z. Marshall¹⁸, M.U.F. Martensson¹⁷¹, S. Marti-Garcia¹⁷³, C.B. Martin¹²⁷, T.A. Martin¹⁷⁷, V.J. Martin⁵⁰,
 B. Martin dit Latour¹⁷, L. Martinelli^{75a,75b}, M. Martinez^{14,w}, P. Martinez Agullo¹⁷³,
 V.I. Martinez Outschoorn¹⁰³, S. Martin-Haugh¹⁴³, V.S. Martoiu^{27b}, A.C. Martyniuk⁹⁵, A. Marzin³⁶,
 S.R. Maschek¹¹⁵, L. Masetti¹⁰⁰, T. Mashimo¹⁶², R. Mashinistov¹¹¹, J. Masik¹⁰¹, A.L. Maslennikov^{122b,122a},
 L. Massa^{23b,23a}, P. Massarotti^{70a,70b}, P. Mastrandrea^{72a,72b}, A. Mastroberardino^{41b,41a}, T. Masubuchi¹⁶²,
 D. Matakias²⁹, A. Matic¹¹⁴, N. Matsuzawa¹⁶², P. Mättig²⁴, J. Maurer^{27b}, B. Maček⁹²,
 D.A. Maximov^{122b,122a}, R. Mazini¹⁵⁷, I. Maznas¹⁶¹, S.M. Mazza¹⁴⁵, J.P. Mc Gowan¹⁰⁴, S.P. Mc Kee¹⁰⁶,
 T.G. McCarthy¹¹⁵, W.P. McCormack¹⁸, E.F. McDonald¹⁰⁵, J.A. Mcfayden³⁶, G. Mchedlidze^{158b},
 M.A. McKay⁴², K.D. McLean¹⁷⁵, S.J. McMahan¹⁴³, P.C. McNamara¹⁰⁵, C.J. McNicol¹⁷⁷,
 R.A. McPherson^{175,ab}, J.E. Mdhluhi^{33e}, Z.A. Meadows¹⁰³, S. Meehan³⁶, T. Megy³⁸, S. Mehlhase¹¹⁴,
 A. Mehta⁹¹, B. Meirose⁴³, D. Melini¹⁵⁹, B.R. Mellado Garcia^{33e}, J.D. Mellenthin⁵³, M. Melo^{28a},
 F. Meloni⁴⁶, A. Melzer²⁴, E.D. Mendes Gouveia^{139a,139e}, L. Meng³⁶, X.T. Meng¹⁰⁶, S. Menke¹¹⁵,
 E. Meoni^{41b,41a}, S. Mergelmeyer¹⁹, S.A.M. Merkt¹³⁸, C. Merlassino¹³⁴, P. Mermod⁵⁴, L. Merola^{70a,70b},
 C. Meroni^{69a}, G. Merz¹⁰⁶, O. Meshkov^{113,111}, J.K.R. Meshreki¹⁵⁰, J. Metcalfe⁶, A.S. Mete⁶, C. Meyer⁶⁶,
 J-P. Meyer¹⁴⁴, M. Michetti¹⁹, R.P. Middleton¹⁴³, L. Mijovic⁵⁰, G. Mikenberg¹⁷⁹, M. Mikesikova¹⁴⁰,
 M. Mikuž⁹², H. Mildner¹⁴⁸, A. Milic¹⁶⁶, C.D. Milke⁴², D.W. Miller³⁷, A. Milov¹⁷⁹, D.A. Milstead^{45a,45b},
 R.A. Mina¹⁵², A.A. Minaenko¹²³, I.A. Minashvili^{158b}, A.I. Mincer¹²⁵, B. Mindur^{84a}, M. Mineev⁸⁰,
 Y. Minegishi¹⁶², L.M. Mir¹⁴, M. Mironova¹³⁴, A. Mirto^{68a,68b}, K.P. Mistry¹³⁶, T. Mitani¹⁷⁸,

J. Mitrevski¹¹⁴, V.A. Mitsou¹⁷³, M. Mittal^{60c}, O. Miu¹⁶⁶, A. Miucci²⁰, P.S. Miyagawa⁹³, A. Mizukami⁸², J.U. Mjörnmark⁹⁷, T. Mkrtchyan^{61a}, M. Mlynarikova¹⁴², T. Moa^{45a,45b}, S. Mobius⁵³, K. Mochizuki¹¹⁰, P. Mogg¹¹⁴, S. Mohapatra³⁹, R. Moles-Valls²⁴, K. Mönig⁴⁶, E. Monnier¹⁰², A. Montalbano¹⁵¹, J. Montejo Berlingen³⁶, M. Montella⁹⁵, F. Monticelli⁸⁹, S. Monzani^{69a}, N. Morange⁶⁵, A.L. Moreira De Carvalho^{139a}, D. Moreno^{22a}, M. Moreno Llácer¹⁷³, C. Moreno Martinez¹⁴, P. Morettini^{55b}, M. Morgenstern¹⁵⁹, S. Morgenstern⁴⁸, D. Mori¹⁵¹, M. Morii⁵⁹, M. Morinaga¹⁷⁸, V. Morisbak¹³³, A.K. Morley³⁶, G. Mornacchi³⁶, A.P. Morris⁹⁵, L. Morvaj¹⁵⁴, P. Moschovakos³⁶, B. Moser¹²⁰, M. Mosidze^{158b}, T. Moskalets¹⁴⁴, J. Moss^{31,m}, E.J.W. Moyse¹⁰³, S. Muanza¹⁰², J. Mueller¹³⁸, R.S.P. Mueller¹¹⁴, D. Muenstermann⁹⁰, G.A. Mullier⁹⁷, D.P. Mungo^{69a,69b}, J.L. Munoz Martinez¹⁴, F.J. Munoz Sanchez¹⁰¹, P. Murin^{28b}, W.J. Murray^{177,143}, A. Murrone^{69a,69b}, J.M. Muse¹²⁸, M. Muškinja¹⁸, C. Mwewa^{33a}, A.G. Myagkov^{123,ag}, A.A. Myers¹³⁸, G. Myers⁶⁶, J. Myers¹³¹, M. Myska¹⁴¹, B.P. Nachman¹⁸, O. Nackenhorst⁴⁷, A.Nag Nag⁴⁸, K. Nagai¹³⁴, K. Nagano⁸², Y. Nagasaka⁶², J.L. Nagle²⁹, E. Nagy¹⁰², A.M. Nairz³⁶, Y. Nakahama¹¹⁷, K. Nakamura⁸², T. Nakamura¹⁶², H. Nanjo¹³², F. Napolitano^{61a}, R.F. Naranjo Garcia⁴⁶, R. Narayan⁴², I. Naryshkin¹³⁷, T. Naumann⁴⁶, G. Navarro^{22a}, P.Y. Nechaeva¹¹¹, F. Nechansky⁴⁶, T.J. Neep²¹, A. Negri^{71a,71b}, M. Negrini^{23b}, C. Nellist¹¹⁹, C. Nelson¹⁰⁴, M.E. Nelson^{45a,45b}, S. Nemecek¹⁴⁰, M. Nessi^{36,e}, M.S. Neubauer¹⁷², F. Neuhaus¹⁰⁰, M. Neumann¹⁸¹, R. Newhouse¹⁷⁴, P.R. Newman²¹, C.W. Ng¹³⁸, Y.S. Ng¹⁹, Y.W.Y. Ng¹⁷⁰, B. Ngair^{35e}, H.D.N. Nguyen¹⁰², T. Nguyen Manh¹¹⁰, E. Nibigira³⁸, R.B. Nickerson¹³⁴, R. Nicolaidou¹⁴⁴, D.S. Nielsen⁴⁰, J. Nielsen¹⁴⁵, M. Niemeyer⁵³, N. Nikipforou¹¹, V. Nikolaenko^{123,ag}, I. Nikolic-Audit¹³⁵, K. Nikolopoulos²¹, P. Nilsson²⁹, H.R. Nindhito⁵⁴, Y. Ninomiya⁸², A. Nisati^{73a}, N. Nishu^{60c}, R. Nisius¹¹⁵, I. Nitsche⁴⁷, T. Nitta¹⁷⁸, T. Nobe¹⁶², D.L. Noel³², Y. Noguchi⁸⁶, I. Nomidis¹³⁵, M.A. Nomura²⁹, M. Nordberg³⁶, J. Novak⁹², T. Novak⁹², O. Novgorodova⁴⁸, R. Novotny¹⁴¹, L. Nozka¹³⁰, K. Ntekas¹⁷⁰, E. Nurse⁹⁵, F.G. Oakham^{34,al}, H. Oberlack¹¹⁵, J. Ocariz¹³⁵, A. Ochi⁸³, I. Ochoa³⁹, J.P. Ochoa-Ricoux^{146a}, K. O'Connor²⁶, S. Oda⁸⁸, S. Odaka⁸², S. Oerdek⁵³, A. Ogrodnik^{84a}, A. Oh¹⁰¹, C.C. Ohm¹⁵³, H. Oide¹⁶⁴, M.L. Ojeda¹⁶⁶, H. Okawa¹⁶⁸, Y. Okazaki⁸⁶, M.W. O'Keefe⁹¹, Y. Okumura¹⁶², T. Okuyama⁸², A. Olariu^{27b}, L.F. Oleiro Seabra^{139a}, S.A. Olivares Pino^{146a}, D. Oliveira Damazio²⁹, J.L. Oliver¹, M.J.R. Olsson¹⁷⁰, A. Olszewski⁸⁵, J. Olszowska⁸⁵, Ö.O. Öncel²⁴, D.C. O'Neil¹⁵¹, A.P. O'Neill¹³⁴, A. Onofre^{139a,139e}, P.U.E. Onyisi¹¹, H. Oppen¹³³, R.G. Oreamuno Madriz¹²¹, M.J. Oreglia³⁷, G.E. Orellana⁸⁹, D. Orestano^{75a,75b}, N. Orlando¹⁴, R.S. Orr¹⁶⁶, V. O'Shea⁵⁷, R. Ospanov^{60a}, G. Otero y Garzon³⁰, H. Otono⁸⁸, P.S. Ott^{61a}, G.J. Ottino¹⁸, M. Ouchrif^{35d}, J. Ouellette²⁹, F. Ould-Saada¹³³, A. Ouraou¹⁴⁴, Q. Ouyang^{15a}, M. Owen⁵⁷, R.E. Owen¹⁴³, V.E. Ozcan^{12c}, N. Ozturk⁸, J. Pacalt¹³⁰, H.A. Pacey³², K. Pachal⁴⁹, A. Pacheco Pages¹⁴, C. Padilla Aranda¹⁴, S. Pagan Griso¹⁸, G. Palacino⁶⁶, S. Palazzo⁵⁰, S. Palestini³⁶, M. Palka^{84b}, P. Palni^{84a}, C.E. Pandini⁵⁴, J.G. Panduro Vazquez⁹⁴, P. Pani⁴⁶, G. Panizzo^{67a,67c}, L. Paolozzi⁵⁴, C. Papadatos¹¹⁰, K. Papageorgiou^{9,g}, S. Parajuli⁴², A. Paramonov⁶, C. Paraskevopoulos¹⁰, D. Paredes Hernandez^{63b}, S.R. Paredes Saenz¹³⁴, B. Parida¹⁷⁹, T.H. Park¹⁶⁶, A.J. Parker³¹, M.A. Parker³², F. Parodi^{55b,55a}, E.W. Parrish¹²¹, J.A. Parsons³⁹, U. Parzefall⁵², L. Pascual Dominguez¹³⁵, V.R. Pascuzzi¹⁸, J.M.P. Pasner¹⁴⁵, F. Pasquali¹²⁰, E. Pasqualucci^{73a}, S. Passaggio^{55b}, F. Pastore⁹⁴, P. Pasuwan^{45a,45b}, S. Patariaia¹⁰⁰, J.R. Pater¹⁰¹, A. Pathak^{180,i}, J. Patton⁹¹, T. Pauly³⁶, J. Parkes¹⁵², B. Pearson¹¹⁵, M. Pedersen¹³³, L. Pedraza Diaz¹¹⁹, R. Pedro^{139a}, T. Peiffer⁵³, S.V. Peleganchuk^{122b,122a}, O. Penc¹⁴⁰, H. Peng^{60a}, B.S. Peralva^{81a}, M.M. Perego⁶⁵, A.P. Pereira Peixoto^{139a}, L. Pereira Sanchez^{45a,45b}, D.V. Perepelitsa²⁹, E. Perez Codina^{167a}, F. Peri¹⁹, L. Perini^{69a,69b}, H. Pernegger³⁶, S. Perrella³⁶, A. Perrevoort¹²⁰, K. Peters⁴⁶, R.F.Y. Peters¹⁰¹, B.A. Petersen³⁶, T.C. Petersen⁴⁰, E. Petit¹⁰², V. Petousis¹⁴¹, A. Petridis¹, C. Petridou¹⁶¹, P. Petroff⁶⁵, F. Petrucci^{75a,75b}, M. Pettee¹⁸², N.E. Pettersson¹⁰³, K. Petukhova¹⁴², A. Peyaud¹⁴⁴, R. Pezoa^{146d}, L. Pezzotti^{71a,71b}, T. Pham¹⁰⁵, F.H. Phillips¹⁰⁷, P.W. Phillips¹⁴³, M.W. Phipps¹⁷², G. Piacquadio¹⁵⁴, E. Pianori¹⁸, A. Picazio¹⁰³, R.H. Pickles¹⁰¹, R. Piegai³⁰, D. Pietreanu^{27b}, J.E. Pilcher³⁷, A.D. Pilkington¹⁰¹, M. Pinamonti^{67a,67c}, J.L. Pinfold³, C. Pitman Donaldson⁹⁵, M. Pitt¹⁶⁰, L. Pizzimento^{74a,74b}, A. Pizzini¹²⁰, M.-A. Pleier²⁹, V. Plesanovs⁵²,

V. Pleskot¹⁴², E. Plotnikova⁸⁰, P. Podberezko^{122b,122a}, R. Poettgen⁹⁷, R. Poggi⁵⁴, L. Poggioli¹³⁵, I. Pogrebnyak¹⁰⁷, D. Pohl²⁴, I. Pokharel⁵³, G. Polesello^{71a}, A. Poley^{151,167a}, A. Policicchio^{73a,73b}, R. Polifka¹⁴², A. Polini^{23b}, C.S. Pollard⁴⁶, V. Polychronakos²⁹, D. Ponomarenko¹¹², L. Pontecorvo³⁶, S. Popa^{27a}, G.A. Popeneciu^{27d}, L. Portales⁵, D.M. Portillo Quintero⁵⁸, S. Pospisil¹⁴¹, K. Potamianos⁴⁶, I.N. Potrap⁸⁰, C.J. Potter³², H. Potti¹¹, T. Poulsen⁹⁷, J. Poveda¹⁷³, T.D. Powell¹⁴⁸, G. Pownall⁴⁶, M.E. Pozo Astigarraga³⁶, P. Pralavorio¹⁰², S. Prell⁷⁹, D. Price¹⁰¹, M. Primavera^{68a}, M.L. Proffitt¹⁴⁷, N. Proklova¹¹², K. Prokofiev^{63c}, F. Prokoshin⁸⁰, S. Protopopescu²⁹, J. Proudfoot⁶, M. Przybycien^{84a}, D. Pudzha¹³⁷, A. Puri¹⁷², P. Puzo⁶⁵, D. Pyatiizbyantseva¹¹², J. Qian¹⁰⁶, Y. Qin¹⁰¹, A. Quadt⁵³, M. Queitsch-Maitland³⁶, M. Racko^{28a}, F. Ragusa^{69a,69b}, G. Rahal⁹⁸, J.A. Raine⁵⁴, S. Rajagopalan²⁹, A. Ramirez Morales⁹³, K. Ran^{15a,15d}, D.M. Rauch⁴⁶, F. Rauscher¹¹⁴, S. Rave¹⁰⁰, B. Ravina¹⁴⁸, I. Ravinovich¹⁷⁹, J.H. Rawling¹⁰¹, M. Raymond³⁶, A.L. Read¹³³, N.P. Readioff¹⁴⁸, M. Reale^{68a,68b}, D.M. Rebuzzi^{71a,71b}, G. Redlinger²⁹, K. Reeves⁴³, J. Reichert¹³⁶, D. Reikher¹⁶⁰, A. Reiss¹⁰⁰, A. Rej¹⁵⁰, C. Rembser³⁶, A. Renardi⁴⁶, M. Renda^{27b}, M.B. Rendel¹¹⁵, A.G. Rennie⁵⁷, S. Resconi^{69a}, E.D. Resseguie¹⁸, S. Rettie⁹⁵, B. Reynolds¹²⁷, E. Reynolds²¹, O.L. Rezanova^{122b,122a}, P. Reznicek¹⁴², E. Ricci^{76a,76b}, R. Richter¹¹⁵, S. Richter⁴⁶, E. Richter-Was^{84b}, M. Ridel¹³⁵, P. Rieck¹¹⁵, O. Rifki⁴⁶, M. Rijssenbeek¹⁵⁴, A. Rimoldi^{71a,71b}, M. Rimoldi⁴⁶, L. Rinaldi^{23b}, T.T. Rinn¹⁷², G. Ripellino¹⁵³, I. Riu¹⁴, P. Rivadeneira⁴⁶, J.C. Rivera Vergara¹⁷⁵, F. Rizatdinova¹²⁹, E. Rizvi⁹³, C. Rizzi³⁶, S.H. Robertson^{104,ab}, M. Robin⁴⁶, D. Robinson³², C.M. Robles Gajardo^{146d}, M. Robles Manzano¹⁰⁰, A. Robson⁵⁷, A. Rocchi^{74a,74b}, E. Rocco¹⁰⁰, C. Roda^{72a,72b}, S. Rodriguez Bosca¹⁷³, A.M. Rodriguez Vera^{167b}, S. Roe³⁶, J. Roggel¹⁸¹, O. Røhne¹³³, R. Röhrig¹¹⁵, R.A. Rojas^{146d}, B. Roland⁵², C.P.A. Roland⁶⁶, J. Roloff²⁹, A. Romaniouk¹¹², M. Romano^{23b,23a}, N. Rompotis⁹¹, M. Ronzani¹²⁵, L. Roos¹³⁵, S. Rosati^{73a}, G. Rosin¹⁰³, B.J. Rosser¹³⁶, E. Rossi⁴⁶, E. Rossi^{75a,75b}, E. Rossi^{70a,70b}, L.P. Rossi^{55b}, L. Rossini⁴⁶, R. Rosten¹⁴, M. Rotaru^{27b}, B. Rottler⁵², D. Rousseau⁶⁵, G. Rovelli^{71a,71b}, A. Roy¹¹, D. Roy^{33e}, A. Rozanov¹⁰², Y. Rozen¹⁵⁹, X. Ruan^{33e}, T.A. Ruggeri¹, F. Rühr⁵², A. Ruiz-Martinez¹⁷³, A. Rummeler³⁶, Z. Rurikova⁵², N.A. Rusakovich⁸⁰, H.L. Russell¹⁰⁴, L. Rustige^{38,47}, J.P. Rutherford⁷, E.M. Rüttinger¹⁴⁸, M. Rybar¹⁴², G. Rybkin⁶⁵, E.B. Rye¹³³, A. Ryzhov¹²³, J.A. Sabater Iglesias⁴⁶, P. Sabatini⁵³, L. Sabetta^{73a,73b}, S. Sacerdoti⁶⁵, H.F.W. Sadrozinski¹⁴⁵, R. Sadykov⁸⁰, F. Safai Tehrani^{73a}, B. Safarzadeh Samani¹⁵⁵, M. Safdari¹⁵², P. Saha¹²¹, S. Saha¹⁰⁴, M. Sahinsoy¹¹⁵, A. Sahu¹⁸¹, M. Saimpert³⁶, M. Saito¹⁶², T. Saito¹⁶², H. Sakamoto¹⁶², D. Salamani⁵⁴, G. Salamanna^{75a,75b}, A. Salnikov¹⁵², J. Salt¹⁷³, A. Salvador Salas¹⁴, D. Salvatore^{41b,41a}, F. Salvatore¹⁵⁵, A. Salvucci^{63a,63b,63c}, A. Salzburger³⁶, J. Samarati³⁶, D. Sammel⁵², D. Sampsonidis¹⁶¹, D. Sampsonidou¹⁶¹, J. Sánchez¹⁷³, A. Sanchez Pineda^{67a,36,67c}, H. Sandaker¹³³, C.O. Sander⁴⁶, I.G. Sanderswood⁹⁰, M. Sandhoff¹⁸¹, C. Sandoval^{22b}, D.P.C. Sankey¹⁴³, M. Sannino^{55b,55a}, Y. Sano¹¹⁷, A. Sansoni⁵¹, C. Santoni³⁸, H. Santos^{139a,139b}, S.N. Santpur¹⁸, A. Santra¹⁷³, K.A. Saoucha¹⁴⁸, A. Sapronov⁸⁰, J.G. Saraiva^{139a,139d}, O. Sasaki⁸², K. Sato¹⁶⁸, F. Sauerburger⁵², E. Sauvan⁵, P. Savard^{166,al}, R. Sawada¹⁶², C. Sawyer¹⁴³, L. Sawyer^{96,af}, I. Sayago Galvan¹⁷³, C. Sbarra^{23b}, A. Sbrizzi^{67a,67c}, T. Scanlon⁹⁵, J. Schaarschmidt¹⁴⁷, P. Schacht¹¹⁵, D. Schaefer³⁷, L. Schaefer¹³⁶, S. Schaepe³⁶, U. Schäfer¹⁰⁰, A.C. Schaffer⁶⁵, D. Schaile¹¹⁴, R.D. Schamberger¹⁵⁴, E. Schanet¹¹⁴, C. Scharf¹⁹, N. Scharmberg¹⁰¹, V.A. Schegelsky¹³⁷, D. Scheirich¹⁴², F. Schenck¹⁹, M. Schernau¹⁷⁰, C. Schiavi^{55b,55a}, L.K. Schildgen²⁴, Z.M. Schillaci²⁶, E.J. Schioppa^{68a,68b}, M. Schioppa^{41b,41a}, K.E. Schleicher⁵², S. Schlenker³⁶, K.R. Schmidt-Sommerfeld¹¹⁵, K. Schmieden³⁶, C. Schmitt¹⁰⁰, S. Schmitt⁴⁶, J.C. Schmoedel⁴⁶, L. Schoeffel¹⁴⁴, A. Schoening^{61b}, P.G. Scholer⁵², E. Schopf¹³⁴, M. Schott¹⁰⁰, J.F.P. Schouwenberg¹¹⁹, J. Schovancova³⁶, S. Schramm⁵⁴, F. Schroeder¹⁸¹, A. Schulte¹⁰⁰, H-C. Schultz-Coulon^{61a}, M. Schumacher⁵², B.A. Schumm¹⁴⁵, Ph. Schune¹⁴⁴, A. Schwartzman¹⁵², T.A. Schwarz¹⁰⁶, Ph. Schwemling¹⁴⁴, R. Schwienhorst¹⁰⁷, A. Sciandra¹⁴⁵, G. Sciolla²⁶, M. Scornajenghi^{41b,41a}, F. Scuri^{72a}, F. Scutti¹⁰⁵, L.M. Scyboz¹¹⁵, C.D. Sebastiani⁹¹, P. Seema¹⁹, S.C. Seidel¹¹⁸, A. Seiden¹⁴⁵, B.D. Seidlitz²⁹, T. Seiss³⁷, C. Seitz⁴⁶, J.M. Seixas^{81b}, G. Sekhniaidze^{70a}, S.J. Sekula⁴², N. Semprini-Cesari^{23b,23a}, S. Sen⁴⁹, C. Serfon²⁹, L. Serin⁶⁵, L. Serkin^{67a,67b}, M. Sessa^{60a}, H. Severini¹²⁸, S. Sevova¹⁵², F. Sforza^{55b,55a},

A. Sfyrla⁵⁴, E. Shabalina⁵³, J.D. Shahinian¹⁴⁵, N.W. Shaikh^{45a,45b}, D. Shaked Renous¹⁷⁹, L.Y. Shan^{15a},
 M. Shapiro¹⁸, A. Sharma¹³⁴, A.S. Sharma¹, P.B. Shatalov¹²⁴, K. Shaw¹⁵⁵, S.M. Shaw¹⁰¹, M. Shehade¹⁷⁹,
 Y. Shen¹²⁸, A.D. Sherman²⁵, P. Sherwood⁹⁵, L. Shi⁹⁵, S. Shimizu⁸², C.O. Shimmin¹⁸², Y. Shimogama¹⁷⁸,
 M. Shimojima¹¹⁶, I.P.J. Shipsey¹³⁴, S. Shirabe¹⁶⁴, M. Shiyakova^{80,z}, J. Shlomi¹⁷⁹, A. Shmeleva¹¹¹,
 M.J. Shochet³⁷, J. Shojaii¹⁰⁵, D.R. Shope¹⁵³, S. Shrestha¹²⁷, E.M. Shrif^{33e}, E. Shulga¹⁷⁹, P. Sicho¹⁴⁰,
 A.M. Sickles¹⁷², E. Sideras Haddad^{33e}, O. Sidiropoulou³⁶, A. Sidoti^{23b,23a}, F. Siegert⁴⁸, Dj. Sijacki¹⁶,
 M.Jr. Silva¹⁸⁰, M.V. Silva Oliveira³⁶, S.B. Silverstein^{45a}, S. Simion⁶⁵, R. Simoniello¹⁰⁰,
 C.J. Simpson-allsoy²¹, S. Simsek^{12b}, P. Sinervo¹⁶⁶, V. Sinetckii¹¹³, S. Singh¹⁵¹, M. Sioli^{23b,23a}, I. Siral¹³¹,
 S.Yu. Sivoklov¹¹³, J. Sjölin^{45a,45b}, A. Skaf⁵³, E. Skorda⁹⁷, P. Skubic¹²⁸, M. Slawinska⁸⁵, K. Sliwa¹⁶⁹,
 R. Slovak¹⁴², V. Smakhtin¹⁷⁹, B.H. Smart¹⁴³, J. Smiesko^{28b}, N. Smirnov¹¹², S.Yu. Smirnov¹¹²,
 Y. Smirnov¹¹², L.N. Smirnova^{113,r}, O. Smirnova⁹⁷, E.A. Smith³⁷, H.A. Smith¹³⁴, M. Smizanska⁹⁰,
 K. Smolek¹⁴¹, A. Smykiewicz⁸⁵, A.A. Snesev¹¹¹, H.L. Snoek¹²⁰, I.M. Snyder¹³¹, S. Snyder²⁹,
 R. Sobie^{175,ab}, A. Soffer¹⁶⁰, A. Sogaard⁵⁰, F. Sohns⁵³, C.A. Solans Sanchez³⁶, E.Yu. Soldatov¹¹²,
 U. Soldevila¹⁷³, A.A. Solodkov¹²³, A. Soloshenko⁸⁰, O.V. Solovyanov¹²³, V. Solovyev¹³⁷, P. Sommer¹⁴⁸,
 H. Son¹⁶⁹, W. Song¹⁴³, W.Y. Song^{167b}, A. Sopczak¹⁴¹, A.L. Sopio⁹⁵, F. Sopkova^{28b}, S. Sottocornola^{71a,71b},
 R. Soualah^{67a,67c}, A.M. Soukharev^{122b,122a}, D. South⁴⁶, S. Spagnolo^{68a,68b}, M. Spalla¹¹⁵,
 M. Spangenberg¹⁷⁷, F. Spanò⁹⁴, D. Sperlich⁵², T.M. Spieker^{61a}, G. Spigo³⁶, M. Spina¹⁵⁵, D.P. Spiteri⁵⁷,
 M. Spousta¹⁴², A. Stabile^{69a,69b}, B.L. Stamas¹²¹, R. Stamen^{61a}, M. Stamenkovic¹²⁰, E. Stanecka⁸⁵,
 B. Stanislaus¹³⁴, M.M. Stanitzki⁴⁶, M. Stankaityte¹³⁴, B. Stapi¹²⁰, E.A. Starchenko¹²³, G.H. Stark¹⁴⁵,
 J. Stark⁵⁸, P. Staroba¹⁴⁰, P. Starovoitov^{61a}, S. Stärz¹⁰⁴, R. Staszewski⁸⁵, G. Stavropoulos⁴⁴, M. Stegler⁴⁶,
 P. Steinberg²⁹, A.L. Steinhebel¹³¹, B. Stelzer^{151,167a}, H.J. Stelzer¹³⁸, O. Stelzer-Chilton^{167a}, H. Stenzel⁵⁶,
 T.J. Stevenson¹⁵⁵, G.A. Stewart³⁶, M.C. Stockton³⁶, G. Stoicea^{27b}, M. Stolarski^{139a}, S. Stonjek¹¹⁵,
 A. Straessner⁴⁸, J. Strandberg¹⁵³, S. Strandberg^{45a,45b}, M. Strauss¹²⁸, T. Strebler¹⁰², P. Strizenec^{28b},
 R. Ströhmer¹⁷⁶, D.M. Strom¹³¹, R. Stroynowski⁴², A. Strubig⁵⁰, S.A. Stucci²⁹, B. Stugu¹⁷, J. Stupak¹²⁸,
 N.A. Styles⁴⁶, D. Su¹⁵², W. Su^{60c,147}, X. Su^{60a}, V.V. Sulin¹¹¹, M.J. Sullivan⁹¹, D.M.S. Sultan⁵⁴,
 S. Sultansoy^{4c}, T. Sumida⁸⁶, S. Sun¹⁰⁶, X. Sun¹⁰¹, K. Suruliz¹⁵⁵, C.J.E. Suster¹⁵⁶, M.R. Sutton¹⁵⁵,
 S. Suzuki⁸², M. Svatos¹⁴⁰, M. Swiatlowski^{167a}, S.P. Swift², T. Swirski¹⁷⁶, A. Sydorenko¹⁰⁰, I. Sykora^{28a},
 M. Sykora¹⁴², T. Sykora¹⁴², D. Ta¹⁰⁰, K. Tackmann^{46,x}, J. Taenzer¹⁶⁰, A. Taffard¹⁷⁰, R. Tafirout^{167a},
 E. Tagiev¹²³, R. Takashima⁸⁷, K. Takeda⁸³, T. Takeshita¹⁴⁹, E.P. Takeva⁵⁰, Y. Takubo⁸², M. Talby¹⁰²,
 A.A. Talyshv^{122b,122a}, K.C. Tam^{63b}, N.M. Tamir¹⁶⁰, J. Tanaka¹⁶², R. Tanaka⁶⁵, S. Tapia Araya¹⁷²,
 S. Tapprogge¹⁰⁰, A. Tarek Abouelfadl Mohamed¹⁰⁷, S. Tarem¹⁵⁹, K. Tariq^{60b}, G. Tarna^{27b,d},
 G.F. Tartarelli^{69a}, P. Tas¹⁴², M. Tasevsky¹⁴⁰, T. Tashiro⁸⁶, E. Tassi^{41b,41a}, A. Tavares Delgado^{139a},
 Y. Tayalati^{35e}, A.J. Taylor⁵⁰, G.N. Taylor¹⁰⁵, W. Taylor^{167b}, H. Teagle⁹¹, A.S. Tee⁹⁰,
 R. Teixeira De Lima¹⁵², P. Teixeira-Dias⁹⁴, H. Ten Kate³⁶, J.J. Teoh¹²⁰, S. Terada⁸², K. Terashi¹⁶²,
 J. Terron⁹⁹, S. Terzo¹⁴, M. Testa⁵¹, R.J. Teuscher^{166,ab}, S.J. Thais¹⁸², N. Themistokleous⁵⁰,
 T. Thevenaux-Pelzer⁴⁶, F. Thiele⁴⁰, D.W. Thomas⁹⁴, J.O. Thomas⁴², J.P. Thomas²¹, E.A. Thompson⁴⁶,
 P.D. Thompson²¹, E. Thomson¹³⁶, E.J. Thorpe⁹³, R.E. Tisce Torres⁵³, V.O. Tikhomirov^{111,ah},
 Yu.A. Tikhonov^{122b,122a}, S. Timoshenko¹¹², P. Tipton¹⁸², S. Tisserant¹⁰², K. Todome^{23b,23a},
 S. Todorova-Nova¹⁴², S. Todt⁴⁸, J. Tojo⁸⁸, S. Tokár^{28a}, K. Tokushuku⁸², E. Tolley¹²⁷, R. Tombs³²,
 K.G. Tomiwa^{33e}, M. Tomoto¹¹⁷, L. Tompkins¹⁵², P. Tornambe¹⁰³, E. Torrence¹³¹, H. Torres⁴⁸,
 E. Torrò Pastor¹⁴⁷, C. Toscirì¹³⁴, J. Toth^{102,aa}, D.R. Tovey¹⁴⁸, A. Traet¹⁷, C.J. Treado¹²⁵, T. Trefzger¹⁷⁶,
 F. Tresoldi¹⁵⁵, A. Tricoli²⁹, I.M. Trigger^{167a}, S. Trincaz-Duvoid¹³⁵, D.A. Trischuk¹⁷⁴, W. Trischuk¹⁶⁶,
 B. Trocmé⁵⁸, A. Trofymov⁶⁵, C. Troncon^{69a}, F. Trovato¹⁵⁵, L. Truong^{33c}, M. Trzebinski⁸⁵, A. Trzupek⁸⁵,
 F. Tsai⁴⁶, J.C-L. Tseng¹³⁴, P.V. Tsiarshka^{108,ae}, A. Tsirigotis^{161,u}, V. Tsiskaridze¹⁵⁴, E.G. Tskhadadze^{158a},
 M. Tsopoulou¹⁶¹, I.I. Tsukerman¹²⁴, V. Tsulaia¹⁸, S. Tsuno⁸², D. Tsybychev¹⁵⁴, Y. Tu^{63b}, A. Tudorache^{27b},
 V. Tudorache^{27b}, T.T. Tulbure^{27a}, A.N. Tuna⁵⁹, S. Turchikhin⁸⁰, D. Turgeman¹⁷⁹, I. Turk Cakir^{4b,s},
 R.J. Turner²¹, R. Turra^{69a}, P.M. Tuts³⁹, S. Tzamarias¹⁶¹, E. Tzovara¹⁰⁰, K. Uchida¹⁶², F. Ukegawa¹⁶⁸,

G. Unal³⁶, M. Unal¹¹, A. Undrus²⁹, G. Unel¹⁷⁰, F.C. Ungaro¹⁰⁵, Y. Unno⁸², K. Uno¹⁶², J. Urban^{28b}, P. Urquijo¹⁰⁵, G. Usai⁸, Z. Uysal^{12d}, V. Vacek¹⁴¹, B. Vachon¹⁰⁴, K.O.H. Vadla¹³³, T. Vafeiadis³⁶, A. Vaidya⁹⁵, C. Valderanis¹¹⁴, E. Valdes Santurio^{45a,45b}, M. Valente⁵⁴, S. Valentinetti^{23b,23a}, A. Valero¹⁷³, L. Valéry⁴⁶, R.A. Vallance²¹, A. Vallier³⁶, J.A. Valls Ferrer¹⁷³, T.R. Van Daalen¹⁴, P. Van Gemmeren⁶, S. Van Stroud⁹⁵, I. Van Vulpen¹²⁰, M. Vanadia^{74a,74b}, W. Vandelli³⁶, M. Vandembroucke¹⁴⁴, E.R. Vandewall¹²⁹, A. Vaniachine¹⁶⁵, D. Vannicola^{73a,73b}, R. Vari^{73a}, E.W. Varnes⁷, C. Varni^{55b,55a}, T. Varol¹⁵⁷, D. Varouchas⁶⁵, K.E. Varvell¹⁵⁶, M.E. Vasile^{27b}, G.A. Vasquez¹⁷⁵, F. Vazeille³⁸, D. Vazquez Furelos¹⁴, T. Vazquez Schroeder³⁶, J. Veatch⁵³, V. Vecchio¹⁰¹, M.J. Veen¹²⁰, L.M. Veloce¹⁶⁶, F. Veloso^{139a,139c}, S. Veneziano^{73a}, A. Ventura^{68a,68b}, A. Verbytskyi¹¹⁵, V. Vercesi^{71a}, M. Verducci^{72a,72b}, C.M. Vergel Infante⁷⁹, C. Vergis²⁴, W. Verkerke¹²⁰, A.T. Vermeulen¹²⁰, J.C. Vermeulen¹²⁰, C. Vernieri¹⁵², P.J. Verschuuren⁹⁴, M.C. Vetterli^{151,al}, N. Viaux Maira^{146d}, T. Vickey¹⁴⁸, O.E. Vickey Boeriu¹⁴⁸, G.H.A. Viehhauser¹³⁴, L. Vigani^{61b}, M. Villa^{23b,23a}, M. Villaplana Perez³, E.M. Villhauer⁵⁰, E. Vilucchi⁵¹, M.G. Vinciter³⁴, G.S. Virdee²¹, A. Vishwakarma⁵⁰, C. Vittori^{23b,23a}, I. Vivarelli¹⁵⁵, M. Vogel¹⁸¹, P. Vokac¹⁴¹, S.E. von Buddenbrock^{33e}, E. Von Toerne²⁴, V. Vorobel¹⁴², K. Vorobev¹¹², M. Vos¹⁷³, J.H. Vosseveld⁹¹, M. Vozak¹⁰¹, N. Vranjes¹⁶, M. Vranjes Milosavljevic¹⁶, V. Vrba¹⁴¹, M. Vreeswijk¹²⁰, N.K. Vu¹⁰², R. Vuillermet³⁶, I. Vukotic³⁷, S. Wada¹⁶⁸, P. Wagner²⁴, W. Wagner¹⁸¹, J. Wagner-Kuhr¹¹⁴, S. Wahdan¹⁸¹, H. Wahlberg⁸⁹, R. Wakasa¹⁶⁸, V.M. Walbrecht¹¹⁵, J. Walder¹⁴³, R. Walker¹¹⁴, S.D. Walker⁹⁴, W. Walkowiak¹⁵⁰, V. Wallangen^{45a,45b}, A.M. Wang⁵⁹, A.Z. Wang¹⁸⁰, C. Wang^{60a}, C. Wang^{60c}, F. Wang¹⁸⁰, H. Wang¹⁸, H. Wang³, J. Wang^{63a}, P. Wang⁴², Q. Wang¹²⁸, R.-J. Wang¹⁰⁰, R. Wang^{60a}, R. Wang⁶, S.M. Wang¹⁵⁷, W.T. Wang^{60a}, W. Wang^{15c}, W.X. Wang^{60a}, Y. Wang^{60a}, Z. Wang¹⁰⁶, C. Wanotayaroj⁴⁶, A. Warburton¹⁰⁴, C.P. Ward³², D.R. Wardrope⁹⁵, N. Warrack⁵⁷, A.T. Watson²¹, M.F. Watson²¹, G. Watts¹⁴⁷, B.M. Waugh⁹⁵, A.F. Webb¹¹, C. Weber²⁹, M.S. Weber²⁰, S.A. Weber³⁴, S.M. Weber^{61a}, A.R. Weidberg¹³⁴, J. Weingarten⁴⁷, M. Weirich¹⁰⁰, C. Weiser⁵², P.S. Wells³⁶, T. Wenaus²⁹, B. Wendland⁴⁷, T. Wengler³⁶, S. Wenig³⁶, N. Wermes²⁴, M. Wessels^{61a}, T.D. Weston²⁰, K. Whalen¹³¹, A.M. Wharton⁹⁰, A.S. White¹⁰⁶, A. White⁸, M.J. White¹, D. Whiteson¹⁷⁰, B.W. Whitmore⁹⁰, W. Wiedenmann¹⁸⁰, C. Wiel⁴⁸, M. Wielers¹⁴³, N. Wieseotte¹⁰⁰, C. Wiglesworth⁴⁰, L.A.M. Wiik-Fuchs⁵², H.G. Wilkens³⁶, L.J. Wilkins⁹⁴, H.H. Williams¹³⁶, S. Williams³², S. Willocq¹⁰³, P.J. Windischhofer¹³⁴, I. Wingerter-Seez⁵, E. Winkels¹⁵⁵, F. Winklmeier¹³¹, B.T. Winter⁵², M. Wittgen¹⁵², M. Wobisch⁹⁶, A. Wolf¹⁰⁰, R. Wölker¹³⁴, J. Wollrath⁵², M.W. Wolter⁸⁵, H. Wolters^{139a,139c}, V.W.S. Wong¹⁷⁴, N.L. Woods¹⁴⁵, S.D. Worm⁴⁶, B.K. Wosiek⁸⁵, K.W. Woźniak⁸⁵, K. Wraight⁵⁷, S.L. Wu¹⁸⁰, X. Wu⁵⁴, Y. Wu^{60a}, J. Wuerzinger¹³⁴, T.R. Wyatt¹⁰¹, B.M. Wynne⁵⁰, S. Xella⁴⁰, L. Xia¹⁷⁷, J. Xiang^{63c}, X. Xiao¹⁰⁶, X. Xie^{60a}, I. Xiotidis¹⁵⁵, D. Xu^{15a}, H. Xu^{60a}, H. Xu^{60a}, L. Xu²⁹, T. Xu¹⁴⁴, W. Xu¹⁰⁶, Z. Xu^{60b}, Z. Xu¹⁵², B. Yabsley¹⁵⁶, S. Yacoub^{33a}, K. Yajima¹³², D.P. Yallup⁹⁵, N. Yamaguchi⁸⁸, Y. Yamaguchi¹⁶⁴, A. Yamamoto⁸², M. Yamatani¹⁶², T. Yamazaki¹⁶², Y. Yamazaki⁸³, J. Yan^{60c}, Z. Yan²⁵, H.J. Yang^{60c,60d}, H.T. Yang¹⁸, S. Yang^{60a}, T. Yang^{63c}, X. Yang^{60b,58}, Y. Yang¹⁶², Z. Yang^{60a}, W.-M. Yao¹⁸, Y.C. Yap⁴⁶, Y. Yasu⁸², E. Yatsenko^{60c}, H. Ye^{15c}, J. Ye⁴², S. Ye²⁹, I. Yeletsikh⁸⁰, M.R. Yexley⁹⁰, E. Yigitbasi²⁵, P. Yin³⁹, K. Yorita¹⁷⁸, K. Yoshihara⁷⁹, C.J.S. Young³⁶, C. Young¹⁵², J. Yu⁷⁹, R. Yuan^{60b,h}, X. Yue^{61a}, M. Zaazoua^{35e}, B. Zabinski⁸⁵, G. Zacharis¹⁰, E. Zaffaroni⁵⁴, J. Zahreddine¹³⁵, A.M. Zaitsev^{123,ag}, T. Zakareishvili^{158b}, N. Zakharchuk³⁴, S. Zambito³⁶, D. Zanzi³⁶, D.R. Zaripovas⁵⁷, S.V. Zeißner⁴⁷, C. Zeitnitz¹⁸¹, G. Zemaityte¹³⁴, J.C. Zeng¹⁷², O. Zenin¹²³, T. Ženiš^{28a}, D. Zerwas⁶⁵, M. Zgubić¹³⁴, B. Zhang^{15c}, D.F. Zhang^{15b}, G. Zhang^{15b}, J. Zhang⁶, Kaili. Zhang^{15a}, L. Zhang^{15c}, L. Zhang^{60a}, M. Zhang¹⁷², R. Zhang¹⁸⁰, S. Zhang¹⁰⁶, X. Zhang^{60c}, X. Zhang^{60b}, Y. Zhang^{15a,15d}, Z. Zhang^{63a}, Z. Zhang⁶⁵, P. Zhao⁴⁹, Z. Zhao^{60a}, A. Zhemchugov⁸⁰, Z. Zheng¹⁰⁶, D. Zhong¹⁷², B. Zhou¹⁰⁶, C. Zhou¹⁸⁰, H. Zhou⁷, M.S. Zhou^{15a,15d}, M. Zhou¹⁵⁴, N. Zhou^{60c}, Y. Zhou⁷, C.G. Zhu^{60b}, C. Zhu^{15a,15d}, H.L. Zhu^{60a}, H. Zhu^{15a}, J. Zhu¹⁰⁶, Y. Zhu^{60a}, X. Zhuang^{15a}, K. Zhukov¹¹¹, V. Zhulanov^{122b,122a}, D. Ziemska⁶⁶, N.I. Zimine⁸⁰, S. Zimmermann⁵², Z. Zinonos¹¹⁵, M. Ziolkowski¹⁵⁰, L. Živković¹⁶, G. Zobernig¹⁸⁰, A. Zoccoli^{23b,23a}, K. Zoch⁵³, T.G. Zorbas¹⁴⁸, R. Zou³⁷, L. Zwalinski³⁶.

- ¹Department of Physics, University of Adelaide, Adelaide; Australia.
- ²Physics Department, SUNY Albany, Albany NY; United States of America.
- ³Department of Physics, University of Alberta, Edmonton AB; Canada.
- ⁴(^a)Department of Physics, Ankara University, Ankara; (^b)Istanbul Aydin University, Application and Research Center for Advanced Studies, Istanbul; (^c)Division of Physics, TOBB University of Economics and Technology, Ankara; Turkey.
- ⁵LAPP, Université Grenoble Alpes, Université Savoie Mont Blanc, CNRS/IN2P3, Annecy; France.
- ⁶High Energy Physics Division, Argonne National Laboratory, Argonne IL; United States of America.
- ⁷Department of Physics, University of Arizona, Tucson AZ; United States of America.
- ⁸Department of Physics, University of Texas at Arlington, Arlington TX; United States of America.
- ⁹Physics Department, National and Kapodistrian University of Athens, Athens; Greece.
- ¹⁰Physics Department, National Technical University of Athens, Zografou; Greece.
- ¹¹Department of Physics, University of Texas at Austin, Austin TX; United States of America.
- ¹²(^a)Bahcesehir University, Faculty of Engineering and Natural Sciences, Istanbul; (^b)Istanbul Bilgi University, Faculty of Engineering and Natural Sciences, Istanbul; (^c)Department of Physics, Bogazici University, Istanbul; (^d)Department of Physics Engineering, Gaziantep University, Gaziantep; Turkey.
- ¹³Institute of Physics, Azerbaijan Academy of Sciences, Baku; Azerbaijan.
- ¹⁴Institut de Física d'Altes Energies (IFAE), Barcelona Institute of Science and Technology, Barcelona; Spain.
- ¹⁵(^a)Institute of High Energy Physics, Chinese Academy of Sciences, Beijing; (^b)Physics Department, Tsinghua University, Beijing; (^c)Department of Physics, Nanjing University, Nanjing; (^d)University of Chinese Academy of Science (UCAS), Beijing; China.
- ¹⁶Institute of Physics, University of Belgrade, Belgrade; Serbia.
- ¹⁷Department for Physics and Technology, University of Bergen, Bergen; Norway.
- ¹⁸Physics Division, Lawrence Berkeley National Laboratory and University of California, Berkeley CA; United States of America.
- ¹⁹Institut für Physik, Humboldt Universität zu Berlin, Berlin; Germany.
- ²⁰Albert Einstein Center for Fundamental Physics and Laboratory for High Energy Physics, University of Bern, Bern; Switzerland.
- ²¹School of Physics and Astronomy, University of Birmingham, Birmingham; United Kingdom.
- ²²(^a)Facultad de Ciencias y Centro de Investigaciones, Universidad Antonio Nariño, Bogotá; (^b)Departamento de Física, Universidad Nacional de Colombia, Bogotá, Colombia; Colombia.
- ²³(^a)INFN Bologna and Università di Bologna, Dipartimento di Fisica; (^b)INFN Sezione di Bologna; Italy.
- ²⁴Physikalisches Institut, Universität Bonn, Bonn; Germany.
- ²⁵Department of Physics, Boston University, Boston MA; United States of America.
- ²⁶Department of Physics, Brandeis University, Waltham MA; United States of America.
- ²⁷(^a)Transilvania University of Brasov, Brasov; (^b)Horia Hulubei National Institute of Physics and Nuclear Engineering, Bucharest; (^c)Department of Physics, Alexandru Ioan Cuza University of Iasi, Iasi; (^d)National Institute for Research and Development of Isotopic and Molecular Technologies, Physics Department, Cluj-Napoca; (^e)University Politehnica Bucharest, Bucharest; (^f)West University in Timisoara, Timisoara; Romania.
- ²⁸(^a)Faculty of Mathematics, Physics and Informatics, Comenius University, Bratislava; (^b)Department of Subnuclear Physics, Institute of Experimental Physics of the Slovak Academy of Sciences, Kosice; Slovak Republic.
- ²⁹Physics Department, Brookhaven National Laboratory, Upton NY; United States of America.
- ³⁰Departamento de Física, Universidad de Buenos Aires, Buenos Aires; Argentina.
- ³¹California State University, CA; United States of America.

- ³²Cavendish Laboratory, University of Cambridge, Cambridge; United Kingdom.
- ³³(^a)Department of Physics, University of Cape Town, Cape Town; (^b)iThemba Labs, Western Cape; (^c)Department of Mechanical Engineering Science, University of Johannesburg, Johannesburg; (^d)University of South Africa, Department of Physics, Pretoria; (^e)School of Physics, University of the Witwatersrand, Johannesburg; South Africa.
- ³⁴Department of Physics, Carleton University, Ottawa ON; Canada.
- ³⁵(^a)Faculté des Sciences Ain Chock, Réseau Universitaire de Physique des Hautes Energies - Université Hassan II, Casablanca; (^b)Faculté des Sciences, Université Ibn-Tofail, Kénitra; (^c)Faculté des Sciences Semlalia, Université Cadi Ayyad, LPHEA-Marrakech; (^d)Faculté des Sciences, Université Mohamed Premier and LPTPM, Oujda; (^e)Faculté des sciences, Université Mohammed V, Rabat; Morocco.
- ³⁶CERN, Geneva; Switzerland.
- ³⁷Enrico Fermi Institute, University of Chicago, Chicago IL; United States of America.
- ³⁸LPC, Université Clermont Auvergne, CNRS/IN2P3, Clermont-Ferrand; France.
- ³⁹Nevis Laboratory, Columbia University, Irvington NY; United States of America.
- ⁴⁰Niels Bohr Institute, University of Copenhagen, Copenhagen; Denmark.
- ⁴¹(^a)Dipartimento di Fisica, Università della Calabria, Rende; (^b)INFN Gruppo Collegato di Cosenza, Laboratori Nazionali di Frascati; Italy.
- ⁴²Physics Department, Southern Methodist University, Dallas TX; United States of America.
- ⁴³Physics Department, University of Texas at Dallas, Richardson TX; United States of America.
- ⁴⁴National Centre for Scientific Research "Demokritos", Agia Paraskevi; Greece.
- ⁴⁵(^a)Department of Physics, Stockholm University; (^b)Oskar Klein Centre, Stockholm; Sweden.
- ⁴⁶Deutsches Elektronen-Synchrotron DESY, Hamburg and Zeuthen; Germany.
- ⁴⁷Lehrstuhl für Experimentelle Physik IV, Technische Universität Dortmund, Dortmund; Germany.
- ⁴⁸Institut für Kern- und Teilchenphysik, Technische Universität Dresden, Dresden; Germany.
- ⁴⁹Department of Physics, Duke University, Durham NC; United States of America.
- ⁵⁰SUPA - School of Physics and Astronomy, University of Edinburgh, Edinburgh; United Kingdom.
- ⁵¹INFN e Laboratori Nazionali di Frascati, Frascati; Italy.
- ⁵²Physikalisches Institut, Albert-Ludwigs-Universität Freiburg, Freiburg; Germany.
- ⁵³II. Physikalisches Institut, Georg-August-Universität Göttingen, Göttingen; Germany.
- ⁵⁴Département de Physique Nucléaire et Corpusculaire, Université de Genève, Genève; Switzerland.
- ⁵⁵(^a)Dipartimento di Fisica, Università di Genova, Genova; (^b)INFN Sezione di Genova; Italy.
- ⁵⁶II. Physikalisches Institut, Justus-Liebig-Universität Giessen, Giessen; Germany.
- ⁵⁷SUPA - School of Physics and Astronomy, University of Glasgow, Glasgow; United Kingdom.
- ⁵⁸LPSC, Université Grenoble Alpes, CNRS/IN2P3, Grenoble INP, Grenoble; France.
- ⁵⁹Laboratory for Particle Physics and Cosmology, Harvard University, Cambridge MA; United States of America.
- ⁶⁰(^a)Department of Modern Physics and State Key Laboratory of Particle Detection and Electronics, University of Science and Technology of China, Hefei; (^b)Institute of Frontier and Interdisciplinary Science and Key Laboratory of Particle Physics and Particle Irradiation (MOE), Shandong University, Qingdao; (^c)School of Physics and Astronomy, Shanghai Jiao Tong University, KLPPAC-MoE, SKLPPC, Shanghai; (^d)Tsung-Dao Lee Institute, Shanghai; China.
- ⁶¹(^a)Kirchhoff-Institut für Physik, Ruprecht-Karls-Universität Heidelberg, Heidelberg; (^b)Physikalisches Institut, Ruprecht-Karls-Universität Heidelberg, Heidelberg; Germany.
- ⁶²Faculty of Applied Information Science, Hiroshima Institute of Technology, Hiroshima; Japan.
- ⁶³(^a)Department of Physics, Chinese University of Hong Kong, Shatin, N.T., Hong Kong; (^b)Department of Physics, University of Hong Kong, Hong Kong; (^c)Department of Physics and Institute for Advanced Study, Hong Kong University of Science and Technology, Clear Water Bay, Kowloon, Hong Kong; China.

- ⁶⁴Department of Physics, National Tsing Hua University, Hsinchu; Taiwan.
- ⁶⁵IJCLab, Université Paris-Saclay, CNRS/IN2P3, 91405, Orsay; France.
- ⁶⁶Department of Physics, Indiana University, Bloomington IN; United States of America.
- ⁶⁷(^a)INFN Gruppo Collegato di Udine, Sezione di Trieste, Udine; (^b)ICTP, Trieste; (^c)Dipartimento Politecnico di Ingegneria e Architettura, Università di Udine, Udine; Italy.
- ⁶⁸(^a)INFN Sezione di Lecce; (^b)Dipartimento di Matematica e Fisica, Università del Salento, Lecce; Italy.
- ⁶⁹(^a)INFN Sezione di Milano; (^b)Dipartimento di Fisica, Università di Milano, Milano; Italy.
- ⁷⁰(^a)INFN Sezione di Napoli; (^b)Dipartimento di Fisica, Università di Napoli, Napoli; Italy.
- ⁷¹(^a)INFN Sezione di Pavia; (^b)Dipartimento di Fisica, Università di Pavia, Pavia; Italy.
- ⁷²(^a)INFN Sezione di Pisa; (^b)Dipartimento di Fisica E. Fermi, Università di Pisa, Pisa; Italy.
- ⁷³(^a)INFN Sezione di Roma; (^b)Dipartimento di Fisica, Sapienza Università di Roma, Roma; Italy.
- ⁷⁴(^a)INFN Sezione di Roma Tor Vergata; (^b)Dipartimento di Fisica, Università di Roma Tor Vergata, Roma; Italy.
- ⁷⁵(^a)INFN Sezione di Roma Tre; (^b)Dipartimento di Matematica e Fisica, Università Roma Tre, Roma; Italy.
- ⁷⁶(^a)INFN-TIFPA; (^b)Università degli Studi di Trento, Trento; Italy.
- ⁷⁷Institut für Astro- und Teilchenphysik, Leopold-Franzens-Universität, Innsbruck; Austria.
- ⁷⁸University of Iowa, Iowa City IA; United States of America.
- ⁷⁹Department of Physics and Astronomy, Iowa State University, Ames IA; United States of America.
- ⁸⁰Joint Institute for Nuclear Research, Dubna; Russia.
- ⁸¹(^a)Departamento de Engenharia Elétrica, Universidade Federal de Juiz de Fora (UFJF), Juiz de Fora; (^b)Universidade Federal do Rio De Janeiro COPPE/EE/IF, Rio de Janeiro; (^c)Universidade Federal de São João del Rei (UFSJ), São João del Rei; (^d)Instituto de Física, Universidade de São Paulo, São Paulo; Brazil.
- ⁸²KEK, High Energy Accelerator Research Organization, Tsukuba; Japan.
- ⁸³Graduate School of Science, Kobe University, Kobe; Japan.
- ⁸⁴(^a)AGH University of Science and Technology, Faculty of Physics and Applied Computer Science, Krakow; (^b)Marian Smoluchowski Institute of Physics, Jagiellonian University, Krakow; Poland.
- ⁸⁵Institute of Nuclear Physics Polish Academy of Sciences, Krakow; Poland.
- ⁸⁶Faculty of Science, Kyoto University, Kyoto; Japan.
- ⁸⁷Kyoto University of Education, Kyoto; Japan.
- ⁸⁸Research Center for Advanced Particle Physics and Department of Physics, Kyushu University, Fukuoka ; Japan.
- ⁸⁹Instituto de Física La Plata, Universidad Nacional de La Plata and CONICET, La Plata; Argentina.
- ⁹⁰Physics Department, Lancaster University, Lancaster; United Kingdom.
- ⁹¹Oliver Lodge Laboratory, University of Liverpool, Liverpool; United Kingdom.
- ⁹²Department of Experimental Particle Physics, Jožef Stefan Institute and Department of Physics, University of Ljubljana, Ljubljana; Slovenia.
- ⁹³School of Physics and Astronomy, Queen Mary University of London, London; United Kingdom.
- ⁹⁴Department of Physics, Royal Holloway University of London, Egham; United Kingdom.
- ⁹⁵Department of Physics and Astronomy, University College London, London; United Kingdom.
- ⁹⁶Louisiana Tech University, Ruston LA; United States of America.
- ⁹⁷Fysiska institutionen, Lunds universitet, Lund; Sweden.
- ⁹⁸Centre de Calcul de l'Institut National de Physique Nucléaire et de Physique des Particules (IN2P3), Villeurbanne; France.
- ⁹⁹Departamento de Física Teórica C-15 and CIAFF, Universidad Autónoma de Madrid, Madrid; Spain.
- ¹⁰⁰Institut für Physik, Universität Mainz, Mainz; Germany.

- ¹⁰¹School of Physics and Astronomy, University of Manchester, Manchester; United Kingdom.
- ¹⁰²CPPM, Aix-Marseille Université, CNRS/IN2P3, Marseille; France.
- ¹⁰³Department of Physics, University of Massachusetts, Amherst MA; United States of America.
- ¹⁰⁴Department of Physics, McGill University, Montreal QC; Canada.
- ¹⁰⁵School of Physics, University of Melbourne, Victoria; Australia.
- ¹⁰⁶Department of Physics, University of Michigan, Ann Arbor MI; United States of America.
- ¹⁰⁷Department of Physics and Astronomy, Michigan State University, East Lansing MI; United States of America.
- ¹⁰⁸B.I. Stepanov Institute of Physics, National Academy of Sciences of Belarus, Minsk; Belarus.
- ¹⁰⁹Research Institute for Nuclear Problems of Byelorussian State University, Minsk; Belarus.
- ¹¹⁰Group of Particle Physics, University of Montreal, Montreal QC; Canada.
- ¹¹¹P.N. Lebedev Physical Institute of the Russian Academy of Sciences, Moscow; Russia.
- ¹¹²National Research Nuclear University MEPhI, Moscow; Russia.
- ¹¹³D.V. Skobeltsyn Institute of Nuclear Physics, M.V. Lomonosov Moscow State University, Moscow; Russia.
- ¹¹⁴Fakultät für Physik, Ludwig-Maximilians-Universität München, München; Germany.
- ¹¹⁵Max-Planck-Institut für Physik (Werner-Heisenberg-Institut), München; Germany.
- ¹¹⁶Nagasaki Institute of Applied Science, Nagasaki; Japan.
- ¹¹⁷Graduate School of Science and Kobayashi-Maskawa Institute, Nagoya University, Nagoya; Japan.
- ¹¹⁸Department of Physics and Astronomy, University of New Mexico, Albuquerque NM; United States of America.
- ¹¹⁹Institute for Mathematics, Astrophysics and Particle Physics, Radboud University Nijmegen/Nikhef, Nijmegen; Netherlands.
- ¹²⁰Nikhef National Institute for Subatomic Physics and University of Amsterdam, Amsterdam; Netherlands.
- ¹²¹Department of Physics, Northern Illinois University, DeKalb IL; United States of America.
- ¹²²^(a) Budker Institute of Nuclear Physics and NSU, SB RAS, Novosibirsk; ^(b) Novosibirsk State University Novosibirsk; Russia.
- ¹²³Institute for High Energy Physics of the National Research Centre Kurchatov Institute, Protvino; Russia.
- ¹²⁴Institute for Theoretical and Experimental Physics named by A.I. Alikhanov of National Research Centre "Kurchatov Institute", Moscow; Russia.
- ¹²⁵Department of Physics, New York University, New York NY; United States of America.
- ¹²⁶Ochanomizu University, Otsuka, Bunkyo-ku, Tokyo; Japan.
- ¹²⁷Ohio State University, Columbus OH; United States of America.
- ¹²⁸Homer L. Dodge Department of Physics and Astronomy, University of Oklahoma, Norman OK; United States of America.
- ¹²⁹Department of Physics, Oklahoma State University, Stillwater OK; United States of America.
- ¹³⁰Palacký University, RCPTM, Joint Laboratory of Optics, Olomouc; Czech Republic.
- ¹³¹Institute for Fundamental Science, University of Oregon, Eugene, OR; United States of America.
- ¹³²Graduate School of Science, Osaka University, Osaka; Japan.
- ¹³³Department of Physics, University of Oslo, Oslo; Norway.
- ¹³⁴Department of Physics, Oxford University, Oxford; United Kingdom.
- ¹³⁵LPNHE, Sorbonne Université, Université de Paris, CNRS/IN2P3, Paris; France.
- ¹³⁶Department of Physics, University of Pennsylvania, Philadelphia PA; United States of America.
- ¹³⁷Konstantinov Nuclear Physics Institute of National Research Centre "Kurchatov Institute", PNPI, St. Petersburg; Russia.
- ¹³⁸Department of Physics and Astronomy, University of Pittsburgh, Pittsburgh PA; United States of

America.

¹³⁹(^a) Laboratório de Instrumentação e Física Experimental de Partículas - LIP, Lisboa; (^b) Departamento de Física, Faculdade de Ciências, Universidade de Lisboa, Lisboa; (^c) Departamento de Física, Universidade de Coimbra, Coimbra; (^d) Centro de Física Nuclear da Universidade de Lisboa, Lisboa; (^e) Departamento de Física, Universidade do Minho, Braga; (^f) Departamento de Física Teórica y del Cosmos, Universidad de Granada, Granada (Spain); (^g) Dep Física and CEFITEC of Faculdade de Ciências e Tecnologia, Universidade Nova de Lisboa, Caparica; (^h) Instituto Superior Técnico, Universidade de Lisboa, Lisboa; Portugal.

¹⁴⁰ Institute of Physics of the Czech Academy of Sciences, Prague; Czech Republic.

¹⁴¹ Czech Technical University in Prague, Prague; Czech Republic.

¹⁴² Charles University, Faculty of Mathematics and Physics, Prague; Czech Republic.

¹⁴³ Particle Physics Department, Rutherford Appleton Laboratory, Didcot; United Kingdom.

¹⁴⁴ IRFU, CEA, Université Paris-Saclay, Gif-sur-Yvette; France.

¹⁴⁵ Santa Cruz Institute for Particle Physics, University of California Santa Cruz, Santa Cruz CA; United States of America.

¹⁴⁶(^a) Departamento de Física, Pontificia Universidad Católica de Chile, Santiago; (^b) Universidad Andres Bello, Department of Physics, Santiago; (^c) Instituto de Alta Investigación, Universidad de Tarapacá; (^d) Departamento de Física, Universidad Técnica Federico Santa María, Valparaíso; Chile.

¹⁴⁷ Department of Physics, University of Washington, Seattle WA; United States of America.

¹⁴⁸ Department of Physics and Astronomy, University of Sheffield, Sheffield; United Kingdom.

¹⁴⁹ Department of Physics, Shinshu University, Nagano; Japan.

¹⁵⁰ Department Physik, Universität Siegen, Siegen; Germany.

¹⁵¹ Department of Physics, Simon Fraser University, Burnaby BC; Canada.

¹⁵² SLAC National Accelerator Laboratory, Stanford CA; United States of America.

¹⁵³ Physics Department, Royal Institute of Technology, Stockholm; Sweden.

¹⁵⁴ Departments of Physics and Astronomy, Stony Brook University, Stony Brook NY; United States of America.

¹⁵⁵ Department of Physics and Astronomy, University of Sussex, Brighton; United Kingdom.

¹⁵⁶ School of Physics, University of Sydney, Sydney; Australia.

¹⁵⁷ Institute of Physics, Academia Sinica, Taipei; Taiwan.

¹⁵⁸(^a) E. Andronikashvili Institute of Physics, Iv. Javakhishvili Tbilisi State University, Tbilisi; (^b) High Energy Physics Institute, Tbilisi State University, Tbilisi; Georgia.

¹⁵⁹ Department of Physics, Technion, Israel Institute of Technology, Haifa; Israel.

¹⁶⁰ Raymond and Beverly Sackler School of Physics and Astronomy, Tel Aviv University, Tel Aviv; Israel.

¹⁶¹ Department of Physics, Aristotle University of Thessaloniki, Thessaloniki; Greece.

¹⁶² International Center for Elementary Particle Physics and Department of Physics, University of Tokyo, Tokyo; Japan.

¹⁶³ Graduate School of Science and Technology, Tokyo Metropolitan University, Tokyo; Japan.

¹⁶⁴ Department of Physics, Tokyo Institute of Technology, Tokyo; Japan.

¹⁶⁵ Tomsk State University, Tomsk; Russia.

¹⁶⁶ Department of Physics, University of Toronto, Toronto ON; Canada.

¹⁶⁷(^a) TRIUMF, Vancouver BC; (^b) Department of Physics and Astronomy, York University, Toronto ON; Canada.

¹⁶⁸ Division of Physics and Tomonaga Center for the History of the Universe, Faculty of Pure and Applied Sciences, University of Tsukuba, Tsukuba; Japan.

¹⁶⁹ Department of Physics and Astronomy, Tufts University, Medford MA; United States of America.

¹⁷⁰ Department of Physics and Astronomy, University of California Irvine, Irvine CA; United States of

America.

¹⁷¹Department of Physics and Astronomy, University of Uppsala, Uppsala; Sweden.

¹⁷²Department of Physics, University of Illinois, Urbana IL; United States of America.

¹⁷³Instituto de Física Corpuscular (IFIC), Centro Mixto Universidad de Valencia - CSIC, Valencia; Spain.

¹⁷⁴Department of Physics, University of British Columbia, Vancouver BC; Canada.

¹⁷⁵Department of Physics and Astronomy, University of Victoria, Victoria BC; Canada.

¹⁷⁶Fakultät für Physik und Astronomie, Julius-Maximilians-Universität Würzburg, Würzburg; Germany.

¹⁷⁷Department of Physics, University of Warwick, Coventry; United Kingdom.

¹⁷⁸Waseda University, Tokyo; Japan.

¹⁷⁹Department of Particle Physics, Weizmann Institute of Science, Rehovot; Israel.

¹⁸⁰Department of Physics, University of Wisconsin, Madison WI; United States of America.

¹⁸¹Fakultät für Mathematik und Naturwissenschaften, Fachgruppe Physik, Bergische Universität Wuppertal, Wuppertal; Germany.

¹⁸²Department of Physics, Yale University, New Haven CT; United States of America.

^a Also at Borough of Manhattan Community College, City University of New York, New York NY; United States of America.

^b Also at Centro Studi e Ricerche Enrico Fermi; Italy.

^c Also at CERN, Geneva; Switzerland.

^d Also at CPPM, Aix-Marseille Université, CNRS/IN2P3, Marseille; France.

^e Also at Département de Physique Nucléaire et Corpusculaire, Université de Genève, Genève; Switzerland.

^f Also at Departament de Física de la Universitat Autònoma de Barcelona, Barcelona; Spain.

^g Also at Department of Financial and Management Engineering, University of the Aegean, Chios; Greece.

^h Also at Department of Physics and Astronomy, Michigan State University, East Lansing MI; United States of America.

ⁱ Also at Department of Physics and Astronomy, University of Louisville, Louisville, KY; United States of America.

^j Also at Department of Physics, Ben Gurion University of the Negev, Beer Sheva; Israel.

^k Also at Department of Physics, California State University, East Bay; United States of America.

^l Also at Department of Physics, California State University, Fresno; United States of America.

^m Also at Department of Physics, California State University, Sacramento; United States of America.

ⁿ Also at Department of Physics, King's College London, London; United Kingdom.

^o Also at Department of Physics, St. Petersburg State Polytechnical University, St. Petersburg; Russia.

^p Also at Department of Physics, University of Fribourg, Fribourg; Switzerland.

^q Also at Dipartimento di Matematica, Informatica e Fisica, Università di Udine, Udine; Italy.

^r Also at Faculty of Physics, M.V. Lomonosov Moscow State University, Moscow; Russia.

^s Also at Giresun University, Faculty of Engineering, Giresun; Turkey.

^t Also at Graduate School of Science, Osaka University, Osaka; Japan.

^u Also at Hellenic Open University, Patras; Greece.

^v Also at IJCLab, Université Paris-Saclay, CNRS/IN2P3, 91405, Orsay; France.

^w Also at Institutio Catalana de Recerca i Estudis Avancats, ICREA, Barcelona; Spain.

^x Also at Institut für Experimentalphysik, Universität Hamburg, Hamburg; Germany.

^y Also at Institute for Mathematics, Astrophysics and Particle Physics, Radboud University Nijmegen/Nikhef, Nijmegen; Netherlands.

^z Also at Institute for Nuclear Research and Nuclear Energy (INRNE) of the Bulgarian Academy of Sciences, Sofia; Bulgaria.

^{aa} Also at Institute for Particle and Nuclear Physics, Wigner Research Centre for Physics, Budapest;

Hungary.

ab Also at Institute of Particle Physics (IPP), Vancouver; Canada.

ac Also at Institute of Physics, Azerbaijan Academy of Sciences, Baku; Azerbaijan.

ad Also at Instituto de Fisica Teorica, IFT-UAM/CSIC, Madrid; Spain.

ae Also at Joint Institute for Nuclear Research, Dubna; Russia.

af Also at Louisiana Tech University, Ruston LA; United States of America.

ag Also at Moscow Institute of Physics and Technology State University, Dolgoprudny; Russia.

ah Also at National Research Nuclear University MEPhI, Moscow; Russia.

ai Also at Physics Department, An-Najah National University, Nablus; Palestine.

aj Also at Physikalisches Institut, Albert-Ludwigs-Universität Freiburg, Freiburg; Germany.

ak Also at The City College of New York, New York NY; United States of America.

al Also at TRIUMF, Vancouver BC; Canada.

am Also at Universita di Napoli Parthenope, Napoli; Italy.

an Also at University of Chinese Academy of Sciences (UCAS), Beijing; China.

* Deceased